

Aus dem Institut für Immunologie im Biomedizinischen Centrum der LMU

Institut der Ludwig-Maximilians-Universität München

Leitung: Prof. Dr. rer. nat Thomas Brocker

**Dissection of the molecular requirements for  
T follicular helper cell differentiation and maintenance**



Dissertation  
zum Erwerb des Doktorgrades der Naturwissenschaften  
an der Medizinischen Fakultät der  
Ludwig-Maximilians-Universität München

vorgelegt von

Marc Dominik Alterauge

aus

Augsburg

Jahr  
2020

---

Mit Genehmigung der Medizinischen Fakultät  
der Universität München

Betreuer(in): Prof. Dr. Dirk Baumjohann

Zweitgutachter(in): PD Dr. Hanna-Mari Baldauf

Dekan: Prof. Dr. med. dent. Reinhard Hickel

Tag der mündlichen Prüfung: 04.05.2021

## Eidesstattliche Versicherung

Ich erkläre hiermit an Eides statt, dass ich die vorliegende Dissertation mit dem Thema „Dissection of the molecular requirements for T follicular helper cell differentiation and maintenance“ selbständig verfasst, mich außer der angegebenen keiner weiteren Hilfsmittel bedient und alle Erkenntnisse, die aus dem Schrifttum ganz oder annähernd übernommen sind, als solche kenntlich gemacht und nach ihrer Herkunft unter Bezeichnung der Fundstelle einzeln nachgewiesen habe. Ich erkläre des Weiteren, dass die hier vorgelegte Dissertation nicht in gleicher oder in ähnlicher Form bei einer anderen Stelle zur Erlangung eines akademischen Grades eingereicht wurde.

München, den 19.07.21

Dominik Alterauge

---

„The first draft of anything is shit.” — Ernest Hemingway

## Table of contents

### Table of contents

1. Summary .....	1
2. Zusammenfassung .....	2
3. List of abbreviations.....	3
4. Introduction.....	6
4.1. Defense strategies of the vertebrate immune system .....	6
4.2. Th cells in immune responses .....	7
4.2.1. Differentiation and function of Th cell subsets.....	7
4.2.2. T follicular helper cells.....	8
4.2.2.1. Function.....	8
4.2.2.2. Multistage model of differentiation.....	9
4.2.2.3. Molecular regulation .....	12
4.2.2.3.1. Co-stimulation and post-transcriptional regulation .....	12
4.2.2.3.2. Transcription factor networks .....	13
4.3. The transcriptional repressor Bcl6.....	15
4.3.1. Function, structure and cofactors of Bcl6 .....	15
4.3.2. The function and regulation of Bcl6 in B cell responses.....	15
4.3.3. Bcl6 in Tfh cells .....	16
4.3.3.1. Cell type-dependent functions of Bcl6.....	16
4.3.3.2. The regulation of Bcl6 in CD4 <sup>+</sup> T cells.....	16
4.3.3.3. The role of Bcl6 in Tfh cells .....	17
4.4. Tfh cell plasticity and maintenance.....	18
5. Aim of the thesis .....	20
6. Materials and Methods .....	22
6.1. Resources tables.....	22
6.1.1. Mice.....	22
6.1.2. Virus .....	22
6.1.3. Flow cytometry reagents .....	22
6.1.4. Chemicals, Peptides and Proteins .....	24
6.1.5. Critical commercial assays.....	25
6.1.6. Primers and oligonucleotides .....	26
6.1.7. Custom solutions and buffers.....	26
6.1.8. Consumables .....	27
6.1.9. Instruments.....	27
6.1.10. Deposited data .....	27
6.1.11. Software and algorithms.....	27

Table of contents

6.2. Methods.....	28
6.2.1. Mice.....	28
6.2.2. Immunizations, adoptive cell transfers, infections, and tamoxifen treatment .....	28
6.2.3. Flow cytometry .....	29
6.2.4. Immunohistology .....	29
6.2.5. Quantitative Real-Time qPCR analysis.....	30
6.2.6. SHM analysis .....	30
6.2.7. RNA-sequencing .....	31
6.2.8. Data availability .....	32
6.2.9. Statistical analysis.....	32
7. Results.....	33
7.1. The impact of CD4 <sup>+</sup> T cell-specific <i>Cxcr5</i> -ablation on the GC response .....	33
7.1.1. An inducible Cre recombinase elicits a <i>Cxcr5</i> KO with high efficiency in CD4 <sup>+</sup> T cells.....	33
7.1.2. <i>Cxcr5</i> -ablation in early and mature Tfh cells shows minor effects on T and B cell responses.....	36
7.1.3. Loss of the preferential CD4 <sup>+</sup> T cell LZ localization in the absence of CXCR5.....	38
7.1.4. Enhanced class-switching and plasma cell formation in an acute viral infection upon <i>Cxcr5</i> -deletion .....	39
7.1.5. The transcriptome of CXCR5-sufficient and -deficient Tfh cells highly similar .....	40
7.2. The impact of CD4 <sup>+</sup> T cell-specific <i>Bcl6</i> -ablation on the GC response .....	43
7.2.1. A system for the temporally-guided deletion of <i>Bcl6</i> in CD4 <sup>+</sup> T cells .....	43
7.2.2. Differential requirements of <i>Bcl6</i> for GC Tfh and Tfr cell maintenance.....	46
7.2.3. Altered Th1/Tfh cell ratios upon induced loss of Bcl6 during acute viral infection.....	50
7.2.4. Transdifferentiation of <i>Bcl6</i> -deleted Tfh cell into Th1 cells during acute viral infection.....	52
7.2.5. <i>Bcl6</i> -ablation in the context of a type-II immune response yields enhanced Th2/memory T cell marker expression.....	54
8. Discussion .....	56
8.1. Tamoxifen-inducible KO mouse strains as tools to investigate the requirements of Tfh cell maintenance .....	56
8.2. Induced <i>Cxcr5</i> -deficiency in CD4 <sup>+</sup> T cells does not impair Tfh cell maintenance.....	57
8.3. Potential roles of Bcl6 in established Tfh cells .....	61
8.4. Bcl6 as a gatekeeper of Tfh cell plasticity .....	62
9. Acknowledgement .....	81
10. References .....	66
11. Curriculum Vitae.....	83
12. Publication list.....	84

## 1. Summary

T follicular helper (Tfh) cells are the primary source of T cell help for germinal center (GC) B cells. This cellular interaction is critical for the formation of high-affinity antibodies. By regulating the GC reaction and its cellular output, Tfh cells control humoral immunity in health and disease. While the molecular cues that promote their formation are well known, an adequate definition of the molecular regulation of Tfh cell maintenance is missing. In this thesis, a mouse model for the temporally-guided and CD4<sup>+</sup> T cell-specific ablation of genes was established and applied to examine the requirement of continued expression of two Tfh cell hallmark molecules, CXCR5 and Bcl6, in established Tfh cells. Here, it was found that ongoing expression of the chemokine receptor CXCR5 was largely dispensable for the maintenance of the Tfh cell phenotype, while the transcription factor Bcl6 was strictly needed to sustain Tfh cells and GC B cell responses. *Cxcr5*-ablated Tfh cells continued to express high amounts of Bcl6 and the co-inhibitory receptor PD-1 and were also retained in GCs. Despite a diminished fraction of CD4<sup>+</sup> T cells within GCs and a loss of the characteristic light zone (LZ) polarization, B cell help potency was not grossly impaired. Finally, a global assessment of the transcriptome of *Cxcr5*-deficient Tfh cells by RNA-sequencing revealed that the Tfh cell phenotype was maintained in the absence of CXCR5. In contrast, Bcl6 was required to promote the high expression levels of PD-1 and CXCR5 that are present in GC Tfh cells, and to simultaneously restrain the activity of non-Tfh cell genes, such as *Selplg* and *Ccr7*. Furthermore, the loss of *Bcl6* resulted in a severe impairment of the GC B cell response and particularly immunoglobulin (Ig) class-switched GC B cells were not properly sustained. Strikingly, *Bcl6*-ablation in CD4<sup>+</sup> T cells during an acute viral infection resulted in the transdifferentiation of established Tfh cells into T helper 1 (Th1) cells.

Taken together, these findings challenge the prevailing view of CXCR5 as a requirement of Tfh cell identity- and highlight Bcl6 as a critical gatekeeper of Tfh cell plasticity *in vivo*. Thus, Bcl6 might represent a promising therapeutic target in autoimmunity and certain types of cancers, such as follicular lymphoma or angioimmunoblastic T cell lymphoma.

## 2. Zusammenfassung

Follikuläre T-Helferzellen (Tfh) sind die primäre Quelle von T-Zellhilfe für Keimzentren (GC) B-Zellen. Diese zelluläre Interaktion ist ausschlaggebend für die Bildung von hochaffinen Antikörpern. Durch die Regulation der GC Reaktion und der dabei entstehenden Zellen steuern Tfh-Zellen die humorale Immunität unter physiologischen und pathologischen Bedingungen. Während die molekularen Signale, die zu ihrer Entstehung beitragen, bekannt sind, fehlt ein tieferes Verständnis der Regulation von bereits ausdifferenzierten Tfh-Zellen. In dieser Arbeit wurde zuerst ein Mausmodell für die zeitlich-gesteuerte und CD4<sup>+</sup> T-Zell-spezifische Deletion von Genen etabliert. Mit Hilfe dieses Modells wurde untersucht, ob die kontinuierliche Expression von zwei Tfh-Zell-definierenden Markern, CXCR5 und Bcl6, in bereits gebildeten Tfh-Zellen essentiell ist. Diese Analysen ergaben, dass der Chemokinrezeptor CXCR5 für die Aufrechterhaltung von Tfh-Zellen nicht wesentlich erforderlich ist, wohingegen der Transkriptionsfaktor Bcl6 essentiell für die Unterstützung von Tfh-Zellen und GC B-Zellantworten ist. Tfh-Zellen, in denen *Cxcr5* deletiert wurde, zeigten eine unverändert hohe Expression von Bcl6 und dem co-inhibitorischen Rezeptor PD-1 und befanden sich weiterhin in GCs. Obwohl die Anzahl von CD4<sup>+</sup> T Zellen in GCs reduziert war und ein Verlust der charakteristischen Polarisierung in der hellen Zone (LZ) beobachtet wurde, war die Potenz der B-Zellhilfe nicht stark beeinträchtigt. Abschließend zeigte eine globale Analyse des Transkriptoms von *Cxcr5*-defizienten Tfh-Zellen mittels RNA Sequenzierung, dass der Tfh-Zell Phänotyp in Abwesenheit von CXCR5 erhalten blieb. Im Gegensatz dazu wurde Bcl6 benötigt um die hohe Expression von PD-1 und CXCR5 beizubehalten, die in GC Tfh-Zellen vorliegt, und gleichzeitig die Aktivität von nicht-Tfh-Zell Genen, wie *Selplg* und *Ccr7*, zu unterdrücken. Des Weiteren hatte der Verlust von *Bcl6* eine massive Beeinträchtigung der GC Antwort zur Folge. Vor allem GC B-Zellen, die einen IgG Klassenwechsel durchlaufen hatten, konnten nicht in normalem Umfang aufrechterhalten werden. Überraschenderweise führte die Deletion von *Bcl6* in CD4<sup>+</sup> T-Zellen, im Zuge einer akuten viralen Infektion, zu einer Transdifferenzierung von etablierten Tfh-Zellen zu Typ1 T-Helferzellen (Th1).

Zusammengenommen stellen diese Beobachtungen die Bedeutung von CXCR5 für die Tfh-Zell-Identität in Frage und betonen die zentrale Rolle von Bcl6 als Regulator der Plastizität von Tfh-Zellen *in vivo*. Demzufolge könnte Bcl6 ein vielversprechendes therapeutisches Zielmolekül für die Behandlung von Autoimmunerkrankungen und bestimmten Krebsarten, wie z.B. follikulärem Lymphom oder angioimmunoblastischem T-Zell-Lymphom, darstellen.

### 3. List of abbreviations

APC	Antigen-presenting cell
Ascl2	Achaete-scute homologue 2
Batf	Basic leucine zipper transcriptional factor ATF-like
Bcl6	B cell lymphoma 6
BCR	B cell receptor
Blimp-1	B lymphocyte-induced maturation protein-1
BTB	Bric-a-brac, tramtrack, broad complex
CCR7	C-C chemokine receptor type 7
CD	Cluster of differentiation
ChIP	Chromatin immunoprecipitation
CTL	Cytotoxic lymphocyte
CXCR	CXC chemokine receptor
CXCL	CXC chemokine ligand
DC	Dendritic cell
DNA	Deoxyribonucleic acid
DZ	Dark zone
EBI2	Epstein-Barr virus-induced G protein coupled receptor 2
eYFP	Enhanced yellow fluorescent protein
FDC	Follicular dendritic cell
FOXO1	Forkhead box protein O1
Foxp3	Forkhead box protein 3
GATA3	GATA binding protein 3
GC	Germinal center
gDNA	Genomic DNA
GP	Glycoprotein
HDAC	Histone deacetylase complex
ICOS	Inducible T cell co-stimulator
IFN $\gamma$	Interferon gamma
IFNGR1	IFN gamma receptor 1
Ig	Immunoglobulin
IHC	Immunohistochemistry
IL	Interleukin
i.p.	Intraperitoneal
IRF	Interferon regulatory factor
KI	Knock-in
Klf2	Kruppel-like factor 2

List of abbreviations

KLH	Keyhole limpet hemocyanin
KO	KO
L	Ligand
LCMV	Lymphocytic choriomeningitis virus
LEF-1	Lymphoid enhancer binding factor-1
LN	Lymph node
LZ	Light zone
MAPK	Mitogen-activated protein kinase
MHC	Major histocompatibility complex
min	Minutes
miR	MicroRNA
mRNA	Messenger RNA
MSA	Mouse serum albumin
mTOR	Mammalian target of rapamycin
mTORC1	mTOR complex 1
mTORC2	mTOR complex 2
NP	4-hydroxy-3-nitrophenyl acetyl
PC	Plasma cell
PCA	Principal component analysis
PD-1	Programmed cell death protein 1
PD-L1	Programmed cell death ligand 1
PI3K	Phosphoinositide 3-kinase
PSGL-1	P-selectin glycoprotein ligand-1
RNA	Ribonucleic acid
ROI	Region of interest
ROR $\gamma$ t	Retinoic acid-related orphan receptor gamma
RT	Room temperature
s.c.	Subcutane
s.e.m.	Standard error of the mean
seq	Sequencing
SHM	Somatic hypermutation
SLAM	Signaling lymphocytic activation molecule
SM	SMARTA
STAT	Signal transducer and activator of transcription
Tbet	T-box transcription factor
TCR	T cell receptor
TCF-1	T cell factor-1

List of abbreviations

TF	Transcription factor
Tg	Transgenic
Th	T helper
Thpok	T helper-inducing POZ/Krueppel-like factor
Tfh	T follicular helper cells
Tfr	T follicular regulatory cells
TLR	Toll-like receptors
TNF $\alpha$	Tumor necrosis factor alpha
Treg	Regulatory T cells
UMI	Unique molecular identifiers
UTR	Untranslated region
qPCR	Quantitative polymerase chain reaction
WT	Wildtype

## 4. Introduction

### 4.1. Defense strategies of the vertebrate immune system

Multicellular organisms are exposed to a large variety of endogenous and exogenous threats. Powerful defense strategies have thus evolved to protect the hosts on several levels. The simplest and most common way is to prevent the entry of foreign structures across the outer barriers, while more sophisticated mechanisms encompass degradation and inactivation of the pathogenic molecules. This protection is referred to as immunity, a state of invulnerability to a biological hazard. All organisms are equipped with an immune system and with growing complexity of the hosts, the immune system has coevolved more versatile mechanisms. In plants and animals, components of the innate immune system sense pathogen-associated molecular patterns (PAMPs) such as bacterial RNA, DNA, or constituents of the cell wall (Medzhitov and Janeway, 1997). These structures are bound by a set of extra- or intracellular receptors including toll-like receptors (TLRs) and nucleotide-binding oligomerization domain (NOD)-like receptors (NLRs), respectively. TLR and NLR-triggered signaling cascades result in a strong activation of innate immune cells, such as granulocytes and macrophages, which eliminate infected cells through phagocytosis (Chen et al., 2009; Hemmi et al., 2000). Alternatively, clearance of cells can also be accomplished by the complement system, the humoral branch of the innate immune system. It comprises several soluble molecules that either mediate direct lysis or labeling for subsequent lysis (Tschopp et al., 1986). Besides macrophages, TLR ligands also activate dendritic cells (DCs) (Tada et al., 2005). Through their function as antigen-presenting cells (APCs) they are able to invoke the adaptive branch of the immune system, which has evolved in vertebrates (Boehm et al., 2018; Cooper and Alder, 2006).

In contrast to its innate counterpart, the adaptive immune system is more variable and flexible as it can learn to recognize previously unknown structures through adaptation. Moreover, adaptive immune cells that are able to bind pathogenic structures are maintained as memory cells and promote long-lasting protection. Consequently, pathogens that have evaded innate immune sensors can still be controlled by the adaptive counterpart. This is achieved through two groups of lymphocytes that carry highly variable antigen-binding receptors: T and B lymphocytes. In the course of their development, DNA segments that encode for the T and B cell receptor (TCR and BCR) undergo somatic rearrangement (Davis and Bjorkman, 1988; Tonegawa, 1983). Distinct sets of variable (V), diversity (D), and joining (J) gene segments are joined through recombination and generate an enormous variability. This process occurs almost randomly and can therefore give rise to antigen receptors that recognize self-antigens (Melamed et al., 1998). Self-reactivity needs to be efficiently removed from the organism to prevent immune reactions directed against the host. Therefore, tightly controlled selection processes are required during the maturation of T and B cells. For B cells, this takes place in

the bone marrow where they develop and subsequently migrate into peripheral secondary lymphoid organs, such as lymph nodes (LNs) or the spleen. Here, they scan the environment for exogenous antigens and, upon activation, differentiate into antibody-secreting plasma cells (PCs). B cells mainly act through the secretion of target-specific antibodies that bind, opsonize and neutralize foreign structures (Amir et al., 1990; Farrell and Shellam, 1991). Antibodies depict the humoral component of the adaptive immune response. Additionally, B cells can also act as potent APCs especially for antigens that are recognized by the BCR (Stockinger, 1992).

In contrast, T cell development takes place in the thymus. T cells in the cortex express an immature TCR and both the CD4 and the CD8 co-receptors. Depending on the recognition of peptides presented on either major histocompatibility complex (MHC) I or II molecules, CD4 or CD8 expression is arrested and the cells differentiate into CD8<sup>+</sup> cytotoxic lymphocytes (CTLs) or CD4<sup>+</sup> T helper (Th) cells, respectively. Only cells that show no or very weak binding to presented self-peptides are allowed to enter the periphery as naive T cells. CTLs are able to directly kill cells that present foreign antigens on MHC-I molecules, which is an indicator of viral infections. Th cells, in turn, do not act immediately on compromised cells but mediate their effects by supporting and maintaining immune responses of other immune cell subsets.

## 4.2. Th cells in immune responses

### 4.2.1. Differentiation and function of Th cell subsets

Although Th cells target invading pathogens indirectly, they fulfill particularly vital tasks in the course of an immune response. By providing stimulatory signals, Th cells interact with a variety of immune cells of both the innate and the adaptive immune system. Thereby, CD4<sup>+</sup> T cells have a critical impact on the magnitude of immune responses against a variety of threats. Depending on the type of infection, different subsets of Th cells are generated. Th1 cells promote anti-viral responses, while Th2 and Th17 cells target helminths and fungi, respectively (Zhu et al., 2010). The differentiation of these cells is guided through so called master regulators (Wang et al., 2015a): T-box transcription factor TBX21 (Tbet) in Th1 cells, GATA binding protein 3 (GATA3) in Th2 cells and retinoic acid-related orphan receptor gamma (RORγt) in Th17 cells (Zhu et al., 2010). Upon pathogen encounter, innate immune cells recognize the characteristic PAMPs of these organisms and direct the differentiation of CD4<sup>+</sup> T cells, which have received TCR ligation and co-stimulation, into the corresponding subset through the secretion of particular cytokines (Jain and Pasare, 2017). After priming by DCs, Th cells migrate directly to the site of infection and support vital aspects of local immune responses: activation of CD8<sup>+</sup> T cells (Zhang et al., 2009) and monocytes (Alonso et al., 2011; Sebbag et al., 1997). Th1 cells exhibit their helper function through the secretion of interleukin-2 (IL-2), interferon-gamma (IFNγ) and the tumor necrosis factor alpha (TNFα) (Seder et al., 2008). While Th1 cell-derived IL-2 promotes mostly CTL responses, TNFα acts as a pleiotropic

immune activator (Almishri et al., 2016; Suresh et al., 2005) and regulator of immune cell function. IL-5 and IL-31 are the signature cytokines of Th2 cells (Walker and McKenzie, 2018). While IL-5 is essential for the proliferation and maturation of eosinophils (Coffman et al., 1989; Roufosse, 2018), IL-13 plays a critical role in the clearance of helminths (Wynn, 2003). As the third major subset, Th17 cells are primarily defined by the secretion of IL-17A and IL-17F. However, Th17 cells exhibit phenotypical heterogeneity depending on the cytokine milieu and can be anti-inflammatory when tumor transforming growth factor beta (TGF $\beta$ ) signaling prevails, which stimulates the expression of the regulatory cytokine IL-10 (Ichiyama et al., 2016; McGeachy et al., 2007). In the absence of TGF $\beta$ , Th17 cells exhibit a pro-inflammatory phenotype, which is marked by the co-expression of Tbet together with ROR $\gamma$ t and also IFN $\gamma$  (Lee et al., 2012). Besides immune cell activation and recruitment, it was recently shown that Th1 cells are required to maintain CD8-mediated antiviral immunity in persisting infections (Snell et al., 2016). In summary, Th cells support and amplify innate and adaptive immune responses directly at the site of infection or inflammation.

#### 4.2.2. T follicular helper cells

##### 4.2.2.1. Function

It was generally believed for more than 20 years that Th2 cells are the subset providing T cell help to B cells (Crotty, 2015; Mosmann et al., 1986). It is now clear that, although Th2 cells can stimulate germinal center (GC) B cells *in vitro* through IL-4 secretion, this does not occur *in vivo*, as Th2 cells migrate to the site of infection upon activation (Reinhardt et al., 2009). In contrast, T follicular helper (Tfh) cells do not leave the secondary lymphoid organs to mediate their primary effector functions. After priming, Tfh cells migrate into B cell follicles, where they exert their potent B cell helper functions. Analog to the other subsets, Tfh cells require TCR-ligation, co-stimulation and appropriate cytokine signals (Crotty, 2011; Vinuesa et al., 2016). Following activation, Tfh cells migrate into the adjacent B cell follicle and initiate an intensive crosstalk with B cells. The result of this intimate interaction is the stimulation of B cells to undergo affinity maturation, class switching, memory or PC differentiation. Thereby, Tfh cells promote high-affinity antibody responses that are long-lived and hence protect the host from infections. Furthermore, Tfh cells also control the immunoglobulin (Ig) isotype through the induction of class-switching. This depends strongly on the cytokine milieu in which the antigen is presented, e.g. in viral infections in mice, type I cytokines such as IFN $\gamma$  prevail and direct class-switching towards IgG2a and 2b (Mosmann and Coffman, 1989). IgG2 isotypes in mice mediate the elimination of infected cells through antibody-dependent cellular cytotoxicity (ADCC) and complement-dependent cytotoxicity (CDC) via their fragment crystallizable region (Fc region) (Kipps et al., 1985; Klaus et al., 1979). In contrast, antigens from extracellular pathogens elicit IgG1 antibodies, which are poor inducers of ADCC and CDC, but efficiently

induce the clearance of antigen:antibody complexes (Hazenbos et al., 1998; Lilienthal et al., 2018; Zakroff et al., 1989).

Although the promotion of antibody isotype class-switching is not exclusive to Tfh cells (Miyachi et al., 2016), it is generally accepted that Tfh cells guide the isotype switching of B cells that underwent somatic hypermutation (SHM) of their Ig genes. (De Silva and Klein, 2015). Additionally, Tfh cells support the differentiation of B cells into antibody-secreting PCs (Krautler et al., 2017; Zhang et al., 2018). Several studies have investigated the roles of IL-4 and IL-21 signals that are delivered during short-lived intercellular contacts in this process (De Silva and Klein, 2015). The exact roles could not be clearly deciphered, potentially due to redundancy and context-dependent functions (Ozaki et al., 2004; Weinstein et al., 2016). Clearly, Tfh cell-derived CD40L stimulates PC differentiation by promoting stable interferon regulatory factor 4 (IRF4) expression (Li et al., 2018). The most substantial property of Tfh cells is, however, their capability to enable antibody affinity maturation. This is achieved through iterative rounds of selection and SHM in the GC reaction, orchestrated by Tfh cells (Shulman et al., 2014; Victora et al., 2010). Impaired Tfh cell formation and function in humans is reported to cause immune deficiency (Coffey et al., 1998; Grimbacher et al., 2003), while exaggerated Tfh responses are associated with autoimmunity (Li et al., 2012; Ma et al., 2012; Simpson et al., 2010) and cancer (Ame-Thomas et al., 2012; Ochando and Braza, 2017).

#### 4.2.2.2. Multistage model of differentiation

Approaches to harness the potential of Tfh cells to improve vaccines or to inhibit Tfh function in autoimmune diseases and certain types of cancer are currently investigated (Ame-Thomas et al., 2012; Blanco et al., 2016; Niessl and Kaufmann, 2018; Ochando and Braza, 2017; Streeck et al., 2013; Ueno, 2019). To enhance and optimize these strategies it is crucial to obtain a deeper understanding of the molecular mechanisms driving Tfh cell generation. The commonly proposed model of Tfh cell differentiation is a multifactorial process that encompasses three developmental stages (**Fig. 1**): priming by DCs in the T cell zone, transient interactions with B cells at the T-B cell border and stable cognate interactions with B cells in the GC (Crotty, 2019; Qi, 2016; Vinuesa et al., 2016). Due to the complexity of these spatial and temporal steps, Tfh cell formation is controlled by a variety of checkpoints.

During the initial priming phase in the T cell zone, DCs present MHC-II-loaded peptides that are recognized by the TCR of naive CD4<sup>+</sup> T cells (**Fig. 1, left**) (Baumjohann et al., 2011; Choi et al., 2011; Goenka et al., 2011). Akin to other Th cell subsets, Tfh cells require a second signal, mediated by the co-stimulatory receptors CD28 and inducible T cell co-stimulator (ICOS), which are activated by the respective ligands on DCs (Choi et al., 2011; Watanabe et al., 2017). The third signal for Tfh cell induction is delivered via cytokines. IL-6 acts as a positive regulator by inducing the expression of the transcription factor (TF) B cell lymphoma 6 (Bcl6)

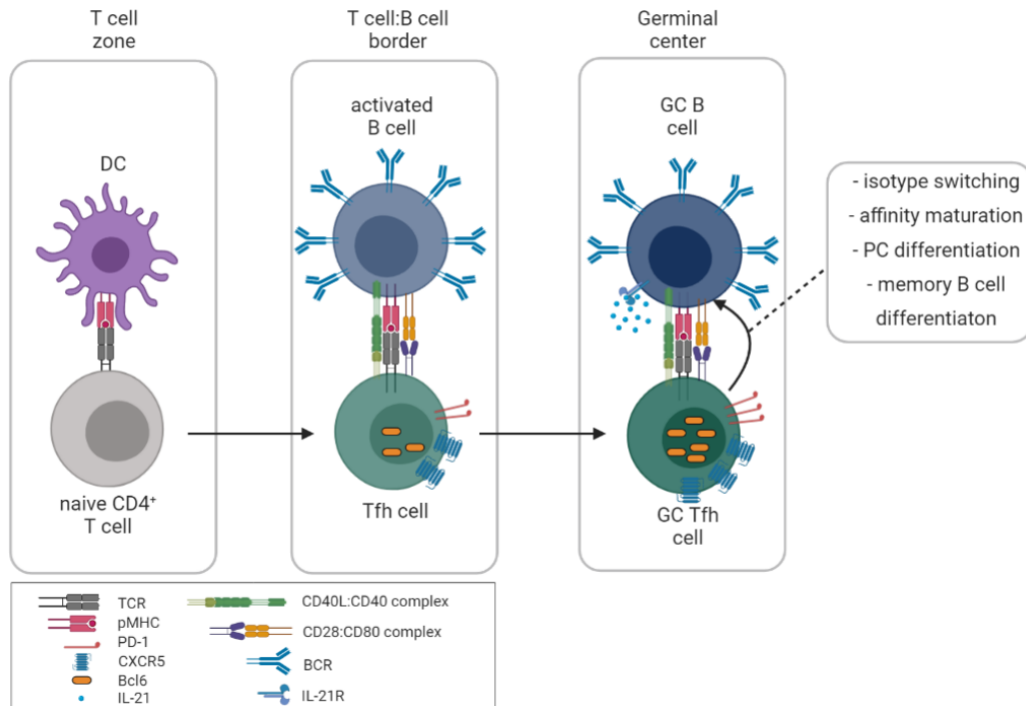


**Figure 1: Tfh cell differentiation multi-step model.** Priming of naive CD4<sup>+</sup> T cells by DCs occurs in the T cell zone. Differentiating Tfh cells undergo changes in their chemokine receptor repertoire and migrate to the T-B cell zone border where antigen presentation is taken over by activated B cells. After further migration into the B cell follicle, Tfh and GC B cells establish GCs and interact closely via receptor-ligand interactions and cytokines. Ultimately, GC B cells are stimulated to undergo isotype switching, affinity maturation and differentiate into PCs or memory B cells.

(Nurieva et al., 2009). IL-2 signaling, in turn, stimulates the expression of B lymphocyte-induced maturation protein-1 (Blimp-1), which is encoded by *Prdm1* and counteracts Tfh cell differentiation (Johnston et al., 2009). Bcl6 was identified to be necessary and sufficient for the induction of Tfh cell differentiation and is referred to as the master regulator of this subset (Johnston et al., 2009; Nurieva et al., 2009; Yu et al., 2009). In ensuing studies, several functions could be ascribed to Bcl6 in Tfh cells, e.g. inhibition of alternative T cell fates, instruction of the Tfh cell metabolic program and induction of migration (Crotty, 2014; Hatzi et al., 2015). While Bcl6 promotes migration through dampening the expression of molecules that would retain the cells within the T cell zone (Yu et al., 2009), the CXC chemokine receptor 5 (CXCR5) directs the migration towards the B cell follicle (Ansel et al., 1999; Arnold et al., 2007; Haynes et al., 2007). Although the expression of Bcl6 coincides with CXCR5 upregulation (Baumjohann et al., 2011), no clear causal relationship was proven. In the secondary differentiation phase, CD4<sup>+</sup> T cells that strongly increase CXCR5 expression can migrate along the CXC chemokine ligand (CXCL) 13 gradient into the B cell follicle (**Fig. 1, middle**). Concomitantly, the expression of C-C chemokine receptor type 7 (CCR7) and P-selectin glycoprotein ligand-1 (PSGL-1, encoded by *Selp/g*) that retain cells within the T cell zone, is needed to be downregulated (Haynes et al., 2007; Poholek et al., 2010).

At the T-B cell border, cognate B cells act as sources for antigens as well as co-stimulation for early Tfh cells (**Fig. 1, middle**) (Choi et al., 2013a; Deenick et al., 2010; Nurieva et al., 2008). The significant role of co-stimulation was emphasized by the finding that the absence of ICOSL on B cells results in a severe decrease of Tfh cell frequencies (Nurieva et al., 2008). Moreover, cognate interactions with B cells are indispensable to maintain the Tfh cell phenotype beyond this point (Baumjohann et al., 2013b; Haynes et al., 2007; Nurieva et al., 2008).

Through a yet incompletely understood selection process, certain Tfh cells at the T-B cell border are allowed to enter the B cell follicle and form GCs where they finally acquire the GC Tfh cell phenotype (**Fig. 1, right**). One of the requirements to gain the right to enter is high levels of ICOS (Shi et al., 2018; Xu et al., 2013). The receptor is engaged by ICOSL, expressed on activated B cells. ICOS signaling in Tfh cells needs to counter-balance the strong inhibitory signals delivered by bystander B cells through programmed cell death-ligand 1 (PD-L1) by binding to PD-1 on T cells (Shi et al., 2018). This leads to an enrichment of highly activated CD4<sup>+</sup> T cells within GCs that possess potent B cell helper abilities. The correct localization of Tfh cells in the LZ of the GC (Breitfeld et al., 2000; Kelsoe, 1996), seems to be vital for their proper function (Greczmiel et al., 2017). GC positioning is generally achieved through downregulation of chemokine receptors that mediate migration towards the T cell or the B cell zone, such as CCR7, PSGL-1, Sphingosine 1-phosphate receptor 1 (S1PR1) or Epstein-Barr virus-induced G-protein coupled receptor 2 (EBI2), respectively (Qi, 2016; Suan et al., 2015; Vinuesa and Cyster, 2011). This is additionally enforced through increased levels of molecules that sense GC factors (CXCR5, CXCR4) (Allen et al., 2004; Cyster et al., 2000; Elsner et al., 2012).

In the dark zone (DZ), B cells divide and introduce mutations into their BCR through the process of SHM (Victora et al., 2012; Victora et al., 2010). Subsequently, they migrate into the LZ and test their edited BCRs for improved antigen binding and compete for selection signals from Tfh cells (Haynes et al., 2007; Victora et al., 2010). While B cells that have lost the potential to bind antigens enter apoptosis, B cells with moderate affinities are likely to re-enter the DZ to undergo additional cycles of mutation and selection. High affinity B cells, in contrast, differentiate into PCs or memory cells (Shinnakasu and Kurosaki, 2017; Suan et al., 2017). This is believed to be determined by the duration of the T-B cell interaction (Ise et al., 2018). In order to form conjugates that are stable for up to 60 min (Haynes et al., 2007), GC Tfh cells exhibit high expression of receptors of the signaling lymphocyte activation molecule (SLAM) family, which bind to other SLAM family members on GC B cells, and also of the intracellular adaptor molecule signaling lymphocytic activation molecule-associated protein (SAP) (Cannons et al., 2010; Qi et al., 2008). SAP antagonizes the inhibitory effect of SLAM family 6 (SLAMF6) and thereby allows an ongoing interaction between T and B cells (Kageyama et al.,

2012) during which they exchange co-stimulatory signals and secrete cytokines. Pivotal for complete GC Tfh cell differentiation is the migration into GCs followed by an exact positioning within the LZ and the establishment of stable cell-cell contacts with B cells.

#### 4.2.2.3. Molecular regulation

##### 4.2.2.3.1. Co-stimulation and post-transcriptional regulation

Since the discovery and characterization of Tfh cells, a number of molecular determinants that control Tfh cell differentiation were described. Interestingly, many of these molecules converge on the phosphoinositide 3-kinase (PI3K)-serine/threonine-protein kinase (Akt) signaling pathway, which is vital for Tfh cells (Gigoux et al., 2009; Rolf et al., 2010). T cell co-stimulation results in PI3K activation and subsequent induction of the Akt and mammalian target of rapamycin (mTOR) signaling (Chi, 2012). Co-stimulation via ICOS and CD28 are both indispensable for GC formation (Dong et al., 2001; Ferguson et al., 1996; Mittrucker et al., 1999; Tafuri et al., 2001) and Tfh cell induction (Choi et al., 2011; Wang et al., 2015b). Although they have largely overlapping functions (Hutloff et al., 1999; Rudd and Schneider, 2003) they play different roles in Tfh cell development and are involved in different phases. Furthermore, ICOS is the more potent inducer of PI3K signaling compared to CD28 (Gigoux et al., 2009).

During the initial priming phase of naive CD4<sup>+</sup> T cells by DCs in the T cell zone, CD28 is the main co-stimulatory molecule; as DCs express high amounts of its ligands CD80 and CD86. Hence, CD28 deficiency abrogates Tfh cell induction (Weber et al., 2015). After the migration of early Tfh cells to the T-B cell border, antigen presentation and co-stimulation are taken over by B cells (Deenick et al., 2010), which express lower levels of CD28 ligands compared to DCs (Lenschow et al., 1993) but are highly positive for ICOSL (Liang et al., 2002). Continued ICOS stimulation on Tfh cells is important for maintaining the Tfh cell phenotype (Akiba et al., 2005; Baumjohann et al., 2013b; Tahiliani et al., 2017; Weber et al., 2015). ICOS expression levels are regulated by a variety of post-transcriptional mechanisms. The RNA-binding protein Roquin promotes the degradation of *Icos* and other Tfh-cell associated genes, such as *I $\delta$ ra* and *I $\delta$ st*, in CD4<sup>+</sup> T cells by recruiting the RNA decay machinery (Glasmacher et al., 2010). Upon strong TCR stimulation, Roquin is cleaved and its target transcripts accumulate, which represents a link between TCR stimulation strength and Tfh cell differentiation (Jeltsch et al., 2014; Vogel et al., 2013). Whether or not differentiating Tfh cells require strong TCR signals is still a matter of discussion. While several studies have shown that T cells with high affinity TCRs are more prone to give rise to Tfh cells (Fazilleau et al., 2009) others have reported opposing observations (Krishnamoorthy et al., 2017; Snook et al., 2018).

MicroRNAs (miRs) depict a second class of post-transcriptional regulators involved in several critical aspects of Tfh cell differentiation (Maul et al., 2019). For instance, mRNA levels of *Icos* and *Icosl* in Tfh and GC B cells, respectively, are regulated by miR146a (Pratama et al., 2015).

Beyond control on the transcript level, the strength of ICOS signaling can be dampened through the PI3K-inactivating phosphatases phosphatase and tensin homologue (PTEN) and PH domain leucine-rich repeat-containing protein phosphatase 2 (PHLPP2), which, in turn, are targeted by several members of the miR17~92 cluster (Baumjohann et al., 2013a; Kang et al., 2013). Successful induction of PI3K activity leads to the activation of several downstream signaling molecules. Among those are the mTOR complexes mTORC1 and mTORC2 that are both essentially involved in Tfh cell formation by promoting proliferation (Yang et al., 2016), glucose metabolism (Zeng et al., 2016) and the inactivation of the negative Tfh cell regulator forkhead box protein O1 (FOXO1) through the stimulation of Akt and itchy homolog E3 ubiquitin protein ligase (Itch) (Stone et al., 2015; Xiao et al., 2014).

#### 4.2.2.3.2. Transcription factor networks

TFs act as determinants of cellular identity by adjusting chromatin accessibility, imposing characteristic expression patterns and repressing inappropriate genes. T cell factor-1 (TCF-1), for instance, establishes the identity of T cells by opening up epigenetically silenced regions of chromatin in which T cell restricted genes are localized (Johnson et al., 2018). These patterns of accessible chromatin are maintained and are a requirement for T cell stability. The T cell fate is dictated by master regulators that act beyond these pioneering TFs, e.g. Tbet and GATA3 (Dong and Flavell, 2000).

Although the concept of exclusive master regulators holds true for certain cell types, a model of a network of co-operating and counteracting TFs might be more accurate for others. Transcriptional regulation of Tfh cells is complex and has been the subject of numerous studies (Liu et al., 2013). Nevertheless, it is not clear what the precise contributions of the individual factors are. They can be grouped based on their functions or phase-specific expression patterns. Lymphoid enhancer binding factor-1 (LEF-1) and TCF-1 belong to the class of early initiation factors and help to launch the Tfh cell differentiation program (Choi et al., 2015; Xu et al., 2015). Many aspects of LEF-1 and TCF-1 regulated gene expression support a strong and stable induction of *Bcl6* while preventing Blimp-1 driven T effector cell formation. This is achieved through direct binding and upregulation of genes encoding components of the Tfh-cell promoting IL-6 signaling pathway e.g. *Il6ra* and *Il6st*, *Icos* and *Bcl6* itself, and simultaneous repression of *Prdm1* (Choi et al., 2015). Nevertheless, even combined deficiency of both TCF-1 and LEF-1 is not sufficient to fully abrogate Tfh cell generation (Choi et al., 2015). Besides this prominent role in early Tfh cell differentiation, TCF-1 was also shown to be required to retain B cell helper abilities during the maintenance phase (Xu et al., 2015).

After successful *Bcl6* induction, Tfh cells migrate towards the T-B cell border, where they interact with B cells. This requires a change in the chemokine receptor repertoire and is controlled by *Bcl6*, achaete-scute homologue 2 (*Ascl2*) and Kruppel-like factor 2 (*Klf2*). *Klf2*

acts as a negative regulator of Tfh cell differentiation by repressing *Cxcr5* and promoting *Selplg* and *Ccr7* (Weber et al., 2015), which, in sum, enforces T cell zone localization. Due to the prior upregulation of ICOS on early Tfh cells, the expression of *Klf2* is potently silenced through downstream signaling events that are initiated by the ligation of ICOSL, resulting in the inactivation of the *Klf2* promoting factor FOXO1 (Weber et al., 2015). The *Cxcr5* locus thus becomes inducible for factors such as *Ascl2*, which was shown to directly bind to and upregulate its expression (Liu et al., 2014). Additionally, *Ascl2* also represses *Selplg* and *Ccr7*, thereby further stabilizing the Tfh cell-promoting chemokine receptor pattern. The importance of a complete and tight downregulation of CCR7 and PSGL-1 is emphasized by an additional direct repression of the respective mRNAs via *Bcl6* (Hatzi et al., 2015). To enter and exhibit effector functions in GCs, Tfh cells require high levels of ICOS (Shi et al., 2018; Xu et al., 2013), continued repression of T cell zone chemokine receptors (Haynes et al., 2007), additional downregulation of B cell zone chemokine receptors (Suan et al., 2015) and finally an upregulation of effector molecules, such as CD40L, IL-4 and IL-21 (Liu et al., 2015; Weinstein et al., 2016).

The TFs Maf and basic leucine zipper transcriptional factor ATF-like (Batf), which also play important roles in other subsets of Th cells, are associated with the expression of Tfh effector molecules IL-4, IL-21 and CD40L (Ise et al., 2011; Kroenke et al., 2012). These factors mediate the B cell helper function of GC Tfh cells to induce affinity maturation and PC differentiation in GC B cells (Crotty, 2014). Mechanistically, Batf acts upstream of Maf and induces its expression as well as that of *Bcl6* (Ise et al., 2011).

In general, TFs associated with Tfh cell differentiation serve one or more of four different purposes: repression of *Blimp-1* (TCF-1, *Bcl6*) (Choi et al., 2015; Crotty et al., 2010; Johnston et al., 2009; Xu et al., 2015), induction of Maf and/or Batf expression (*Bcl6*) (Kroenke et al., 2012; Vacchio et al., 2019), establishing and maintaining the Tfh cell chemokine repertoire (*Ascl2*, *Bcl6*) (Liu et al., 2014; Poholek et al., 2010) and upregulation of *Bcl6* (Batf, TCF-1) (Choi et al., 2015; Ise et al., 2011). Recently, T helper-inducing POZ/Krueppel-like factor (Thpok) was identified as an important transcriptional regulator and shown to have pleiotropic function in Tfh cells, i.e. repression of *Blimp-1*, upregulation of *Bcl6* and induction of Tfh cell effector genes (Vacchio et al., 2019). In conclusion, TCF-1, LEF-1 and Thpok install a stable induction of *Bcl6* while steadily repressing *Blimp-1*. Migration into the B cell follicle and GCs is promoted by an appropriate chemokine expression pattern, established and maintained by *Bcl6* and *Ascl2* and finally T cell help through Tfh cell effector molecules is mediated by Maf, Batf and Thpok.

### 4.3. The transcriptional repressor Bcl6

#### 4.3.1. Function, structure and cofactors of Bcl6

In contrast to the master regulators of other Th cell subsets, Bcl6 confers the Tfh cell transcription program by repressing instead of activating gene promoter activity. Within the immune cell compartment, Bcl6 is substantially expressed in Tfh cells, GC B cells and macrophages (Cattoretti et al., 1995; Johnston et al., 2009; Toney et al., 2000). Bcl6 is a member of the pox virus and zinc finger/bric-a-brac, tramtrack, broad complex (POZ/BTB) family of TFs. It comprises three domains: the BTB domain, the middle region and a DNA-binding domain. The latter consists of six zinc fingers and binds to specific DNA sequence motifs. The BTB domain is required for Bcl6 transcriptional activity (Ahmad et al., 2003) as it interacts with co-repressor complexes or recruits histone deacetylase complexes (HDACs) (Lemercier et al., 2002). By exchanging its co-repressor, Bcl6 can modulate its set of target genes, e.g. by interacting with AP1 or signal transducer and activator of transcription (STAT), Bcl6 can indirectly bind to the respective consensus sequences and suppress transcriptional activity (Hatzi et al., 2015). The Bcl6 middle domain harbors an additional interaction site for the binding of the co-repressor metastasis-associated protein 3 (MTA3) (Fujita et al., 2004). However, the primary function of this domain is to modulate protein stability and activity. It comprises three so-called PEST regions that are associated with rapid degradation upon phosphorylation (Rogers et al., 1986), indicating a short half-life of Bcl6 protein.

#### 4.3.2. The function and regulation of Bcl6 in B cell responses

Prior to the recognition of its central role in Tfh cell differentiation, the transcriptional repressor Bcl6 was mainly examined in the context of B cell biology. Herein, it was shown to be selectively expressed at the GC B cell stage where it inhibits DNA damage-induced apoptosis, which occurs during BCR affinity maturation through SHM (Phan et al., 2007). As a second function, Bcl6 prevents premature differentiation of GC B cells into memory or PCs (Basso and Dalla-Favera, 2012). Consequently, Bcl6 target genes comprise a set of DNA damage response genes (Ranuncolo et al., 2007; Ranuncolo et al., 2008) as well as factors promoting plasma or memory cell differentiation, such as Blimp-1 and IRF4 (Ci et al., 2009; Tunyaplin et al., 2004). Bcl6 transcription is induced by IRF8 in differentiating GC B cells (Lee et al., 2006) and exaggerated induction is prevented by autoregulation as Bcl6 binds to and represses its own promoter (Pasqualucci et al., 2003). When GC B cells are selected to become PCs, Bcl6 is downregulated through complementary mechanisms. BCRs with increased affinity for the antigen induce strong downstream signaling resulting in the activation of mitogen-activated protein kinase (MAPK), which phosphorylates Bcl6 leading to its proteasomal degradation (Niu et al., 1998). Selected GC B cell clones further obtain strong helper signals from Tfh cells through the CD40L-CD40 signaling axis. CD40L binding ultimately leads to the silencing of Bcl6 transcription through IRF4-mediated repression (Saito et al., 2007).

### 4.3.3. Bcl6 in Tfh cells

#### 4.3.3.1. Cell type-dependent functions of Bcl6

Overlapping functions of certain TFs in distinct cell types have been described (Liu et al., 2016a; Myles et al., 2017). Nevertheless, the mutual and essential function of Bcl6 in Tfh and GC B cells is still surprising, as the characteristics of the two cell types in the GC are very different. GC B cells are highly migratory and cycle between LZ and DZ where they proliferate strongly and mutate their BCR (Victoria et al., 2010). Tfh cells, in turn, are stationary in the LZ where they fulfill a control function by instructing the fate of GC B cells (Crotty, 2014). How Bcl6 achieves different functions in a cell-context dependent manner has been discussed in a previous chapter (see 4.3.). In an extensive study that analyzed the cistrome of Bcl6 in human GC Tfh cells using chromatin immunoprecipitation DNA-sequencing (ChIP-seq), it was found that Bcl6 binding motifs were only present in a fraction of the Bcl6 bound genes (Hatzi et al., 2015). Through physical association with other TFs, such as activator protein-1 (AP-1), Bcl6 is able to hijack its cofactors' DNA binding motifs to regulate different gene sets. This can be modulated in a cell-specific context and also explains how Bcl6 can fulfill profoundly different tasks in GC B cells (DNA damage tolerance) and Tfh cells (inhibition of alternative fates and migration) (Hatzi et al., 2013; Hatzi et al., 2015).

#### 4.3.3.2. The regulation of Bcl6 in CD4<sup>+</sup> T cells

Despite its central role in the regulation of Tfh cell differentiation, it is still not clear how Bcl6 expression is induced in naive CD4<sup>+</sup> T cells. *In vitro* stimulation of murine CD4<sup>+</sup> T cells with anti-CD3 and anti-CD28 in the presence of IL-6 yielded increased *Bcl6* mRNA without inducing Bcl6 protein levels (Eto et al., 2011). When naive CD4<sup>+</sup> T cells were first cultured in the presence of Th1 cell-polarizing conditions followed by a resting period, the IL-2 concentration in the media inversely correlated with Bcl6 protein levels (Oestreich et al., 2012). In fact, IL-2 signaling via STAT5 induced the Bcl6 antagonist Blimp-1 and resulted in lower Bcl6 levels (Johnston et al., 2012; Nurieva et al., 2012).

Most of the reported *in vitro* Tfh conditions include APCs for antigen presentation and co-stimulation (Lu et al., 2011). ICOS co-stimulation is indispensable for Tfh cell generation and leads to Bcl6 upregulation (Choi et al., 2011; Stone et al., 2015). ICOS appears to induce Bcl6 through distinct mechanisms that all depend on PI3K signaling. On the one hand ICOS-mediated PI3K stimulation leads to the activation of mTORC2, followed by stimulation of Akt, which then releases the inhibition of Bcl6 transcription through FOXO1 by promoting its nuclear exclusion and degradation (Stone et al., 2015). On the other hand, ICOS ligation results in the activation of the mTORC1 (Zeng et al., 2016). mTORC1 was linked to Bcl6 expression through the mTORC1-4E-BP-eIF4E axis that promotes Bcl6 translation (Yi et al., 2017). This finding was supported by several studies that reported a severe impairment of Tfh cell differentiation

in the absence of the mTORC1 adaptor protein Raptor (regulatory associated protein of mTOR) (Yang et al., 2016; Zeng et al., 2016). Moreover, ICOS signaling stimulates the nuclear translocation and binding of osteopontin (OPN) to Bcl6, thereby impeding its proteasomal degradation (Leavenworth et al., 2015). This highlights the complex and outstanding role of ICOS signaling in Tfh cell differentiation. Early after the administration of a TD antigen, Bcl6 appeared to be expressed in Tfh cells in two distinct waves (Baumjohann et al., 2011). Surprisingly, Bcl6 was observed to be downregulated after the peak of the GC response on day seven (Kitano et al., 2011).

#### 4.3.3.3. The role of Bcl6 in Tfh cells

The importance of Bcl6 as the master regulator of Tfh cells was recognized by several labs in parallel in 2009 (Johnston et al., 2009; Nurieva et al., 2009; Yu et al., 2009). CD4<sup>+</sup> T cells deficient for *Bcl6* are not able to upregulate the Tfh markers CXCR5 and PD-1 or to support GC responses (Johnston et al., 2009; Nurieva et al., 2009; Yu et al., 2009). Mice with a T cell-specific *Bcl6*-deletion are phenotypically normal, but are unable to mount a GC response upon immunization with a thymus-dependent (TD) antigen (Hollister et al., 2013).

It is still a conundrum how a transcriptional repressor alone is able to install the Tfh cell transcriptional program. A possible mode of action is that Bcl6 restrains the expression of factors that act as inhibitors of the Tfh cell gene program. These genes thereby become inducible and sensitive towards Tfh promoting factors. One prominent example is the TF *Klf2* that acts as a repressor of the Tfh hallmark chemokine receptor CXCR5 and activator of the Th1 genes *Ccr7* and *Selplg* (Lee et al., 2015; Weber et al., 2015). By repressing *Klf2*, Bcl6 enables the induction of *Cxcr5* transcription (Hatzi et al., 2015). In this setting, Bcl6 achieves upregulation of Tfh genes indirectly. In contrast, Bcl6 can also act directly on cell fate determinants of other Th cell subsets that are incompatible with Tfh cell differentiation. It was discovered that Bcl6 regulated the expression of genes from mainly two distinct modules, i.e. alternative cell fate decisions and Tfh cell migration. To enforce the stability of Tfh cells, Bcl6 prevents the expression of other master regulators from the Th1, Th2, Th17 and regulatory T cell (Treg) subsets as well as their accessory TFs, such as STAT1/STAT4 complexes (Th1) or STAT3 (Th17) (O'Shea et al., 2011). Even the components of the signaling pathways that would eventually result in the upregulation of these inappropriate TFs are inhibited. Prominent examples include receptors that sense the presence of characteristic cytokines, e.g. IL-2 by CD25 or IFN $\gamma$  by IFN gamma receptor 1 (IFNGR1), and downstream signaling transducers e.g. MAPK and mTOR.

Control of Tfh cell migration and localization through Bcl6 is achieved by a direct repression of several T cell (PSGL-1, CCR7) or B cell zone (EBI2) migratory receptors, which would impair GC entry (Hatzi et al., 2015). Moreover, repression of *Klf2* results in *Cxcr5* upregulation and

facilitates the entry into the follicle and GCs (Weber et al., 2015). Additionally, Bcl6 regulates the Tfh cell metabolic program by repressing several genes of the glycolysis pathway (Oestreich et al., 2014). Based on the current knowledge, it appears feasible to assume that the function of Bcl6 in established Tfh cells is to repress TFs and signaling components that are associated with other Th helper cell subsets, and additionally to maintain a suitable repertoire of migratory molecules compatible with GC localization. Nevertheless, Bcl6 does not directly promote the expression of crucial Tfh cell molecules and gene repression can also be achieved through long-lasting epigenetic modifications (Almouzni and Cedar, 2016). Indeed, Bcl6 was reported to interact with HDACs and alter chromatin accessibility (Lemercier et al., 2002; Yang and Green, 2019). Therefore, it seems feasible that Bcl6 might only be required during Tfh cell development to set up repressive histone marks that silence Tfh cell inappropriate genes. At later stages of the Tfh cell differentiation, continued Bcl6 expression might not be crucial.

#### 4.4. Tfh cell plasticity and maintenance

In the classical view of Th cell lineages, these can be distinguished by unique sets of secreted cytokines, exclusive expression of one master regulator and a stable lineage commitment. Tfh cells depict an exception as they fulfill neither of these criteria in a strict manner. The most abundantly secreted cytokines are IL-4 and IL-21, which are also produced by Th2 and Th1 cells, respectively. Beyond that, Tfh cells in viral infections also secrete the Th1 cytokine IFN $\gamma$  (Yusuf et al., 2010). Although Bcl6 clearly marks Tfh cells, other master regulators, such as Tbet (Yusuf et al., 2010) or forkhead box protein 3 (Foxp3) (Chung et al., 2011; Linterman et al., 2011) can be co-expressed. Thirdly, Tfh cells are associated with a high degree of plasticity (Cannons et al., 2013). *Ex vivo* Tfh cells can be polarized *in vitro* to increase Th1, Th2 or Th17 cytokine expression (Lu et al., 2011). Even fully differentiated Tfh cells maintain positive histone marks at the IFN $\gamma$ , IL-4 and IL-17 loci. Further, a study reported that Tfh cells were the source of pathogenic Th2 cells in the context of an allergy model (Ballesteros-Tato et al., 2016). This flexibility of Tfh cells appears quite logical in the light of their functionality. In contrast to Th1, Th2 and Th17 responses, which rarely coincide, Tfh cells act complementary by promoting antibody responses, compatible with other T effector cell function. In viral infections, Th1 and Tfh cells act jointly (Yusuf et al., 2010). While Th1 cells activate and support innate immune cells and CTLs (Suresh et al., 2005), Tfh cells orchestrate GC responses.

Despite the high degree of plasticity, Tfh cells are fate committed and their phenotype is maintained during primary and secondary immune responses (Choi et al., 2013b; Hale et al., 2013). Although studies addressing the early phase of Tfh cell formation prevail, some factors that contribute to the maintenance of Tfh cells have been previously identified. The stability of adoptively transferred, established Tfh cells strongly depends on continued antigen availability and the presence of GC B cells (Baumjohann et al., 2013b). When co-stimulation through ICOS

or TNF receptor superfamily member 4 (Ox40) is blocked, Tfh cell maintenance is strongly impaired (Akiba et al., 2005; Baumjohann et al., 2013b; Tahiliani et al., 2017; Weber et al., 2015). The importance of co-stimulation for Tfh cell maintenance was most extensively studied for ICOS. One explanation how ICOS enables Tfh cell stability is by enhancing Bcl6 expression, which involves increased *Bcl6* transcription (Stone et al., 2015; Xiao et al., 2014) and translation (Yi et al., 2017). Additionally, ICOS signaling via the TANK-binding kinase 1 (TBK1) is critical for GC Tfh cells and GC development while early Tfh cell differentiation is unaffected (Pedros et al., 2016).

Although a sound understanding of the TF networks that operate in early Tfh cells was elaborated, deeper insights into the transcriptional regulation of Tfh cell maintenance are scarce. While TCF-1 deficiency in naive CD4<sup>+</sup> T cells almost completely abrogated Tfh cell differentiation, induced-deletion at later timepoints did not affect the phenotype, but significantly impaired the functionality of Tfh cells (Xu et al., 2015). Furthermore, in the setting of an acute viral infection, Tbet is essential to maintain Tfh cell numbers by promoting proliferation and limiting apoptosis (Wang et al., 2019).

## 5. Aim of the thesis

The humoral and cellular branches of the adaptive immune system are required to clear pathogens that escape the control by the innate system. Humoral immunity is controlled by Tfh cells through their potent B cell helper abilities, which determine type, affinity and longevity of antibody responses. The induction of protective antibodies together with memory formation are the foundation of efficacious vaccines. Nevertheless, aberrant Tfh cell functions can also contribute to the formation and progression of diseases such as autoimmunity and cancer.

Targeting Tfh cells to harness their potential in vaccinations or restrain their actions in diseases, requires a deep understanding of how established Tfh cells function and what cell-intrinsic and extrinsic cues they rely on. Despite the broad knowledge about the molecular regulation of Tfh cell formation and development, an adequate understanding of Tfh cell maintenance is still missing. To address this issue, the first aim of the present work was to establish a functional system that enables the temporally-controlled deletion of genes in CD4<sup>+</sup> T cells. As several tamoxifen-inducible CreERT2 mouse strains were available, two fundamentally different *Cd4-CreERT2* alleles were compared in terms of efficiency, congruence with Cre reporter alleles and potential off-target effects.

The central aim of the thesis was the utilization of the inducible knock-out (KO) system to systematically analyze the impact of an acute loss of the Tfh cell hallmark molecules CXCR5 (**Fig. 2**) and Bcl6 (**Fig. 3**) in pre-formed Tfh cells. As the chemokine receptor CXCR5 is an important mediator of Tfh cell migration, it was vital for this aim to examine if Tfh cell localization

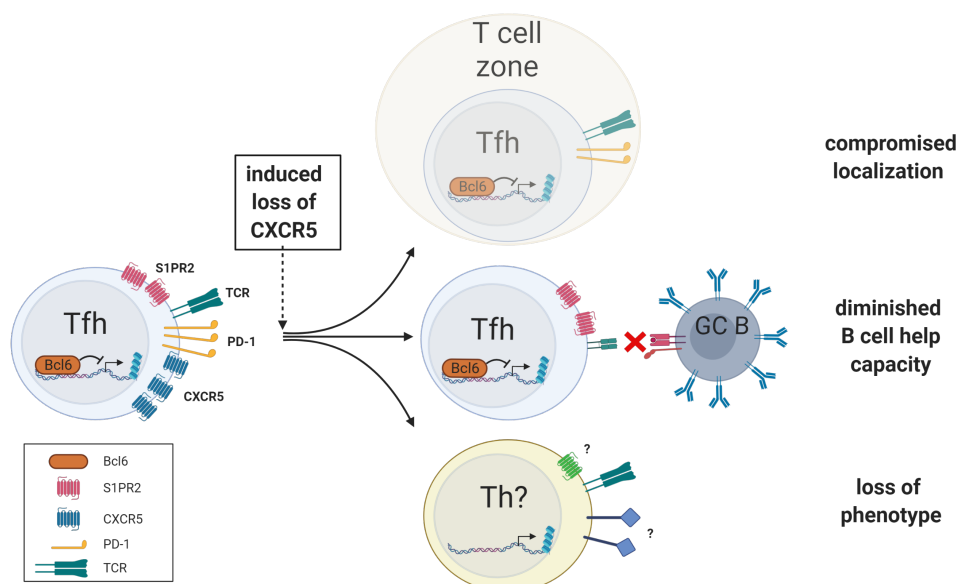


**Figure 2: Hypotheses for the impact of an induced loss of CXCR5 on preformed Tfh cells.** In the absence of CXCR5, Tfh cell migration could be compromised and result in a defective localization (top). Alternatively, the GC B cell helper functions might be diminished (middle). Finally, CXCR5-deficiency may destabilize the phenotype and cause a loss of Tfh cell markers.

was compromised by the deletion (**Fig. 2, top**). Alternatively, the induced loss of CXCR5 might attenuate Tfh cell B cell helper capabilities (**Fig. 2, middle**). As the anatomical site is a determining factor for Tfh cells, it was further explored if *Cxcr5*-ablation had an effect on the stability of the Tfh cell phenotype (**Fig. 2, bottom**).

Additionally, the impact of an induced loss of *Bcl6* in established Tfh cells was examined. Owing to its function as a transcriptional repressor, the focus here was to assess changes in the Tfh cell-characteristic gene expression upon *Bcl6*-ablation (**Fig. 3, top**). Further, B cell helper functions were investigated, as they might be affected by alterations in the synthesis of Tfh cell effector molecules (**Fig. 3, middle**). Despite the important role of Bcl6 in Tfh cell development, it is also feasible that Bcl6 is not required for the maintenance of established Tfh cells (**Fig. 3, bottom**).

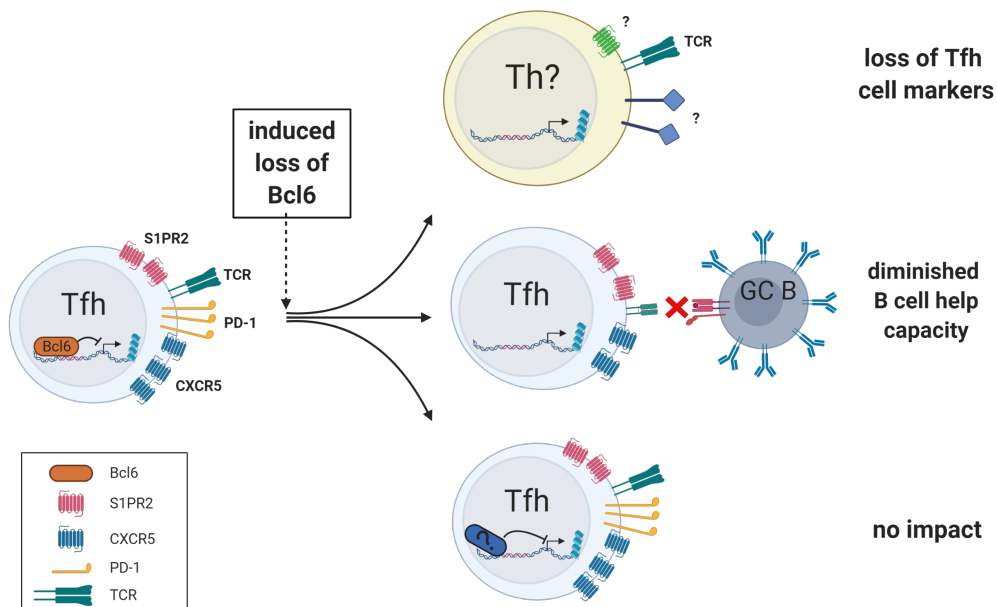


**Figure 3: Hypotheses for the impact of an induced loss of Bcl6 on preformed Tfh cells.** In the absence of Bcl6, Tfh cells might lose characteristic marker expression (top). Alternatively, the capacity to interact with GC B cells might be compromised (middle). As a third scenario, Tfh cells might not be affected by the loss of Bcl6 and continue to maintain the phenotype (bottom).

## 6. Materials and Methods

## 6.1. Resources tables

## 6.1.1. Mice

Strain	Source	Identifier
<i>Bcl6</i> <sup>Δ7-9</sup> ( <i>Bcl6</i> <sup>tm1.1Dent</sup> )	The Jackson Laboratory	JAX #023727
<i>Bcl6</i> <sup>Δ5-10</sup> ( <i>Bcl6</i> <sup>tm1.1Mamu</sup> )	Markus Müschen (Geng et al., 2015)	n/a
C57BL/6	Charles River or Janvier Laboratories	n/a
CD45.1 (Ptprc <sup>a</sup> Pepc <sup>b</sup> /BoyJ)	The Jackson Laboratory	JAX #002014
<i>Cd4-CreERT2</i> knock-in ( <i>CD4</i> <sup>tm1(CreERT2)ThBu</sup> )	Thorsten Buch (Sledzinska et al., 2013)	n/a
<i>Cd4-CreERT2</i> transgenic ( <i>Tg(Cd4-cre/ERT2)11Gnri/J</i> )	The Jackson Laboratory	JAX #022356
<i>Cxcr5</i> <sup>Ffl/fl</sup> ( <i>Cxcr5</i> <sup>tm1.Namt</sup> )	Neil Mabbott (Bradford et al., 2017)	n/a
<i>Rosa26</i> <sup>fl-Stop-fl-eYFP</sup> ( <i>Gt(ROSA)26Sor</i> <sup>tm1(eYFP)Cos</sup> )	The Jackson Laboratory	JAX #006148
SMARTA ( <i>Tg(TcrLCMV)1Aox/PpmJ</i> )	The Jackson Laboratory	JAX #030450
B6.Cg-Cd4 <sup>tm1(cre/ERT2)Thbu</sup> - <i>Cxcr5</i> <sup>tm1.Namt</sup>	This work	n/a
B6.Cg-Tg(TcrLCMV)Aox-Ptprc <sup>a</sup> Pepc <sup>b</sup> -Cd4 <sup>tm1(cre/ERT2)Thbu</sup>	This work	n/a
B6.Cg-Tg(TcrLCMV)Aox-Ptprc <sup>a</sup> Pepc <sup>b</sup> -Cd4 <sup>tm1(cre/ERT2)Thbu</sup> - <i>Cxcr5</i> <sup>tm1.1Namt</sup>	This work	n/a
B6.Cg-Cd4 <sup>tm1(cre/ERT2)Thbu</sup> - <i>Gt(ROSA)26Sor</i> <sup>tm1(EYFP)Cos</sup>	This work	n/a
B6.Cg-Cd4 <sup>tm1(cre/ERT2)Thbu</sup> - <i>Bcl6</i> <sup>tm1.1Dent</sup> - <i>Gt(ROSA)26Sor</i> <sup>tm1(EYFP)Cos</sup>	This work	n/a
B6.Cg-Tg(TcrLCMV)Aox-Ptprc <sup>a</sup> Pepc <sup>b</sup> -Cd4 <sup>tm1(cre/ERT2)Thbu</sup> - <i>Gt(ROSA)26Sor</i> <sup>tm1(EYFP)Cos</sup>	This work	n/a
B6.Cg-Tg(TcrLCMV)Aox-Ptprc <sup>a</sup> Pepc <sup>b</sup> -Cd4 <sup>tm1(cre/ERT2)Thbu</sup> - <i>Bcl6</i> <sup>tm1.1Dent</sup> - <i>Gt(ROSA)26Sor</i> <sup>tm1(EYFP)Cos</sup>	This work	n/a

## 6.1.2. Virus

Name	Source	Identifier
LCMV Armstrong	In house (Dutko and Oldstone, 1983)	n/a

## 6.1.3. Flow cytometry reagents

Antigen	Source	Identifier
7-AAD	Thermo Fisher Scientific	Cat# 00-6993-50
<i>Bcl6</i> (K112-91)	BD Biosciences	Cat# 561522 (PE); Cat# 561525 (AF647)
CD4 (GK1.5)	BIOTREND	Cat# C1637-100 (DyLight® 550)

Materials and methods

<b>Antigen</b>	<b>Source</b>	<b>Identifier</b>
CD4 (RM4-5)	BioLegend	Cat# 100531 (Pacific Blue); Cat# 100559 (BV510)
CD4 (RM4-5)	BD Biosciences	Cat# 740208 (BUV395)
CD16/CD32	BD Biosciences	Cat# 562896 (BV421)
CD16/CD32	BioLegend	Cat# 101302 (purified)
CD19 (6D5)	BioLegend	Cat# 115540 (BV605); Cat# 115546 (BV510); Cat# 115521 (AF488)
CD38 (90)	BioLegend	Cat# 102717 (PE-Cy7); Cat# 102729 (PE/Dazzle 594)
CD44 (IM7)	BioLegend	Cat# 103026 (AF700)
CD45.1 (A20)	BioLegend	Cat# 110713 (APC); Cat# 110741 (BV510); Cat# 10706 (FITC)
CD45.2 (104)	Thermo Fisher Scientific	Cat# 11-0454 (FITC)
CD45.2 (104)	BD Biosciences	Cat# 560697 (V450)
CD62L (MEL-14)	Tonbo Biosciences	Cat# 60-0621-U100 (PE-Cy7)
CD86 (GL1)	BD Biosciences	Cat# 564200 (BV650)
CD95 or Fas (JO2)	BD Biosciences	Cat# 557653 (PE-Cy7); Cat# 740367 (BV605)
CD138 (281-2)	BD Biosciences	Cat# 558626 (APC)
CD162 or PSGL-1 (2PH1)	BD Biosciences	Cat# 563448 (BV510)
CD164 or CXCR4 (2B11)	Thermo Fisher Scientific	Cat# 48-9991-80 (eF450)
CD185 or CXCR5 (L138D7)	BioLegend	Cat# 145509 (Biotin)
CD197 or CCR7 (4B12)	Thermo Fisher Scientific	Cat# 17-1971-82 (APC)
CD274 or PD-1 (29F.1A12)	BioLegend	Cat# 135231 (BV711)
CD274 or PD-1 (5E7)	Thermo Fisher Scientific	Cat# 61-9985 (PE-eF610)
CD274 or PD-1 (J43)	Thermo Fisher Scientific	Cat# 12-9985-82 (PE)
CD357 or GITR (DTA-1)	BD Biosciences	Cat# 563390 (BV711)

Materials and methods

<b>Antigen</b>	<b>Source</b>	<b>Identifier</b>
Fixable Viability Dye eFluor 780	Thermo Fisher Scientific	Cat# 65-0865-14
Foxp3 (FJK-16s)	Thermo Fisher Scientific	Cat# 25-5773-82 (PE-Cy7); Cat# 53-5773-82 (AF488)
GATA3 (TWAJ)	Thermo Fisher Scientific	Cat# 46-9966-42 (PerCP-eF710)
GL7 (GL-7)	BioLegend	Cat# 144605 (AF647)
I-A(b) CLIP-control PVSKMRMATPLLMQA Tetramer	NIH Tetramer Core Facility	Cat# n/a (BV421)
I-A(b) LCMV GP <sub>66-77</sub> DIYKGVYQFKSV tetramer	NIH Tetramer Core Facility	Cat# n/a (BV421)
IgD (11-26c.2a)	BD Biosciences	Cat# 563618 (BV786)
IgD (11-26c.2a)	BioLegend	Cat# 405718 (AF488)
IgG1 (A85-1)	BD Biosciences	Cat# 562580 (BV421); Cat# 553443 (FITC)
IgG2a/c (R19-15)	BD Biosciences	Cat# 553388 (Biotin)
Mouse/rat serum	Thermo Fisher Scientific	Cat# 31881
NP <sub>28</sub> -PE or 4-hydroxy-3-nitrophenylacetyl hapten conjugated to phycoerythrin (PE)	Biosearch Technologies	Cat# N-5070 (PE)
RORgt (Q31-378)	BD Biosciences	Cat# 564723 (BV786)
SLAM (TC15-12F12.2)	BioLegend	Cat# 115931 (BV650)
Streptavidin	BioLegend	Cat# 405207 (APC); Cat# 405204 (PE)
Tbet (4B10)	Thermo Fisher Scientific	Cat# 25-5825-82 (PE-Cy7)
Tbet (4B10)	BioLegend	Cat# 644817 (BV605)

6.1.4. Chemicals, Peptides and Proteins

<b>Name</b>	<b>Source</b>	<b>Identifier</b>
2-mercaptoethanol	Sigma-Aldrich	Cat# M6250
Agarose	Applchem	Cat# A8963
Albumin Fraktion V	Carl Roth	Cat# 8076.3
Corn oil	Sigma-Aldrich	Cat# C8267
dNTPs (100 mM each)	ThermoFisher Scientific	Cat# R0182
Dulbecco's PBS (w/o Mg <sup>2+</sup> , w/o Ca <sup>2+</sup> )	Gibco	Cat# 14190144
Ethanol, absolute	Applchem	Cat# A1613
Exonuclease I	NEB	Cat# M0293

Materials and methods

<b>Name</b>	<b>Source</b>	<b>Identifier</b>
Fluoromount G	Thermo Fisher Scientific	Cat# 00-4958-02
Guanidine hydrochloride	Sigma-Aldrich	Cat# G3272
IGEPAL CA-630	Sigma Aldrich	Cat# I8896
Imject Alum	Thermo Fisher Scientific	Cat# 77161
Maxima H Minus Reverse Transcriptase	Thermo Fisher Scientific	Cat# EP0753
NP <sub>24</sub> -KLH or 4-hydroxy-3-nitrophenylacetyl conjugated to keyhole limpet hemocyanin	Biosearch Technologies	Cat# N-5060
NP-SM-MSA or 4-hydroxy-3-nitrophenylacetyl conjugated to LCMV-GP <sub>61-80</sub> bound to mouse serum albumin	Andreas Hutloff (Vu Van et al., 2016)	n/a
Phusion HF buffer	NEB	Cat# B0518S
Polyethylene glycol 8000	Sigma Aldrich	Cat# 89510
Proteinase K solution	Ambion	Cat# AM2546
RNasin Plus RNase Inhibitor	Promega	Cat# N2615
Sodium Chloride, NaCl	Sigma Aldrich	Cat# S5150-1L
Tamoxifen	Sigma-Aldrich	Cat# T5648
Taq Polymerase	NEB	Cat# M0273S
Terra PCR Direct Polymerase Mix	Takara Bio	Cat# 639287
Tissue-Tek O.C.T. Compound	Sakura Finetek	Cat# SA62550-01
Trizma hydrochloride solution 1M, pH 8.0	Sigma Aldrich	Cat# T2694
UltraPure DNase/RNase-Free Distilled Water	Thermo Fisher Scientific	Cat# 10977-049

6.1.5. Critical commercial assays

<b>Name</b>	<b>Source</b>	<b>Identifier</b>
CD4 <sup>+</sup> T cell Isolation Kit, mouse	Miltenyi Biotec	Cat# 130-104-454
CleanNGS	CleanNA	Cat# CNGS-0050
EasySep Mouse Naive CD4 <sup>+</sup> T cell Isolation Kit	STEMCELL Technologies	Cat# 19765
Foxp3 / Transcription Factor Staining buffer set	Thermo Fisher Scientific	Cat# 00-5523-00
High Sensitivity DNA Analysis Kits	Agilent Technologies	Cat# 5067-4626
MinElute Gel Extraction Kit	Qiagen	Cat# 28606
MinElute PCR Purification Kit	Qiagen	Cat# 28004
Nextera XT DNA Sample Preparation Kit	Illumina	Cat# FC-131-1024 and Cat# FC-131-1001
Quant-iT PicoGreen dsDNA Assay Kit	ThermoFisher Scientific	Cat# P11496
SensiFAST Probe No-ROX One-Step Kit	Bioline	Cat# BIO-76001

## 6.1.6. Primers and oligonucleotides

Name	Source	Identifier
PrimeTime primer: <i>Bcl6</i>	IDTDNA	Assay ID: Mm.PT.58.117896 6; FAM
PrimerTime primer: <i>Actb</i>	IDTDNA	Assay ID: Mm.PT.58.332573 76.gs; HEX
PrimeTime primer: genomic <i>Bcl6</i> F: 5'-ACCACTGACCCAGAGGATTA-3' R: 5'- GCTTCAAATCCCAGCAAAGG -3'; FAM	IDTDNA	Custom
PrimeTime primer: genomic <i>Cxcr5</i> F: 5'-ACATCCTGGTGCTGGTAATC-3' R: 5'- ACTAAGAGAAGGTTCGGCTACT-3' HEX;	IDTDNA	Custom
Random Hexamers (50µM)	ThermoFisher Scientific	Cat# N8080127
External 186.2 5'-GCTGTATCATGCTCTTCTTG-3'	IDTDNA (McHeyzer-Williams et al., 1991)	Custom
External Cy1 5'-GGATGACTCATCCCAGGGTCA CCATGGAGT-3'	IDTDNA (McHeyzer-Williams et al., 1991)	Custom
Internal 186.2 5'-GGTGTCCTCCAGGTCCA-3'	IDTDNA (McHeyzer-Williams et al., 1991)	Custom
Internal Cy1 5'-CCAGGGGCCAGTGGATAGAC-3'	IDTDNA (McHeyzer-Williams et al., 1991)	Custom
Barcoded adapter E3V6NEXT (2µM) TruGrade 5'-Biotin-ACACTCTTTCCCTACACGACGCTCTTC CGATCT[BC6][UMI10][T30]VN-3'	IDTDNA	Custom
Template switching oligo E5V6NEXT (100µM) HPLC 5'ACACTCTTTCCCTACACGACGCrGrGrG-3'	IDTDNA	Custom
SINGV6 (10µM) 5'-Biotin-ACACTCTTTCCCTACACGACGC-3'	IDTDNA	Custom
P5NEXTPT5 (5 µM) AATGATACGGCGACCCAGAGATCTACACTCT TTCCCTACACGACGCTCTTCCG*A*T*C*T*	IDTDNA	Custom
i7 Index Primer (5 µM) TruGrade CAAGCAGAAGACGGCATAACGAGAT[i7]GTCTCG TGGGCTCGG	Eurogentec/IDTDNA	Custom

## 6.1.7. Custom solutions and buffers

Name	Components
Bead binding buffer	22% PEG (w/v), NaCl 1M, Tris-HCl 1mM, Igepal 0.01% (v/v) in UltraPure DNase/RNase-Free Distilled Water
Flow cytometry blocking solution	1% (v/v) anti-CD16/32, 2% normal mouse serum, 2% normal rat serum in flow cytometry staining buffer
Flow cytometry staining buffer	2% FBS, 2mM EDTA in DPBS
IHC blocking buffer	1.5% bovine serum albumin, 5% normal mouse serum in DPBS
IHC staining buffer	1.5% bovine serum albumin in Dulbecco's PBS

## Materials and methods

qPCR lysis buffer	0.2% (v/v) Phusion HF buffer in UltraPure DNase/RNase-Free Distilled Water
RNA-seq lysis buffer	5M Guanidine HCl, 1% (v/v) 2-mercaptoethanol, 0.2% (v/v) Phusion HF buffer in UltraPure DNase/RNase-Free Distilled Water

### 6.1.8. Consumables

Name	Source	Identifier
96-Well, Non-Treated, U-Shaped-Bottom Microplate	Falcon	Cat #351177
E-Gel EX Agarose Gels, 2%	Thermo Fisher Scientific	Cat# G402002
5ML polypropylene round bottom tubes	Falcon	Cat# 352063
96-well plate, conical, polystyrene	Sarstedt	Cat# 82.1583.001
twin.tec PCR Plate 96 LoBind, skirted	Eppendorf	Cat# EP0030129512
DNA LoBind Tubes 1.5mL	Eppendorf	Cat# EP0030108051

### 6.1.9. Instruments

Name	Source
BD LSRFortessa	BD Biosciences
BD FACSAria Fusion	BD Biosciences
BD FACSCanto II	BD Biosciences
LightCycler 480	Roche Diagnostics
Agilent 2100 Bioanalyzer	Agilent Technologies
Leica CM1950	Leica Biosystems
ProFlex 96-Well-PCR-System	Thermo Fisher Scientific
Sorvall Legend XT Centrifuge	Thermo Fisher Scientific
Zeiss Microscope 471202	Carl Zeiss Microscopy
HiSeq 1500	Illumina
E-Gel iBase Power System	Thermo Fisher Scientific
Olympus BX41 fluorescence microscope	Olympus

### 6.1.10. Deposited data

Name	Source	Identifier
RNA-Sequencing data	This work	GEO: GSE142229

### 6.1.11. Software and algorithms

Name	Source
Biorender	<a href="http://biorender.com">http://biorender.com</a> ; personal license
Complex Heatmaps	(Gu et al., 2016)
Cowplot	<a href="https://github.com/wilkelab/cowplot/">github.com/wilkelab/cowplot/</a>
DESeq2	(Love et al., 2014)
FACSDiva	BD Biosciences
FlowJo software	TreeStar
Ggplot2	(Wickham, 2016)
ImageJ	<a href="https://imagej.net">https://imagej.net</a>
Light Cycler 480 SW 1.5.1	Roche
Prism 8	GraphPad
STAR 2.6.0a	(Dobin et al., 2013)
zUMIs	(Bagnoli et al., 2018)

## 6.2. Methods

### 6.2.1. Mice

All mice used in this work are listed in the table in 6.1.1. For adoptive transfer experiments, the respective mouse lines were bred with lymphocytic choriomeningitis virus (LCMV) glycoprotein<sub>61-80</sub> (GP<sub>61-80</sub>)-specific TCR-transgenic (Tg) SMARTA mice (Oxenius et al., 1998) and CD45.1 alleles. All Mice were held under specific pathogen free conditions in individually ventilated cages. Experiments involving mice were performed in accordance with Federal Law and European Regulation and approved by the Regierung von Oberbayern. Experimentally used mice were 8-12 weeks of age. Experimental groups were age and sex-matched.

### 6.2.2. Immunizations, adoptive cell transfers, infections, and tamoxifen treatment

For immunizations, 4-hydroxy-3-nitrophenylacetyl conjugated to keyhole limpet hemocyanin (NP<sub>24</sub>-KLH) or 4-hydroxy-3-nitrophenylacetyl and SMARTA peptide GP<sub>61-80</sub> bound to mouse serum albumin (NP-SM-MSA) was mixed 1:1 with Imject Alum adjuvant and rotated for 45min at room temperature (RT) prior to immunization. Mice were anesthetized by isoflurane inhalation and 10µg of antigen was injected subcutaneously (s.c.) into the hock of each hind limb using an insulin syringe. For adoptive cell transfers of SMARTA cells into wildtype (WT) hosts, naive CD4<sup>+</sup> T cells were isolated from LNs and spleens of SMARTA mice through negative selection using the EasySep Mouse Naive CD4<sup>+</sup> T cell isolation kit. For most experiments, 1x10<sup>4</sup> naive SMARTA cells were washed and resuspended in PBS and subsequently transferred into WT recipients by tail vein injection. 24-72h later, 2x10<sup>5</sup>pfu LCMV Armstrong were injected intraperitoneally (i.p.) in 200µL plain RPMI media without supplements. For the retransfer experiment, 0.5x10<sup>6</sup> naive SMARTA cells were adoptively transferred into WT recipient mice to yield sufficient cells on day 4 for the transfer into secondary hosts. 24h later the recipients were injected i.p. with 1x10<sup>6</sup>pfu LCMV Armstrong, a 5x higher viral load, to account for the higher number of transferred cells. Th1 and Tfh cells that had differentiated from the transferred CD45.1/1 *Cd4-CreERT2<sup>+</sup>Bcl6<sup>ΔΔ</sup>* and CD45.1/2 *Cd4-CreERT2<sup>+</sup>Bcl6<sup>+/+</sup>* SMARTA cells were sorted as CXCR5<sup>-</sup>PSGL-1<sup>hi</sup> and CXCR5<sup>+</sup>PSGL-1<sup>lo</sup>, respectively, into PBS including 2% FCS. The sorted cells were washed with PBS twice and quantified. 2x10<sup>4</sup> Tfh or Th1 cells of both genotypes were co-transferred into infection-matched secondary WT recipients. On the two days following the adoptive co-transfer, recipient mice were given tamoxifen for a total of four times. For immunizations with NP-SM-MSA, 0.3x10<sup>6</sup> naive SMARTA cells were transferred into WT recipients by tail vein injection, followed by immunization with NP-SM-MSA. Conditional genetic deletions in CD4<sup>+</sup> T cells were induced by administering tamoxifen to CD4<sup>tm1(CreERT2)ThBu</sup> and Tg(*Cd4-cre/ERT2*)11*Gnri/J* mice. These mice express a CreERT2 fusion protein that translocates to the nucleus when tamoxifen is present and subsequently mediates gene excision. Tamoxifen for mouse injections was prepared by dissolving in 100% Ethanol at a concentration of 1g/ml. Then, corn oil was added

to obtain a concentration of 33.3mg/ml, followed by incubation at 56°C in a water bath until tamoxifen was fully dissolved. Aliquots were stored at -20°C and thawed freshly for each round of injections. Mice were given 5mg of tamoxifen in 150µl volume by oral gavage twice daily (morning and afternoon) on two consecutive days.

### 6.2.3. Flow cytometry

Spleens or LNs prepared from euthanized mice were collected and kept in PBS on ice. The tissues were minced between the frosted ends of glass slides to obtain single-cell suspensions. Live-dead discrimination was achieved using 7-AAD for surface marker analyses or with the fixable viability dye eFluor780 for intracellular stainings. Fc receptors were blocked prior to fluorophore-conjugated antibody staining for 5min at 4°C with flow cytometry blocking solution (see 6.1.7.). The table in chapter 6.1.3. contains the antibodies that were used in this work. The antibodies were incubated with the cells in flow cytometry staining buffer (see 6.1.7.). For the staining of CXCR5, biotinylated anti-CXCR5 was added together with the other antibodies. After two washes with staining buffer, the cells were incubated with streptavidin conjugated to APC or PE for 15min on ice (Baumjohann and Ansel, 2015). Intracellular stainings were performed with the Foxp3 Transcription Factor Staining Buffer Set. Fixation was conducted for 15 min at RT. NP-specific B cells were identified by bound NP-PE (conjugation ratio 28:1). When analyzing the polyclonal LCMV-specific response in mice, LCMV-specific cells were identified with specific tetramers. To this end, the cells were incubated with I-A(b) LCMV GP<sub>66-77</sub> tetramer or a human CLIP peptide-containing negative control conjugated to BV421. Samples were acquired on a three-laser BD FACSCanto II or a 5-laser BD LSRFortessa. Cell sorting was performed on a BD FACSAria Fusion using the 70µm nozzle. Data analysis was conducted using FlowJo software.

### 6.2.4. Immunohistology

Draining LNs from immunized mice were embedded in OCT Tissue Tek in plastic molds and frozen on top of a mixture of isopropanol and dry ice and subsequently stored at -80°C. Cryosections were cut at 7-9µm on a cryostat, dried and stored at -80°C until antibody staining. After fixation in acetone for 10min at -20°C, the slides were dried, rehydrated in PBS and then blocked with immunohistochemistry (IHC) blocking buffer for 30min at RT in PBS. After blocking, the slides were stained with CD16/32-BV421, IgD-AF488, CD4-Dylight550, GL7-AF647 in IHC staining buffer for 1h at RT. After three washes with PBS, the slides were dried for 5min and then mounted using Fluoromount G. Images of antibody-stained tissue sections were acquired on an Olympus BX41 fluorescence microscope. For the quantification of CD4<sup>+</sup> T cells and their location within GCs, such GCs were chosen that showed an accumulation of GL7<sup>+</sup> GC B cells and also an established network of CD16/32<sup>+</sup> follicular dendritic cells (FCDs), allowing the discrimination of LZ and DZ. Using ImageJ, the GC was drawn as a region of

interest (ROI) around areas containing of GL7<sup>+</sup> GC B cells and CD16/32<sup>+</sup> FDCs. Then the LZ ROI was drawn around areas containing CD16/32<sup>+</sup> FDCs. The DZ ROI was marked by GL7<sup>+</sup> GC B cells without infiltrating CD16/32<sup>+</sup> FDCs. CD4<sup>+</sup> cells within the DZ and LZ ROIs were manually marked and automatically counted using ImageJ. The area of the GC was also calculated by the software.

#### 6.2.5. Quantitative Real-Time qPCR analysis

Real-Time quantitative Polymerase Chain Reaction (qPCR) was used to quantify the deletion of *Bcl6* in genomic DNA (gDNA) and mRNA. 200-500 Tfh cells (CXCR5<sup>+</sup> PD-1<sup>+</sup>) cells were sorted into the wells of a 96 well LightCycler 480 Multiwell plate containing 5µl qPCR lysis buffer (see 6.1.7.). A proteinase K digest was conducted at 55°C for 10min to remove cell debris. This was followed by desiccation at 95°C for 10min with an open lid and without sealing of the plate to reduce the volume and inactivate proteinase K. For the quantification of *Bcl6* mRNA, total RNA was subsequently reverse transcribed into cDNA using the SensiFast One-Step Real-Time PCR kit. Expression was then measured by qPCR using PrimeTime gene expression probes for exons 6-7 of *Bcl6* and the housekeeper *Actb* (see 6.1.6). For *Bcl6*-deletion in gDNA, the reverse transcriptase step was omitted and custom PrimeTime probes for genomic *Bcl6* as well as the control gene *Cxcr5* were utilized. The expression was measured on a LightCycler 480 device. Analysis was done using the Delta C(T) method (Livak and Schmittgen, 2001).

#### 6.2.6. SHM analysis

Day 3+4 tamoxifen-treated *Bcl6*<sup>+/+</sup> and *Bcl6*<sup>Δ/Δ</sup> mice that had been immunized with NP-KLH/alum (see 6.2.2.) were sacrificed on day 14. Single NP-specific GC B cells from the drainings LNs were sorted as live CD19<sup>+</sup>IgD<sup>lo</sup>Fas<sup>hi</sup>IgG1<sup>+</sup>NP<sup>+</sup>CD4<sup>-</sup> lymphocytes in 96-well plates containing qPCR lysis buffer (see 6.1.7). Plates were spun down and frozen on dry ice. Proteinase K digest was conducted at 55°C for 10min, followed by desiccation at 95°C for 10min with an open lid without sealing. Immediately after desiccation, the reverse transcription mix was added, containing 2mM dNTPs, 12U/µl Maxima H Minus reverse transcriptase, 10µM random hexamer primers, 1U RNasin Ribonuclease Inhibitor and incubated for at 42°C for 90min. The total volume of the reaction was 10µl. To specifically amplify the VH186 region, PCR was performed using 2.5µL of the obtained cDNA with Taq polymerase for 39 cycles at 54°C using the primers External 186.2 and External Cy1 (see 6.1.6). The obtained PCR product was diluted 1:30 in nuclease-free water and 1µL was used as input for a nested PCR. The second PCR was performed with Taq polymerase for 29 cycles using the primers Internal 186.2 and Internal Cy1 (see 6.1.6). PCR products were visualized using 1% agarose gels and positive clones were purified using the MinElute PCR purification kit and sent to Eurofins for sequencing using the internal Cy1 primer. Mutations in the sequences were identified by

blasting against the mouse germline anti-NP antibody IgH chain V186.2 gene (M60252, IGMT). Specifically, the reported high-affinity substitutions W33L and R59K were quantified (Allen et al., 1988; Cumano and Rajewsky, 1986; Xiong et al., 2012).

#### 6.2.7. RNA-sequencing

For RNA-sequencing (RNA-seq) analysis, 1,000-2,000 cells were sorted into a 96-well plate containing 50µl RNA-seq lysis buffer (see 6.1.7.) using a BD FACSAria Fusion cell sorter. After sorting, the plate was briefly centrifuged and frozen on dry ice. cDNA was then generated using a modified version of the single-cell RNA-seq protocol mcSCRB (Bagnoli et al., 2018). Cellular components were removed via proteinase K digest at 55°C for 10min, followed by an inactivation step at 75°C for 10min. Nucleic acids from the cell lysate were then bound to polyethyleneglycol (PEG)-beads, washed twice with 80% ethanol and DNA was digested on the beads using DNase I for 10min at RT. Subsequently, DNase was inactivated for 5min at 65°C and beads were washed twice with 80% ethanol followed by elution and resuspension in the reverse transcription mix. The mix contained 12.5mM dNTPs, 7.5% PEG, 2U/µl Maxima H Minus reverse transcriptase, 2µM template switch oligo E5V6NEXT, 0.2µM barcoded oligo-dT primers E3V6NEXT and was incubated with the beads for 90 min at 42°C. Afterwards, the beads were removed using a magnetic stand and the remaining primers were digested with exonuclease I at 37°C for 20min, followed by heat inactivation at 80°C for 10min. cDNA was amplified using Terra polymerase for 17 cycles. After bead purification, cDNA was quantified using Quant-iT PicoGreen dsDNA Assay Kit and the size distribution was analyzed on an Agilent 2100 Bioanalyzer using a high-sensitivity DNA chip. Samples with a distribution between 500bp–6000kb were tagmented with the Nextera XT DNA Library Preparation Kit using 0.8ng cDNA for 10min at 55°C. 0.1µM Custom i5 primers (P5NEXTPT5) were used for the enrichment of 3' ends of tagmented cDNA together with individual i7 index primers. The generated libraries were size-selected between 300-900bp on a 2% agarose E-Gel, followed by extraction using the MinElute Gel Extraction Kit. Libraries were sequenced paired-end on high-output flow cells of an Illumina HiSeq 1500 instrument at LAFUGA Genomics (LMU Munich). The first read sequenced sixteen bases to obtain cellular barcodes from the barcoded oligo-dT primer and the second read sequenced 50 bases of the cDNA fragment. Additionally, a third read contained 8 bases to obtain the i7 barcode. All primer sequences are listed in 6.1.6.

Processing and analysis of the raw data and ensuing analysis of the obtained RNA-seq data, including visualization was performed by Johannes Bagnoli. First, raw fastq data was processed with zUMIs (Parekh et al., 2018), followed by mapping to the mouse reference genome (mm10) using STAR 2.6.0a (Dobin et al., 2013). Ensembl gene annotations were used (GRCm38.75). The i7 index was used to identify the respective samples and where it was

feasible the cellular barcode additionally used to confirm the identity. For both, phred filtering allowed 2 bases below 20bases. The generated count matrices were used for gene expression analysis conducted in R. Rarely detected genes were filtered out via unique molecular identifiers (UMI) per genes and also overall detection in all samples (>1 UMI). Libraries normalization and identification of differentially expressed genes was done using DESeq2 (Love et al., 2014). All plots were generated using cowplot and ggplot2.

#### 6.2.8. Data availability

The sequencing data that support the findings of this study have been deposited in GEO with the accession code GSE142229.

#### 6.2.9. Statistical analysis

Statistical analyses were performed with Prism 8 and are specified in each corresponding figure legend.

## 7. Results

### 7.1. The impact of CD4<sup>+</sup> T cell-specific *Cxcr5*-ablation on the GC response

#### 7.1.1. An inducible Cre recombinase elicits a *Cxcr5* KO with high efficiency in CD4<sup>+</sup> T cells

To assess the requirements of hallmark Tfh cell markers in established Tfh cells, it was vital to establish a system for the temporally-guided ablation of genes specifically in CD4<sup>+</sup> T cells. This can be accomplished using tamoxifen-inducible Cre recombinase systems. Due to reported differences in the efficiency of some of these systems (Becher et al., 2018; Kurachi et al., 2019), two mouse strains were compared, which differ in the strategies that were used to obtain Cre expression in a CD4<sup>+</sup> T cell-specific manner. One mouse line was generated through random integration of a transgene comprising the *Cd4* promoter and the *CreERT2* coding sequence into the genome (Aghajani et al., 2012). This mouse is referred to as CreTg here. In the second strain, the *CreERT2* sequence was knocked-in (KI) directly into the endogenous *Cd4* locus and will therefore be called CreKI (Sledzinska et al., 2013). First, we bred the two lines with mice bearing a *Rosa26*<sup>fl-stop-fl-eYFP</sup> Cre activity reporter allele (Srinivas et al., 2001). Expression of enhanced yellow fluorescent protein (eYFP) from the ubiquitous *Rosa26* locus is only induced upon Cre-mediated excision of a stop cassette. Subsequently, we crossed in a conditional *Cxcr5* allele (Bradford et al., 2017), yielding *Cd4*<sup>CreTg</sup>*Cxcr5*<sup>fl/fl</sup> and *Cd4*<sup>CreKI</sup>*Cxcr5*<sup>fl/fl</sup> inducible KO mice and the respective controls, *Cd4*<sup>CreTg</sup>*Cxcr5*<sup>+/+</sup> and *Cd4*<sup>CreKI</sup>*Cxcr5*<sup>+/+</sup>, which express Cre, but lack the floxed allele. Upon tamoxifen administration, *Cxcr5* is deleted through Cre mediated recombination specifically in CD4<sup>+</sup> T cells.

In a pilot experiment we immunized mice with the model antigen NP-KLH in the adjuvant alum (NP-KLH/alum), which induces the formation of Tfh cells and a T-cell dependent B cell response. On day 3+4 after immunization, tamoxifen was applied orally via gavage two times per day (**Fig. 4a**). On day 10 after immunization, Cre efficiency was assessed based on the expression of the eYFP Cre activity reporter allele and the frequency of cells that had lost CXCR5 protein expression relative to control mice. Here, it became apparent that CreTg mice (**Fig. 4b; upper and lower panel**) showed higher frequencies of cells expressing eYFP compared to CreKI (**Fig. 4c; upper and lower panel**). As eYFP<sup>+</sup> expression identifies cells that have experienced Cre mediated recombination, we first analyzed the CXCR5 KO with respect to the eYFP signal. Additionally, as CXCR5 is only expressed upon activation of CD4<sup>+</sup> T cells, we pre-gated on activated CD44<sup>hi</sup> CD4<sup>+</sup> T cells. In line with the function as Cre reporter, CXCR5<sup>+</sup> cells were almost completely absent in the eYFP<sup>+</sup> fraction in both the Tg and the KI Cre mice (**Fig. 4b,c; lower panel, lower row**). Surprisingly, CXCR5 was also efficiently abrogated in eYFP<sup>-</sup> cells from *Cd4*<sup>CreKI</sup>*Cxcr5*<sup>fl/fl</sup> mice, while the eYFP<sup>-</sup> fraction in the *Cd4*<sup>CreTg</sup>*Cxcr5*<sup>fl/fl</sup> mice was only mildly affected (**Fig. 4b,c; lower panel, upper row**). Besides an apparent difference in the overlap of recombination at the *Rosa26* and the *Cxcr5* locus, we

additionally observed a striking deviation in the activation status of the CD4<sup>+</sup> T cells among Cre reporter-positive cells of the two different strains. The eYFP<sup>+</sup> population of the Tg mice contained only 5-7% activated CD44<sup>hi</sup> CD4<sup>+</sup> T cells, which is an approximate 6-fold reduction compared to the eYFP<sup>+</sup> fraction (**Fig. 4b; upper and lower panel**). This effect was independent of the presence of the floxed *Cxcr5* allele, as it occurred equally in *Cd4<sup>CreTg</sup>Cxcr5<sup>+/+</sup>* and *Cd4<sup>CreTg</sup>Cxcr5<sup>fl/fl</sup>* mice. To a much lower extent, this phenomenon could also be observed in the KI strain (**Fig. 4c; upper and lower panel**). Nevertheless, the total frequency of activated CD4<sup>+</sup> T cells in the CreTg mouse was similar to that observed in the KI strain (**Fig. 4d**). However, as activated cells are the mediators of immune responses, an underrepresentation of CD44<sup>hi</sup> CD4<sup>+</sup> T cells within the population that effectively acquired the KO is problematic. In contrast, CXCR5 was efficiently abrogated in both eYFP<sup>-</sup> and eYFP<sup>+</sup> fractions, indicating that the *Cd4<sup>CreKI</sup>Cxcr5<sup>fl/fl</sup>* mouse depicted a suitable tool to study the effect

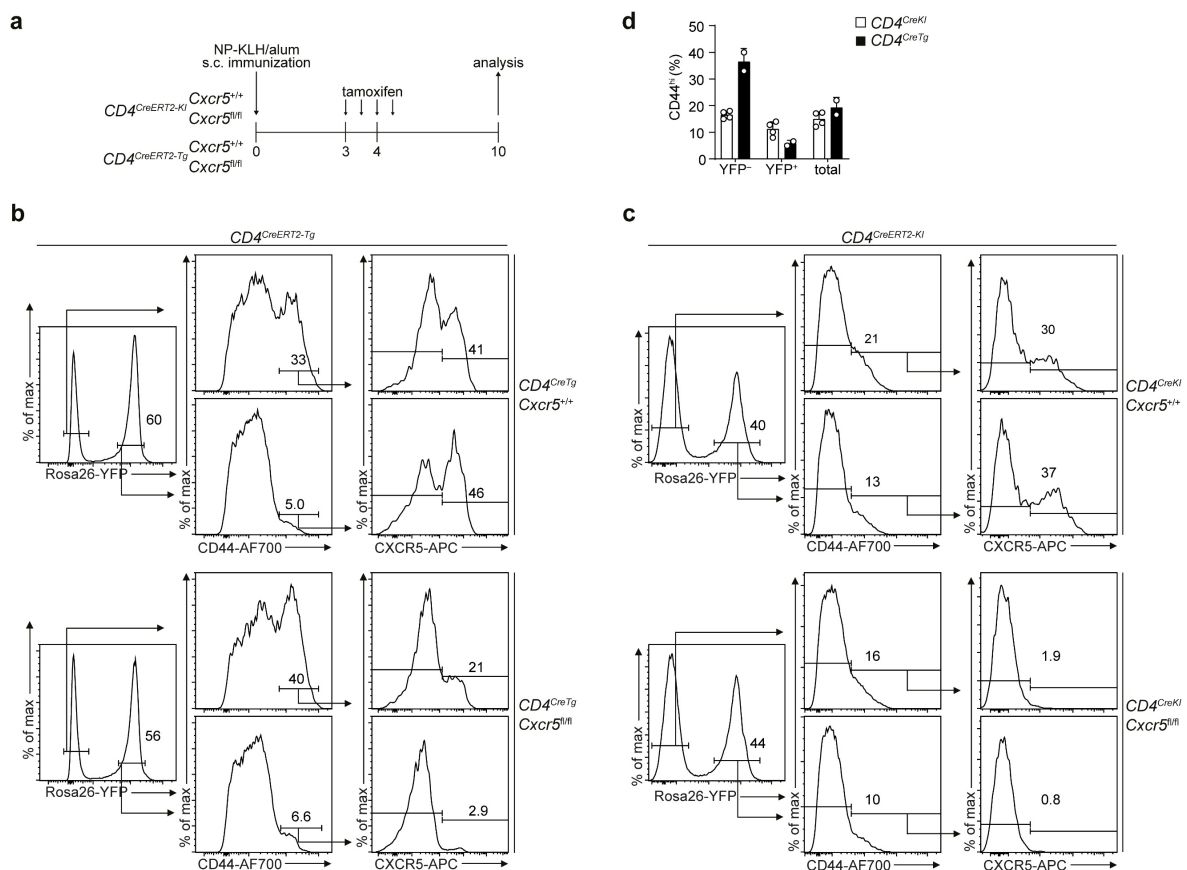


**Figure 4: Tamoxifen-inducible *Cd4-CreERT2* mouse strains differ in recombination efficiency, congruence with reporter-alleles, and activation status.** **a** Experimental scheme for the comparison of two tamoxifen-inducible *Cd4-CreERT2* strains after immunization with NP-KLH/alum. **b** Flow cytometry of CD4<sup>+</sup> T cells from draining LNs of *Cd4<sup>CreTg</sup>Cxcr5<sup>+/+</sup>* and *Cd4<sup>CreTg</sup>Cxcr5<sup>Δ/Δ</sup>* mice on day 10. Cells were pre-gated as live CD4<sup>+</sup>CD19<sup>-</sup> lymphocytes; further gating on YFP<sup>+</sup>/YFP<sup>-</sup> or CD44<sup>hi</sup> cells is indicated by arrows. Gate frequencies indicate percent of eYFP<sup>+</sup>, CD44<sup>hi</sup> or CXCR5<sup>+</sup> cells. **c** Flow cytometry of CD4<sup>+</sup> T cells from draining LNs of *Cd4<sup>CreKI</sup>Cxcr5<sup>+/+</sup>* and *Cd4<sup>CreKI</sup>Cxcr5<sup>Δ/Δ</sup>* mice as in (b). **d** Quantification of flow cytometry data from (b+c), CD44<sup>hi</sup> cells among YFP<sup>-</sup>, YFP<sup>+</sup> and total CD4<sup>+</sup> T cells in *Cd4<sup>CreTg</sup>* or *Cd4<sup>CreKI</sup>* mice. Each symbol represents an individual mouse ( $n(Cd4<sup>CreTg</sup>) = 2$ ;  $n(Cd4<sup>CreKI</sup>) = 4$ ). The data are representative of two independent experiments.

## Results

of an acute loss of CXCR5 in pre-formed Tfh cells and will hereafter be referred to as  $iCxcr5^{\Delta/\Delta}$  (inducible *Cxcr5* KO). For this reason, the CreKI strain was used throughout the thesis for the generation of inducible KOs of *Cxcr5* and *Bcl6*. Moreover, we did not continue to use the *Rosa26<sup>fl-stop-fl-eYFP</sup>* allele in the ensuing experiments.

To further validate the inducible KO system, we first tried to reproduce and confirm previous results described with constitutive *Cxcr5*-deficient  $CD4^+$  T cells (Arnold et al., 2007; Haynes et al., 2007) by applying tamoxifen 2 days prior to immunization (**Fig. 5a**). Strikingly, this yielded an almost complete KO of CXCR5 expression in  $CD4^+$  T cells on day 7 (**Fig. 5b**), with close to a 100% deletion efficiency, which is rare for induced KOs (Becher et al., 2018). GC B cells were also examined, as their quantities can be regarded as a measure of Tfh cell help and functionality. Despite the comprehensive absence of both  $CXCR5^+PD-1^{lo/int}$  Tfh and  $CXCR5^{hi}PD-1^{hi}$  GC Tfh cells, GC B cell frequencies were only intermediately affected in the order of a two-fold reduction (**Fig. 5c; upper row**). Additionally, GC B cells also exhibited a slight decrease in the fraction of class-switched  $IgG1^+$  cells (**Fig. 5c; lower row**). Both, the 50% reduction in GC B cell frequencies and also lower frequencies of class-switched cells were in agreement with earlier studies (Arnold et al., 2007; Haynes et al., 2007). This demonstrated that the combination of the CreKI strain with the conditional *Cxcr5* allele mirrored previous findings with *Cxcr5*-deficient  $CD4^+$  T cells and hence enabled the assessment of the impact on the GC reaction per se.

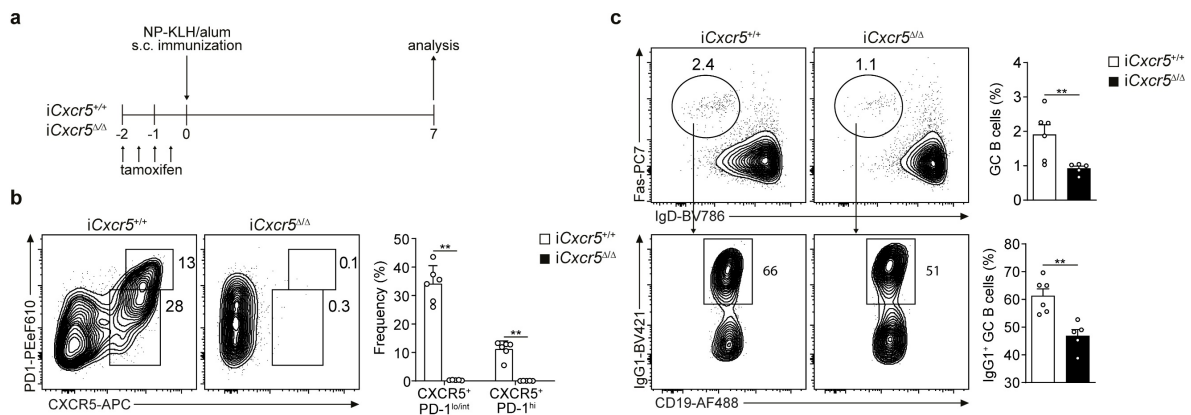


**Figure 5: Tamoxifen-induced *Cxcr5*-ablation prior to GC induction mirrors effects seen with constitutive *Cxcr5*-deficient  $CD4^+$  T cells.** **a** Experimental scheme for the analysis of the impact of tamoxifen-induced and T-cell specific deletion of *Cxcr5* prior to immunization with NP-KLH/alum. **b** Flow cytometry of  $CD4^+$  T cells from draining LNs of  $iCxcr5^{+/+}$  and  $iCxcr5^{\Delta/\Delta}$  mice on day 7. Cells were pre-gated as live  $CD4^+CD44^{hi}CD19^-$  lymphocytes. Gate frequencies indicate percent of  $CXCR5^+PD-1^{int/lo}$  Tfh and  $CXCR5^{hi}PD-1^{hi}$  GC Tfh cells. Quantification of the results (right panel); each symbol represents an individual mouse ( $n = 5-6$ ). **c** Flow cytometry and quantification of B cells from draining LNs as in (b). Cells were pre-gated as live  $CD19^+CD4^-$  lymphocytes (upper row) or live  $CD19^+CD4^-IgD^{lo}Fas^{hi}$  lymphocytes (lower row). Gate frequencies indicate percent of  $IgD^{lo}Fas^{hi}$  GC B cells (upper row) and  $IgG1^+$  class-switched GC B cells (lower row). \*\* $P < 0.01$  two-tailed nonparametric Mann-Whitney test (b, c); mean + s.e.m. in b, c.

### 7.1.2. *Cxcr5*-ablation in early and mature Tfh cells shows minor effects on T and B cell responses

In the previous experiments we established the *iCxcr5*<sup>Δ/Δ</sup> mouse as a suitable tool to analyze the impact of an acute loss of CXCR5 in established Tfh cells. As a next step, *Cxcr5* was deleted during different phases of the GC response. To this end, tamoxifen was administered on day 3+4, depicting an early timepoint after GC induction and in a second group on day 6+7, when the GC reaches its peak (**Fig. 6a**). Similar to the earlier experiments, almost no CXCR5-expressing Tfh and GC Tfh cells were present on day 14, regardless of the timing of KO induction (**Fig. 6b**). Surprisingly, in both settings, a CXCR5<sup>-</sup> population was present that expressed high Tfh cell-characteristic levels of PD-1 (**Fig. 6b**). The frequencies were in the same ranges as in their CXCR5<sup>+</sup> counterpart (**Fig. 6b; upper and lower stats**). Moreover, an analysis of the TF levels upon *Cxcr5*-ablation showed that CXCR5<sup>-</sup> cells even expressed Bcl6 (**Fig. 6c**). Subsequently, we analyzed the frequencies of GC B cells to quantify the impact on the B cell response. Despite the acute loss of *Cxcr5* from CD4<sup>+</sup> T cells, the GC response was only moderately affected (**Fig. 7a**). At the earlier ablation timepoint, we observed a trend towards a diminished fraction of GC B cells, while the effect was more evident for the later

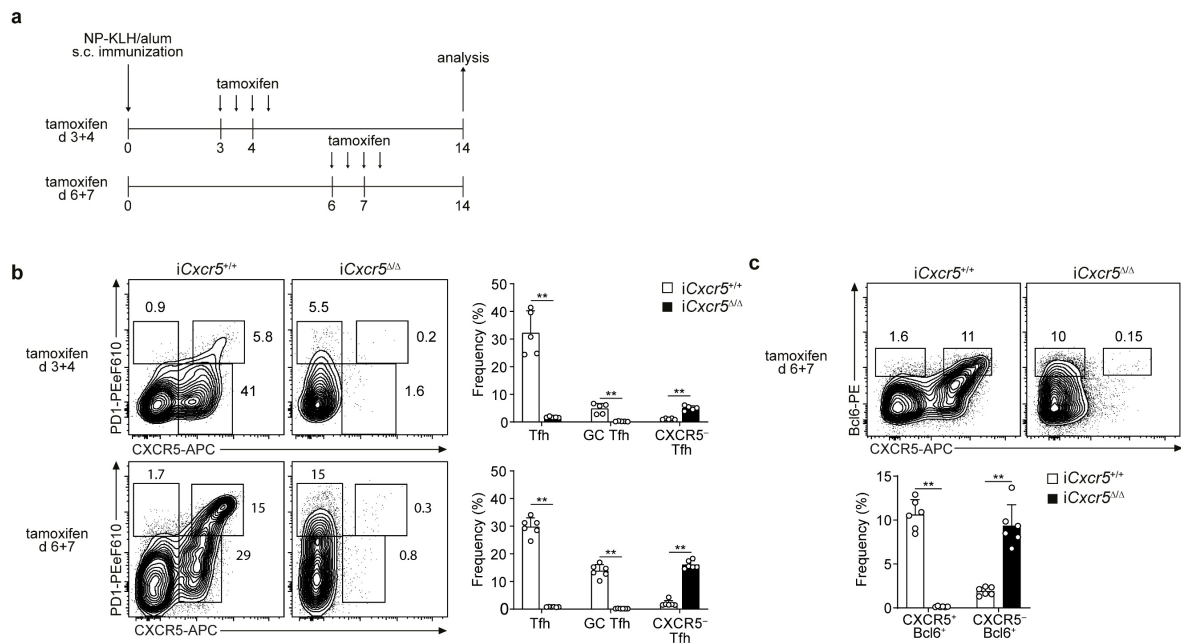


**Figure 6: Continued expression of Tfh cell markers upon T cell-specific deletion of *Cxcr5*.** **a** Experimental scheme for the analysis of the impact of tamoxifen-induced and T-cell specific deletion of *Cxcr5* after immunization with NP-KLH/alum (s.c.). **b** Flow cytometry of CD4<sup>+</sup> T cells from draining LNs of *iCxcr5*<sup>+/+</sup> and *iCxcr5*<sup>Δ/Δ</sup> mice treated with tamoxifen on day 3+4 (upper row) or day 6+7 (lower row) and subsequent analysis on day 14. Cells were pre-gated as live CD4<sup>+</sup>CD44<sup>hi</sup>CD19<sup>-</sup> lymphocytes. Gate frequencies indicate percent of CXCR5<sup>-</sup>PD-1<sup>hi</sup> cells, CXCR5<sup>hi</sup>PD-1<sup>hi</sup> GC Tfh cells and CXCR5<sup>+</sup>PD-1<sup>lo/int</sup> Tfh. Quantification of the results (right panel); each symbol represents an individual mouse (n = 5-6). **c** Intracellular flow cytometry and quantification of CD4<sup>+</sup> T cells as in (b). Gate frequencies indicate percent of CXCR5<sup>-</sup>Bcl6<sup>+</sup> cells and CXCR5<sup>hi</sup>Bcl6<sup>+</sup> GC Tfh cells (n = 6). \*\*P < 0.01 two-tailed nonparametric Mann-Whitney test (b, c); mean + s.e.m. in b, c.

## Results

timepoint (**Fig. 7a**). Tfh cells do not only regulate the abundance of GC B cells, but they also affect isotype class-switching and antigen-specificity of the GC B cells (De Silva and Klein, 2015; Shulman et al., 2014). Nevertheless, the frequencies of both, IgG1<sup>+</sup> and NP<sup>+</sup> GC B cells were not affected by the loss of CXCR5 (**Fig. 7b**). Additionally, IgG1<sup>+</sup>NP<sup>+</sup> cells that later give rise to PCs, were also unaffected. In conclusion, the effects of early versus late ablation of *Cxcr5* were comparable. For the following experiments we focused on the early timepoint of tamoxifen gavage to allow a longer time for the establishment of potential effects in response to the elimination of *Cxcr5* from CD4<sup>+</sup> T cells.

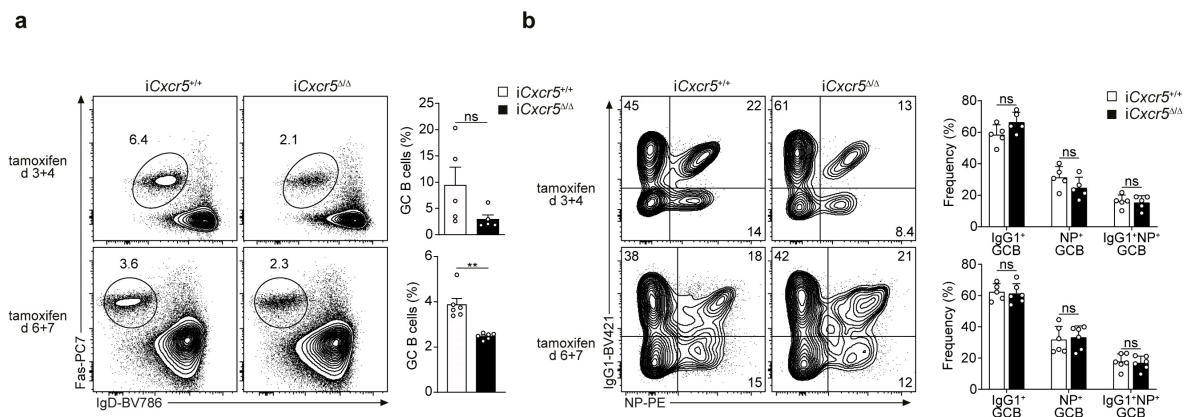


**Figure 7: Decreased GC B cells, but normal class-switching and selection of antigen-specific cells upon loss of CXCR5.** Mice were immunized with NP-KLH/alum (s.c.), treated with tamoxifen and analyzed on day 14. **a** Flow cytometry of B cells from draining LNs of *iCxcr5*<sup>+/+</sup> and *iCxcr5*<sup>ΔΔ</sup> mice treated with tamoxifen on day 3+4 (upper row) or day 6+7 (lower row) and subsequent analysis on day 14. Cells were pre-gated as live CD19<sup>+</sup>CD4<sup>-</sup> lymphocytes. Gate frequencies indicate percent of IgD<sup>lo</sup>Fas<sup>hi</sup> GC B cells. Quantification of the results (right panel); each symbol represents an individual mouse (n = 5-6). **b** Flow cytometry and quantification of B cells as in (b). Cells were pre-gated as live CD19<sup>+</sup>CD4<sup>-</sup>IgD<sup>lo</sup>Fas<sup>hi</sup> lymphocytes. Gate frequencies indicate percent of IgG1<sup>+</sup>NP<sup>-</sup>, IgG1<sup>+</sup>NP<sup>+</sup>, and IgG1<sup>-</sup>NP<sup>+</sup> GC B cells. \*\*P < 0.01, ns = not significant, two-tailed nonparametric Mann-Whitney test (a, b); mean + s.e.m. in a, b.

### 7.1.3. Loss of the preferential CD4<sup>+</sup> T cell LZ localization in the absence of CXCR5

The results from our previous experiments suggested that *Cxcr5*-ablation in established CD4<sup>+</sup> T cells did not impair the expression of important Tfh cell molecules, such as PD-1 and Bcl6, and did also not strongly impede their B cell helper capacities. As CXCR5 is considered the major chemokine receptor that mediates recruitment into follicles and GCs, we next investigated the localization of the *Cxcr5*-ablated CD4<sup>+</sup> T cells. After immunization with NP-KLH/alum, the KO was induced on day 3+4 and histological analyses were conducted on LN

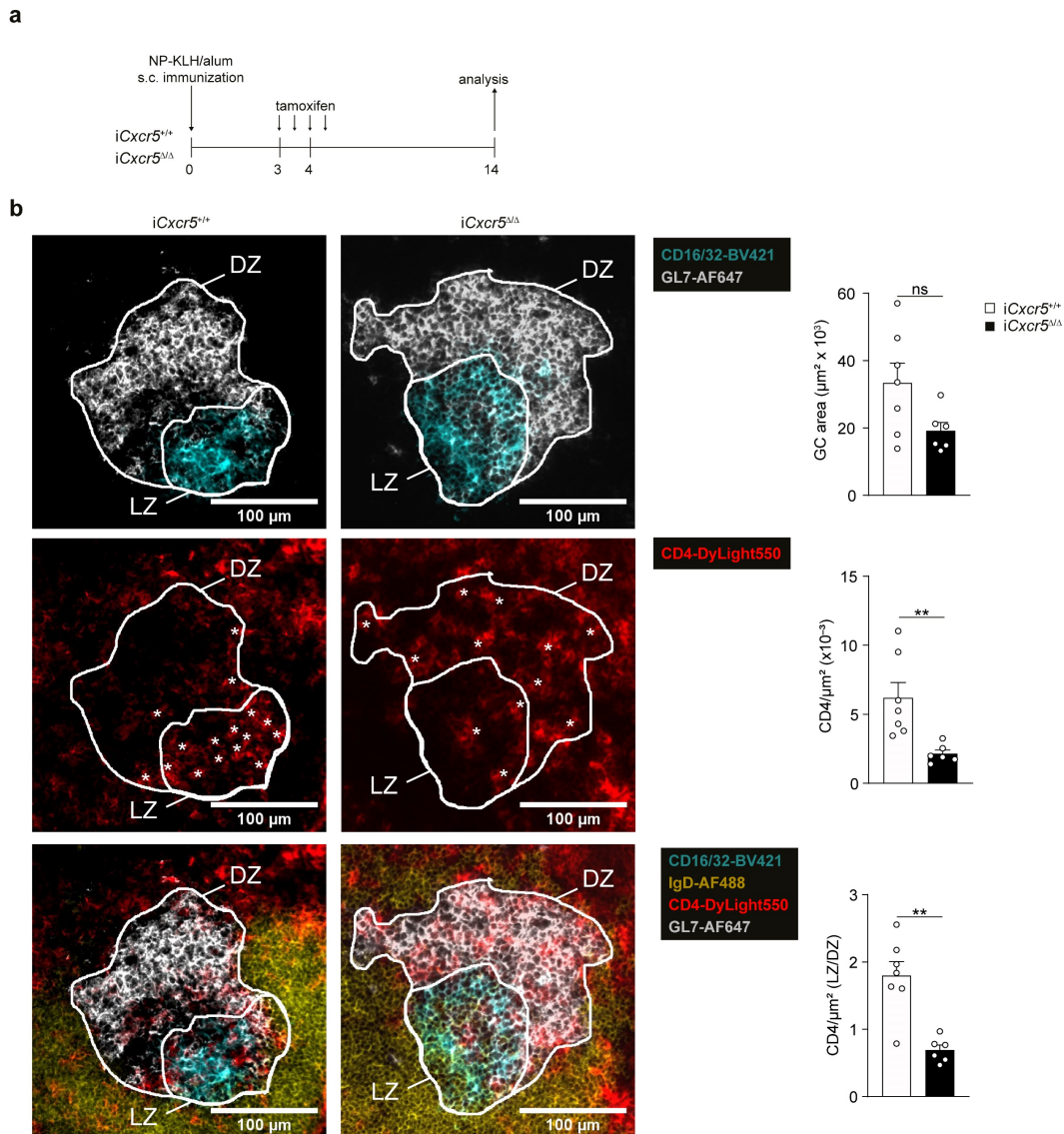


**Figure 8: CD4<sup>+</sup> T cells with induced *Cxcr5*-deficiency stay in GCs, but lose preferential LZ localization.** **a** Experimental scheme for the analysis of the impact of tamoxifen-induced and T-cell specific deletion of *Cxcr5* on day 3+4 after immunization with NP-KLH/alum. **b** Immunofluorescence of GCs in LN sections from immunized and tamoxifen-treated *iCxcr5*<sup>+/+</sup> and *iCxcr5* <sup>$\Delta\Delta$</sup>  mice on day 14. The DZ area was identified based on GL7<sup>+</sup> GC B cells (grey) and absence of CD16/32<sup>+</sup> FDCs (magenta). The LZ area was delineated as CD16/32<sup>+</sup> areas, containing FDCs (top row). CD4<sup>+</sup> T cells within the DZ or LZ in the same sections as above (middle row, asterisks). Full staining of GCs, including the IgD<sup>+</sup> mantle zone (bottom row). Right, quantification of GC area, numbers of CD4<sup>+</sup> T cell per  $\mu\text{m}^2$  of the GC area and ratio of CD4<sup>+</sup> T cells per  $\mu\text{m}^2$  of LZ over DZ area. Each symbol represents one GC ( $n = 2$ ). \*\* $P < 0.01$ , ns = not significant, two-tailed nonparametric Mann-Whitney test (b); mean + s.e.m. in b.

sections obtained on day 14 after immunization (**Fig. 8a**). Identification of GCs and the compartmentalization into the distinct zones was achieved by staining for *T* and *B* cell Activation Marker (GL7)-positive GC B cells, which are primarily localized in the DZ, while CD16/CD32<sup>+</sup> FDCs define the LZ (**Fig. 8b; upper row**). In these micro-anatomical structures, we analyzed the quantities and also the precise localization of CD4<sup>+</sup> T cells. Despite CD4<sup>+</sup> T cell-specific *Cxcr5*-ablation, GCs had normally formed, although a trend towards smaller GCs was apparent (**Fig. 8b; upper row**). The GCs in *iCxcr5*<sup>Δ/Δ</sup> animals contained fewer CD4<sup>+</sup> T cells per GC area, but still substantial numbers (**Fig. 8b; middle row, white asterisks**). However, in contrast to the control mice, the majority of *Cxcr5*-ablated CD4<sup>+</sup> T cells was found in the DZ instead of the LZ (**Fig. 8b; middle row, white asterisks**).

#### 7.1.4. Enhanced class-switching and plasma cell formation in an acute viral infection upon *Cxcr5*-deletion

In the context of classical protein immunization, *Cxcr5*-ablation in CD4<sup>+</sup> T cells appeared not to impair Tfh cell maintenance. During acute viral infections, cell-extrinsic cues that promote Th1 cell responses are abundantly present and must be counteracted by Tfh cells (Papillion et al., 2019). Therefore, we tested Tfh cell stability upon induced CXCR5-loss during an acute infection with LCMV (**Fig. 9a**). For the deletion of *Cxcr5*, tamoxifen was administered on day 3+4. On day 10 post infection, the frequencies of gp66<sup>+</sup>CD4<sup>+</sup> T cells, which are specific for the LCMV epitope GP<sub>66-77</sub>, were similar to those observed in control mice, as assessed by a

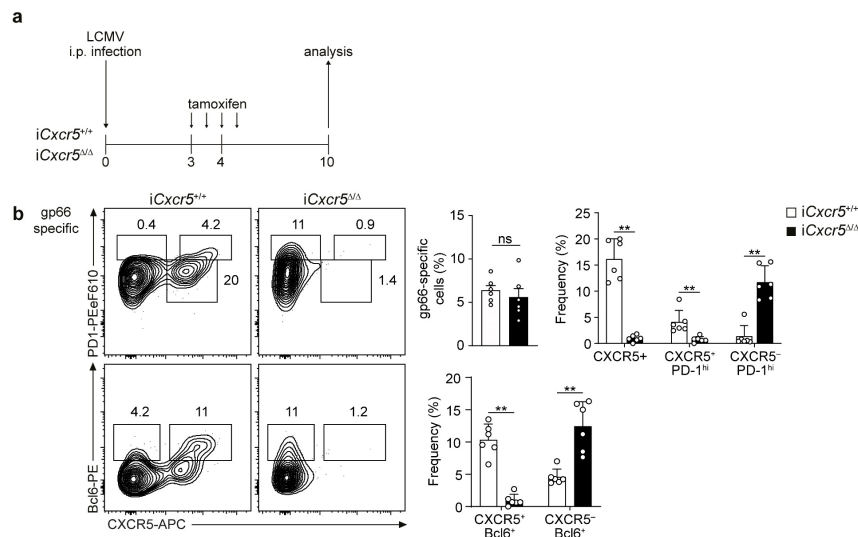


**Figure 9: Continued expression of Tfh cell markers upon *Cxcr5*-ablation during acute LCMV infection.** **a** Experimental scheme for the analysis of the impact of induced CD4<sup>+</sup> T cell-specific ablation of *Cxcr5* during LCMV Armstrong infection (i.p.). **b** Flow cytometry of LCMV GP<sub>66-77</sub> tetramer-positive CD4<sup>+</sup> T cells from the spleen of tamoxifen-treated *iCxcr5*<sup>+/+</sup> and *iCxcr5*<sup>Δ/Δ</sup> mice on day 10 after infection. Pre-gated as live CD4<sup>+</sup>CD44<sup>hi</sup>GP<sub>66-77</sub><sup>+</sup>CD19<sup>-</sup> lymphocytes. Gate frequencies indicate percent of CXCR5-PD-1<sup>hi</sup> cells, CXCR5<sup>hi</sup>PD-1<sup>hi</sup> GC Tfh cells and CXCR5<sup>+</sup>PD-1<sup>int</sup> Tfh cells. Quantification of the results (right panel); each symbol represents an individual mouse (n = 6). ns = not significant, \*\*P < 0.01 two-tailed nonparametric Mann-Whitney test (b); mean + s.e.m. in b.

## Results

staining with a LCMV-specific MHC-II tetramer (**Fig. 9b; quantification**). As before (**Fig. 5, 6**), CXCR5 was efficiently knocked-out, also in antigen-specific cells and CXCR5<sup>-</sup> PD-1<sup>hi</sup> and CXCR5<sup>-</sup> Bcl6<sup>+</sup> populations were again observed (**Fig. 9b**). Further, total GC B cell frequencies were not impaired (**Fig. 10a; left panel**) and the majority of GC B cells in *iCxcr5*<sup>Δ/Δ</sup> mice exhibited a CXCR4<sup>hi</sup>CD86<sup>lo</sup> DZ phenotype akin to control mice (**Fig. 10a; middle panel**). However, a higher proportion of GC B cells underwent class switching towards IgG2c (**Fig. 10a; right panel**), which is the dominant isotype in the response towards LCMV. Moreover, CD138<sup>hi</sup> PC frequencies were increased in animals with a CXCR5-deficient CD4<sup>+</sup> T cell compartment (**Fig. 10b**).

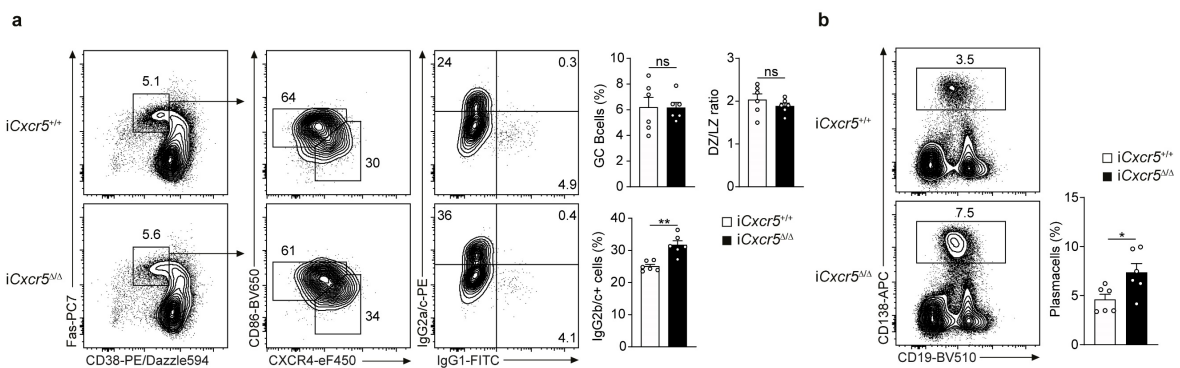


**Figure 10: CD4<sup>+</sup> T cell-specific *Cxcr5*-ablation during acute LCMV infection enhances class-switching and PC differentiation.** Mice were infected with LCMV Armstrong (i.p.), treated with tamoxifen on day 3+4, and analyzed on day 10. **a** Flow cytometry of B cells from spleens of *iCxcr5*<sup>+/+</sup> and *iCxcr5*<sup>Δ/Δ</sup> mice. Cells were pre-gated as live CD19<sup>+</sup>CD4<sup>-</sup> lymphocytes (left panel) or CD19<sup>+</sup>CD4<sup>-</sup>CD38<sup>lo</sup>Fas<sup>hi</sup> lymphocytes (middle and right panel). Gate frequencies indicate percent of CD38<sup>lo</sup>Fas<sup>hi</sup> GC B cells, CXCR4<sup>lo</sup>CD86<sup>hi</sup> DZ and CXCR4<sup>hi</sup>CD86<sup>lo</sup> LZ GC B cells and IgG2c<sup>+</sup>IgG1<sup>-</sup>, IgG2c<sup>+</sup>IgG1<sup>+</sup> or IgG2c<sup>-</sup>IgG1<sup>+</sup> GC B cells. Quantification of the results (right panel); each symbol represents an individual mouse (n = 6). **b** Flow cytometry and quantification of PCs from mice as in (a). Cells were pre-gated as live lymphocytes. Gate frequencies indicate percent of CD19<sup>int</sup>CD138<sup>hi</sup> PCs. ns = not significant, \*P < 0.05, \*\*P < 0.01 two-tailed nonparametric Mann-Whitney test (a, b); mean + s.e.m. in a, b.

### 7.1.5. The transcriptome of CXCR5-sufficient and -deficient Tfh cells is highly similar

The persistence of a population with Tfh cell marker expression upon *Cxcr5*-ablation was confirmed in two independent models in previous experiments (**Fig. 6, 9**). To elucidate the identity of these cells and to examine their relationship to *bona fide* CXCR5-positive Tfh cells, RNA-seq was conducted. In peripheral LNs of naive mice CXCR5<sup>+</sup> CD4<sup>+</sup> T cells are rare and especially cells with a CXCR5<sup>+</sup>PD-1<sup>hi</sup> phenotype are not present. Therefore, CXCR5<sup>+</sup>PD-1<sup>hi</sup> GC Tfh cells can be considered specific for the immunizing antigen. After immunization with NP-KLH and subsequent tamoxifen-treatment (**Fig. 11a**), three populations were sorted for RNA-seq on day 10: CXCR5<sup>-</sup>PD-1<sup>hi</sup> cells from *iCxcr5*<sup>Δ/Δ</sup> mice and CXCR5<sup>+</sup>PD-1<sup>hi</sup> GC Tfh cells as well as CXCR5<sup>-</sup>PD-1<sup>-</sup> non-Tfh cells from *iCxcr5*<sup>+/+</sup> mice (**Fig. 11b**). As Treg cells can express high levels of PD-1 (Stathopoulou et al., 2018) and would therefore contaminate the pool of CXCR5<sup>-</sup> Tfh cells, we excluded them by gating on GITR<sup>-</sup> cells. In the obtained transcriptomic data, we first assessed the expression of important markers that are

## Results

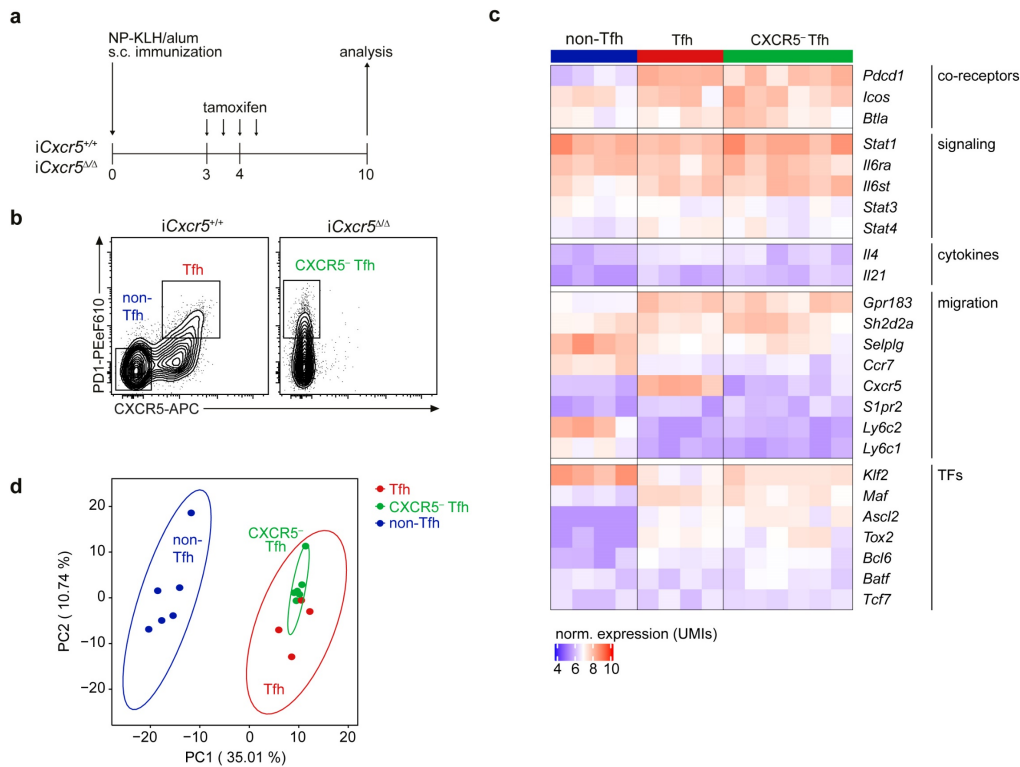


**Figure 11: Maintenance of the Tfh cell phenotype is not impaired by the loss of CXCR5.** **a** Experimental scheme for RNA-seq analysis of the impact of induced CD4<sup>+</sup> T cell-specific ablation of *Cxcr5* after immunization with NP-KLH. **b** Sorting gates of CD4<sup>+</sup> T cell populations from draining LNs of tamoxifen-treated *iCxr5*<sup>+/+</sup> and *iCxr5*<sup>Δ/Δ</sup> mice on day 10 after immunization. Pre-gated as live CD4<sup>+</sup>CD44<sup>hi</sup>GITR<sup>-</sup>CD19<sup>-</sup> lymphocytes. Gates indicate CXCR5<sup>-</sup>PD-1<sup>-</sup> non-Tfh cells, CXCR5<sup>hi</sup>PD-1<sup>hi</sup> Tfh cells and CXCR5<sup>-</sup>PD-1<sup>hi</sup> Tfh cells. **c** Normalized expression of selected Tfh or Th-associated genes (rows) in non-Tfh, Tfh and CXCR5<sup>-</sup> Tfh cells (columns) shown in a heatmap (n = 4-6). **d** PCA of non-Tfh, Tfh and CXCR5<sup>-</sup> Tfh cell transcriptomes derived from samples as in (b). Ellipses surrounding the data points delineate computed confidence ellipses with a 95% confidence level.

differentially expressed between Tfh and non-Tfh cells (Choi et al., 2015; Crotty, 2014) (**Fig. 11c**). Akin to WT Tfh cells, CXCR5<sup>-</sup>PD-1<sup>hi</sup> cells exhibited Tfh cell-characteristic expression of signaling molecules (high *Il6st* and *Il6ra*), inhibitory and stimulatory co-receptors (high *Pdcd1*, *Icos* and *Btla*), migratory receptors (high *Sh2d2a*; low *Selplg*, *Ccr7* and *Ly6c2*) and TFs (increased *Maf*, *Tox2* and *Ascl2*; decreased *Klf2*). Importantly, CXCR5<sup>-</sup> Tfh cells differed clearly from non-Tfh cells, while they exhibited an extensive overlap in marker expression with Tfh cells (**Fig. 11c**). Subsequently, a principal component analysis (PCA) was conducted examining the similarity of the transcriptomes of the individual replicates and between the different cell populations. The first principal component (PC) explained 35% of the variance of the data and separated Tfh and non-Tfh cells (**Fig. 11d**; red and blue dots). Transcriptomes from *Cxcr5*-deficient and *Cxcr5*-sufficient Tfh cell populations were not separated by PC1 and clustered closely (**Fig. 11d**; green and red dots). Although a certain degree of variability among the replicates of the different populations was observed in PC2, the two Tfh cell populations still clustered together. This demonstrated that CXCR5<sup>-</sup>PD-1<sup>hi</sup> cells can indeed be

## Results

considered as CXCR5<sup>-</sup> Tfh cells, as they share the transcriptomic program that operates in WT Tfh cells.

Taken together, the induced and CD4<sup>+</sup> T cell-specific loss of CXCR5 in established Tfh cells, had a minor impact on their function and identity. *Cxcr5*-ablated cells continued to express high levels of PD-1 and Bcl6 protein and were still localized in GCs. Although CD4<sup>+</sup> T cell frequencies and LZ polarization within GCs were reduced, GC B cell helper functions were sustained. Finally, transcriptomic analyses revealed that the identity of Tfh cells was merely altered by the loss of CXCR5.

## 7.2. The impact of CD4<sup>+</sup> T cell-specific *Bcl6*-ablation on the GC response

### 7.2.1. A system for the temporally-guided deletion of *Bcl6* in CD4<sup>+</sup> T cells

Previous studies have addressed the role of *Bcl6* in CD4<sup>+</sup> T cells using either germline or CD4-conditional KO systems (Hollister et al., 2013; Ichii et al., 2007; Johnston et al., 2009; Liu et al., 2016b; Nurieva et al., 2009). However, such systems did not allow for investigating the role of factors that are required for the maintenance of already established Tfh cells.

To overcome this problem, an inducible KO system applying the previously mentioned *Cd4-Cre-ERT2* KI strain was chosen here instead (Sledzinska et al., 2013). As the efficiency of inducible KOs often varies strongly between different conditional alleles, two distinct conditional *Bcl6* alleles were compared to identify a suitable model (**Fig. 12**): On the one hand, a widely used floxed *Bcl6* allele that is well studied and upon Cre-mediated recombination yields a deletion of the DNA-binding domain (referred to as *Bcl6*<sup>Δ7-9</sup>) (Hollister et al., 2013); on the other hand, we used a mouse generated by Geng and colleagues as it differs from previously published mice in several practical aspects (referred to as *Bcl6*<sup>Δ5-10</sup>) (Geng et al., 2015). First, Cre recombination at the *Bcl6* locus does not only result in deletion of the DNA binding domain, but also parts of the middle domain. This is supposed to result in a more comprehensive elimination of *Bcl6* functionality, including DNA-binding independent roles (Oestreich et al., 2011). Second, upon Cre-mediated recombination of the *Bcl6* locus an otherwise silenced *mCherry*-encoding sequence is knocked into the open reading frame, yielding a reporter for *Bcl6* transcription and deletion in Tfh cells, which is particularly useful to assess the efficiency of inducible KOs.

The two mice harboring inducible *Bcl6* KO alleles were compared in the context of a classical protein immunization with NP-KLH in alum. Tamoxifen was given on day 3+4 after immunization to induce *Bcl6*-deletion specifically in CD4<sup>+</sup> T cells (**Fig. 13a**). On day 7,

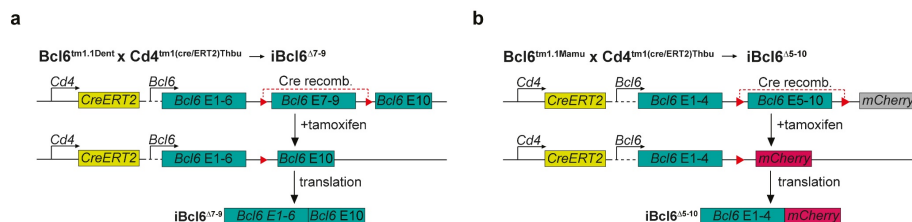


**Figure 12: Genomic structure of the two different *Bcl6* conditional alleles.** Tamoxifen administration to mice harboring a conditional *Bcl6* allele and an inducible CreERT recombinaise results in the excision of the targeted allele. **a** The *Bcl6*<sup>tm1.1Dent</sup> mutant mouse has loxP sites flanking exons 7-9. Following Cre-mediated recombination, a *Bcl6* protein lacking the DNA-binding domain is expressed. **b** In *Bcl6*<sup>tm1.1Mamu</sup> mice, loxP sites were integrated upstream of exon 5 and downstream of exon 10. Additionally, a transcriptionally inactive *mCherry*-encoding sequence was placed in the 3' untranslated region (UTR) of *Bcl6*. Recombination of the locus yields a deletion of the exons 5-10 and transcription of *mCherry* together with *Bcl6*.

## Results

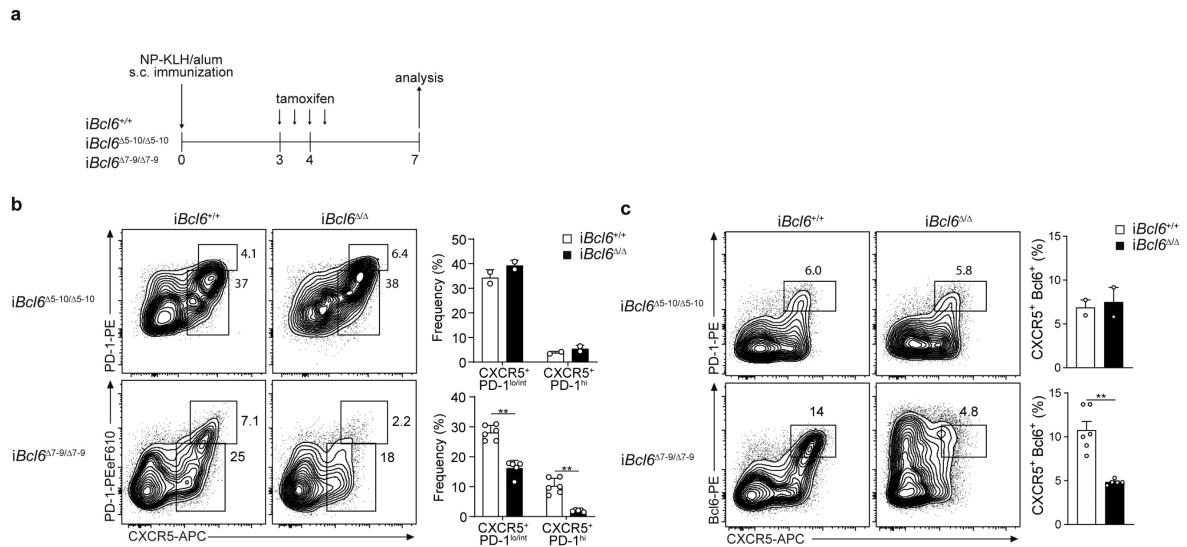


**Figure 13: Differential impact of induced *Bcl6*-ablation on Tfh cell frequencies.** Experimental scheme for the analysis of the impact of tamoxifen-induced and T-cell specific deletion of *Bcl6* after immunization with NP-KLH/alum. **b** Flow cytometry of CD4<sup>+</sup> T cells from LN of *Cd4-CreERT2<sup>+</sup>Bcl6<sup>+/+</sup>* (*iBcl6<sup>+/+</sup>*; top and lower left), *Cd4-CreERT2<sup>+</sup>Bcl6<sup>Δ7-9/Δ7-9</sup>* (*iBcl6<sup>Δ7-9/Δ7-9</sup>*; top right) and *Cd4-CreERT2<sup>+</sup>Bcl6<sup>Δ5-10/Δ5-10</sup>* (*iBcl6<sup>Δ5-10/Δ5-10</sup>*; lower right) mice on day 7. Cells were pre-gated as live CD4<sup>+</sup>CD44<sup>hi</sup>CD19<sup>-</sup> lymphocytes. Gate frequencies indicate percent of CXCR5<sup>+</sup>PD-1<sup>int/lo</sup> Tfh and CXCR5<sup>hi</sup>PD-1<sup>hi</sup> GC Tfh cells. Quantification of the results (right panel); each symbol represents an individual mouse (n = 2-5). Data represents two independent experiments. **c** Flow cytometry and quantification of CD4<sup>+</sup> cells as in (b); gate frequencies indicate percent of CXCR5<sup>+</sup>Bcl6<sup>hi</sup> GC Tfh cells. ns = not significant, \*\*P < 0.01 two-tailed nonparametric Mann-Whitney test (b, c); mean + s.e.m. in b, c.

CXCR5<sup>+</sup> PD-1<sup>lo/int</sup> Tfh and CXCR5<sup>+</sup>PD1<sup>hi</sup> GC Tfh cell populations were observed in the *Cd4-Cre-ERT2<sup>+</sup>Bcl6<sup>+/+</sup>* control mice (referred to as *iBcl6<sup>+/+</sup>*). A significant decrease, especially in CXCR5<sup>hi</sup>PD-1<sup>hi</sup> GC Tfh cells, was seen in *iBcl6<sup>Δ7-9/Δ7-9</sup>*, but not in *iBcl6<sup>Δ5-10/Δ5-10</sup>* mice (**Fig. 13b**). In the latter, the fraction of CXCR5<sup>+</sup>Bcl6<sup>+</sup> T cells was also unaffected, although the utilized antibody is generally able to detect the KO. The increase in *Bcl6* expression observed in *iBcl6<sup>Δ7-9/Δ7-9</sup>* animals (**Fig. 13c**) is probably caused by the loss of *Bcl6* autoregulation that is normally mediated through the DNA-binding domain (Mendez et al., 2008; Pasqualucci et al., 2003; Wang et al., 2002).

Despite unchanged levels of *Bcl6* protein in *iBcl6<sup>Δ5-10/Δ5-10</sup>* mice, Cre-mediated recombination was efficiently induced at the *Bcl6* locus, as indicated by high levels of mCherry in Tfh and GC Tfh cells (**Fig. 14a; middle panel**). Moreover, although CXCR5 and mCherry levels were correlated, the reporter signal was not restricted to CXCR5<sup>+</sup> T cells (**Fig. 14a**). As the *Bcl6<sup>Δ7-9</sup>* mutant could still be detected by the antibody, we quantified Cre-mediated recombination of *Bcl6* via qPCR. This exhibited efficient deletion on gDNA and mRNA level (**Fig. 14b**), at similar efficiencies as in previous reports (Ise et al., 2014). The lower frequencies of GC Tfh cells and the efficient excision of *Bcl6* on the genomic level observed with the conditional *Bcl6<sup>Δ7-9</sup>* allele

## Results

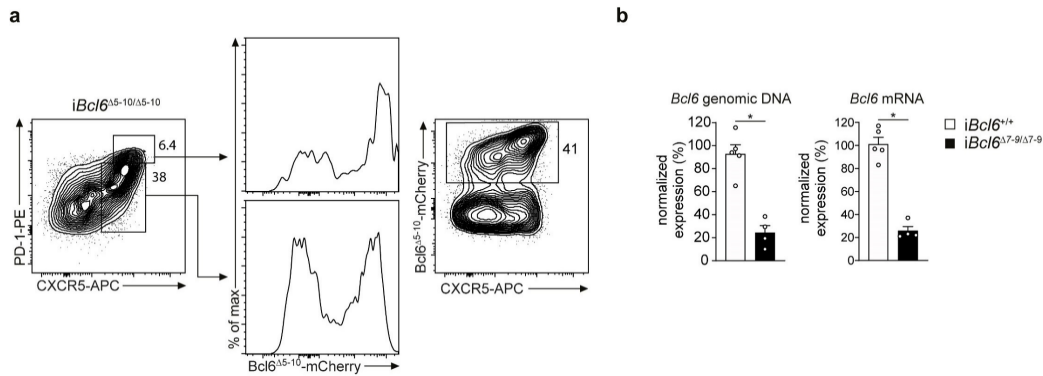


**Figure 14: The Bcl6-mCherry reporter signal is not restricted to Tfh cells.** Mice were immunized with NP-KLH/alum (s.c.), treated with tamoxifen on day 3+4 and analyzed on day 7. **a** Flow cytometry of CD4<sup>+</sup> T cells from LNs of *iBcl6*<sup>Δ5-10/Δ5-10</sup> mice. Cells were pre-gated as live CD4<sup>+</sup>CD44<sup>hi</sup>CD19<sup>-</sup> lymphocytes. Gate frequencies indicate percent of CXCR5<sup>+</sup>PD-1<sup>int/lo</sup> Tfh and CXCR5<sup>hi</sup>PD-1<sup>hi</sup> GC Tfh cells. Bcl6-mCherry histograms are shown for Tfh and GC Tfh cells (middle panel). Correlation of the CXCR5 and Bcl6-mCherry signal (right plot). **b** PCR of *Bcl6* on gDNA (left graph) and mRNA (right graph) of CD4<sup>+</sup>CD44<sup>hi</sup>CXCR5<sup>+</sup>PD-1<sup>+</sup> T cells sorted from LNs of *iBcl6*<sup>+/+</sup> and *iBcl6*<sup>Δ7-9/Δ7-9</sup> mice on day 7 after immunization. *Bcl6* gDNA was normalized to *Cxcr5* gDNA and *Bcl6* mRNA expression was normalized to *Actb*; each symbol represents an individual mouse mean + s.e.m. (n = 4-5). \*P < 0.05, two-tailed nonparametric Mann-Whitney test (a, b); mean + s.e.m. in a, b.

supported the conclusion that the KO was induced promptly and effectively upon tamoxifen administration.

Hence, the *iBcl6*<sup>Δ7-9</sup> mouse proved to be suitable for the analysis of the requirement of Bcl6 during Tfh cell differentiation and maintenance. In contrast, Bcl6 protein levels were unchanged upon tamoxifen-induced *Bcl6*-ablation in the *iBcl6*<sup>Δ5-10/Δ5-10</sup> mouse, potentially due to heterozygous deletion of the floxed allele or generally slower deletion kinetics compared to the other KO allele. Therefore, the *iBcl6*<sup>Δ7-9</sup> mouse was used for the ensuing experiments and is hereafter referred to as *iBcl6*<sup>ΔΔ</sup>.

### 7.2.2. Differential requirements of *Bcl6* for GC Tfh and Tfr cell maintenance

After the establishment of the *iBcl6*<sup>ΔΔ</sup> mouse as a suitable tool for studying Tfh cells, the requirement of continued Bcl6 expression was systematically tested at different timepoints of the GC response. To this end, *Bcl6*-ablation was induced at an early (day 3+4) and a late (day 6+7) timepoint after NP-KLH immunization (**Fig. 15a**). On day 14, CXCR5 and PD-1 surface expression was analyzed by flow cytometry. The frequencies of CXCR5<sup>+</sup> PD-1<sup>lo/int</sup> Tfh cells were slightly reduced by the induced *Bcl6* KO on day 6+7, while the ablation of day 3+4 resulted in a twofold reduction (**Fig. 15b**). Potentially, this is a consequence of the longer period between KO-induction and analysis. Strikingly, for both tamoxifen administration schemes, the fraction of CXCR5<sup>hi</sup>PD-1<sup>hi</sup> GC Tfh cells was almost completely abolished. As mentioned earlier (**Fig. 13, 14**), the KO displayed exaggerated expression levels of non-functional Bcl6 (**Fig. 15c**). Early *Bcl6*-ablation resulted in the appearance of a CXCR5<sup>-</sup>Bcl6<sup>hi</sup> population (**Fig. 15c; top right**). Upon late deletion, some of the cells exhibited a CXCR5<sup>int</sup>Bcl6<sup>hi</sup> phenotype (**Fig. 15c; bottom right**). The loss of Tfh cell markers extended to proteins that are normally downregulated on the surface of the cells, as a PSGL-1<sup>lo</sup> population was absent when *Bcl6*-deficiency was induced on day 6+7 (**Fig. 16a**). Surprisingly, CXCR5<sup>+</sup>Foxp3<sup>+</sup> T follicular regulatory (Tfr) cells, which inhibit GC responses (Chung et al., 2011; Clement et al., 2019;

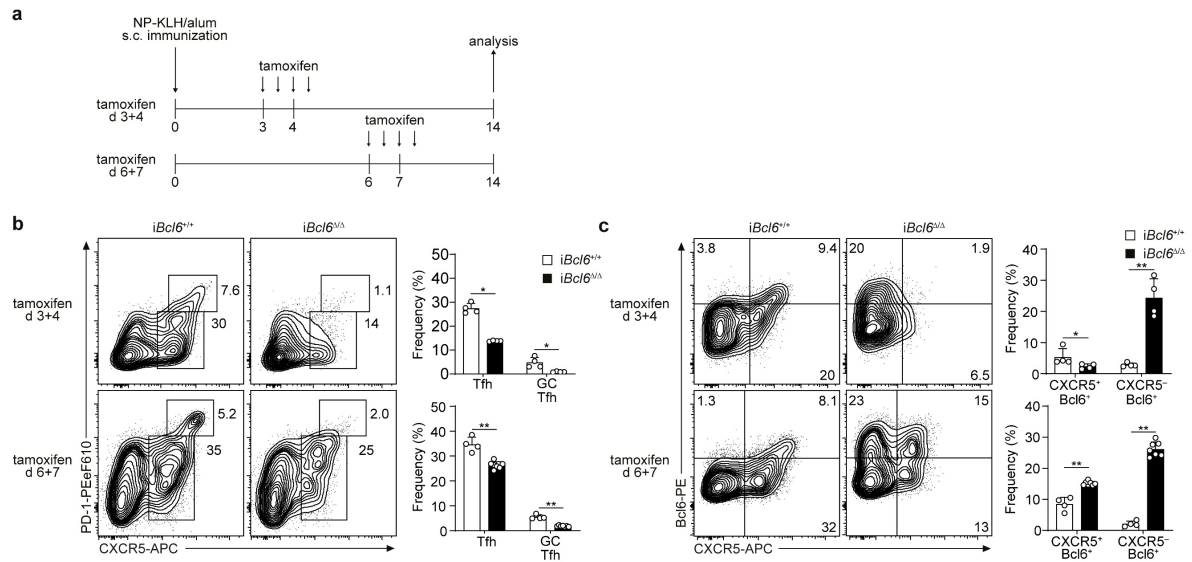


**Figure 15: GC Tfh cells are highly sensitive towards the loss of Bcl6 during Tfh cell differentiation and maintenance.** **a** Experimental scheme for the analysis of the impact of tamoxifen-induced and T-cell specific deletion of *Bcl6* at different timepoints after immunization with NP-KLH/alum. **b** Flow cytometry of CD4<sup>+</sup> T cells from LNs of *iBcl6*<sup>+/+</sup> and *iBcl6*<sup>ΔΔ</sup> mice, treated with tamoxifen early (day 3+4, upper panel) or late (day 6+7, lower panel) and analyzed on day 14. Cells were pre-gated as live CD4<sup>+</sup>CD44<sup>hi</sup>CD19<sup>-</sup> lymphocytes. Gate frequencies indicate percent of CXCR5<sup>+</sup>PD-1<sup>lo/int</sup> Tfh and CXCR5<sup>hi</sup>PD-1<sup>hi</sup> GC Tfh cells. Quantification of the results (right panel); each symbol represents an individual mouse (n = 4-6). **c** Flow cytometry and quantification of CD4<sup>+</sup> T cells as in (b); gate frequencies indicate percent of CXCR5<sup>+</sup>Bcl6<sup>+</sup> cells, CXCR5<sup>+</sup>Bcl6<sup>hi</sup> GC Tfh cells or CXCR5<sup>+</sup>Bcl6<sup>lo</sup> Tfh cells. \*P < 0.05, \*\*P < 0.01 two-tailed nonparametric Mann-Whitney test (b, c); mean + s.e.m. in b, c.

## Results

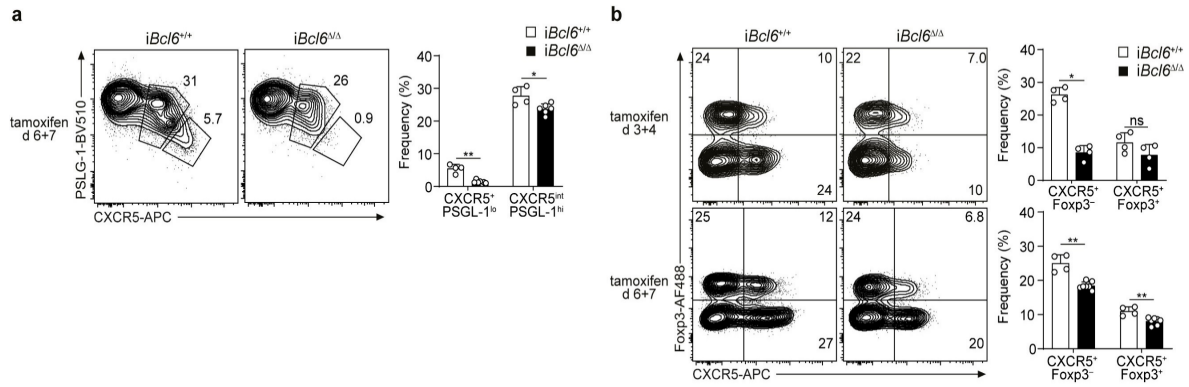


**Figure 16: *Bcl6* is required to maintain the phenotype of GC Tfh, but not Tfr cells.** Mice were immunized with NP-KLH/alum (s.c.), treated with tamoxifen on the respective days and analyzed on day 14. **a** Flow cytometry of CD4<sup>+</sup> T cells from LNs of *iBcl6*<sup>+/+</sup> and *iBcl6*<sup>Δ/Δ</sup> mice treated with tamoxifen on day 6+7. Cells were pre-gated as live CD4<sup>+</sup>CD44<sup>hi</sup>CD19<sup>-</sup> lymphocytes. Gate frequencies indicate percent of CXCR5<sup>int</sup>PSGL-1<sup>lo</sup> Tfh and CXCR5<sup>+</sup>PSGL-1<sup>lo</sup> GC Tfh cells. Quantification of the results (right panel); each symbol represents an individual mouse (n = 4-6). **b** Flow cytometry and quantification of CD4<sup>+</sup> T cells as in (a) treated with tamoxifen early day 3+4 (top row) or late day 6+7 (bottom row). Gate frequencies indicate percent of CXCR5<sup>+</sup>Foxp3<sup>+</sup> Treg, CXCR5<sup>+</sup>Foxp3<sup>-</sup> Tfr or CXCR5<sup>+</sup>Foxp3<sup>-</sup> Tfh cells (n = 4-7). ns = not significant, \*P < 0.05, \*\*P < 0.01 two-tailed nonparametric Mann-Whitney test (a, b); mean + s.e.m. in a, b.

Linterman et al., 2011), were not affected when the KO was induced on day 3+4 (**Fig. 16b; upper panel**). In contrast, day 6+7 deletion affected Tfr cell frequencies only slightly but to a similar extent as CXCR5<sup>+</sup>Foxp3<sup>-</sup> Tfh cells (**Fig. 16b; lower panel**).

Due to their reciprocal interactions, impairment of Tfh cell differentiation and function also affects B cell responses (Crotty, 2011, 2014). Therefore, the frequencies of GC B cells were examined upon early (day 3+4 tam) and late (day 6+7 tam) CD4<sup>+</sup> T cell-specific *Bcl6*-ablation (**Fig. 17a**). In line with the stronger impact on Tfh cells observed in the previous experiments (**Fig. 13, 15**), the day 3+4 tamoxifen application caused a more substantial reduction of about five-fold compared to a two-fold reduction for the late ablation (**Fig. 17b**). In both settings, GC B cells that were specific for the immunizing NP hapten were not preferentially decreased, suggesting that *Bcl6*-ablated CD4<sup>+</sup> T cells were able to support antigen-specific B cells. Nevertheless, we observed a severely diminished fraction of class-switched IgG1<sup>+</sup> GC B cells upon day 3 + 4 tamoxifen administration (**Fig. 17c; upper row**). Concomitantly, IgG1<sup>+</sup>NP<sup>+</sup> cells, which give rise to IgG1-secreting, NP-specific PCs, were also substantially decreased (**Fig. 17c; upper row**). Late *Bcl6*-ablation in turn did not cause any apparent defects in class-switching and NP-specificity (**Fig. 17c; lower row**).

Although no preferential defect in the maintenance of antigen-specific GC B cells was detectable, a mutational analysis of the BCR was conducted to assess potential defects in SHM and ensuing selection of these cells. To this end, single IgG1<sup>+</sup>NP<sup>+</sup> GC B cells were sorted and a segment of the V186.2 heavy chain, containing complementarity determining regions (CDR) 1 and CDR2 (McHeyzer-Williams et al., 1991), was sequenced and examined for the

## Results

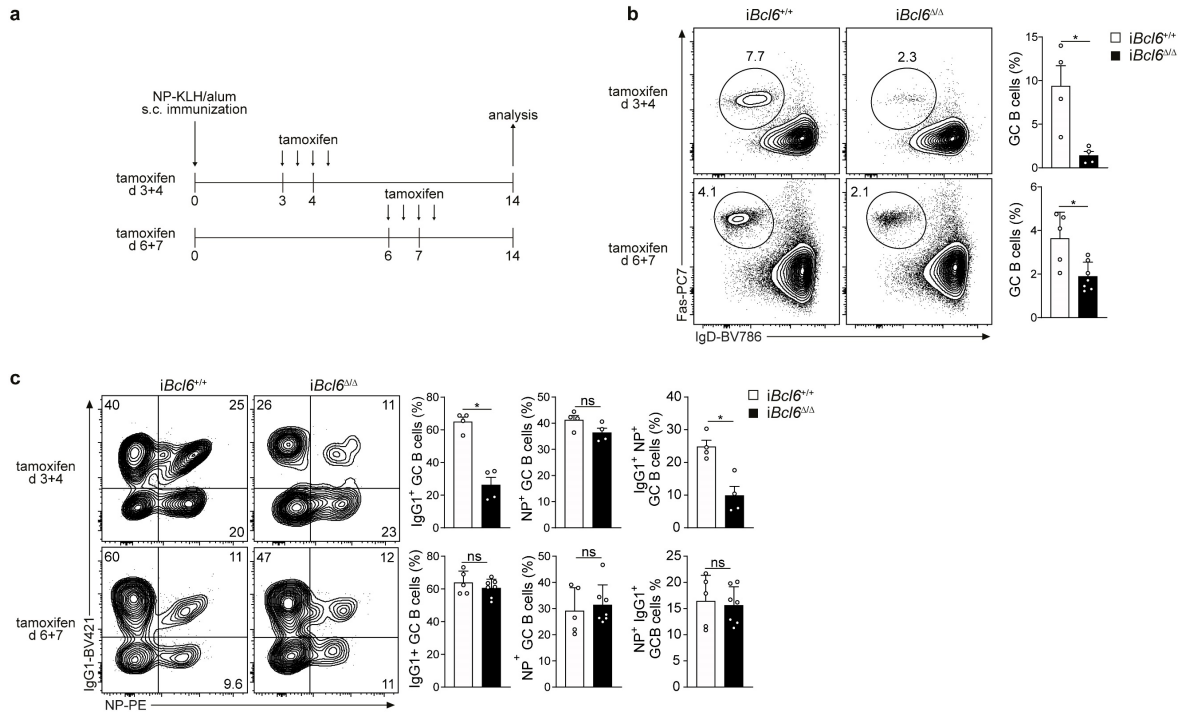


**Figure 17: Defective maintenance of class-switched GC B cells in absence of Bcl6<sup>+</sup> CD4<sup>+</sup> T cells.**  
**a** Experimental scheme for the analysis of the impact of tamoxifen-induced and T-cell specific deletion of *Bcl6* at different timepoints after immunization with NP-KLH/alum. **b** Flow cytometry of B cells from LNs of *iBcl6*<sup>+/+</sup> and *iBcl6*<sup>Δ/Δ</sup> mice, treated with tamoxifen early (day 3+4, upper panel) or late (day 6+7, lower panel) and analyzed on day 14. Cells were pre-gated as live CD19<sup>+</sup>CD4<sup>-</sup> lymphocytes. Gate frequencies indicate percent of IgD<sup>lo</sup>Fas<sup>hi</sup> GC B cells. Quantification of the results (right panel); each symbol represents an individual mouse (n = 4-5). **c** Flow cytometry and quantification of GC B cells from mice as in (b). Cells were pre-gated as live CD19<sup>+</sup>CD4<sup>-</sup>IgD<sup>lo</sup>Fas<sup>hi</sup> lymphocytes. Gate frequencies indicate percent of IgG1<sup>+</sup>NP<sup>-</sup>, IgG1<sup>+</sup>NP<sup>+</sup>, and IgG1<sup>-</sup>NP<sup>+</sup> GC B cells. ns = not significant, \*P < 0.05, \*\*P < 0.01 two-tailed nonparametric Mann-Whitney test (b, c); mean + s.e.m. in b, c.

presence of affinity-increasing mutations (Allen et al., 1988; Cumano and Rajewsky, 1986; Xiong et al., 2012). Here, we observed a strong trend towards lower incidence of the high-affinity amino acid substitutions W33L and K59R in the GC B cells from *iBcl6*<sup>Δ/Δ</sup> mice (**Fig. 18a**). Due to the small number of clones that could be sequenced, it was not possible to determine if this effect is significant. Nevertheless, this trend was not due to an impaired induction of SHM, as the analysis showed normal levels of acquired mutations per clone (**Fig. 18b**). Instead, it seemed that the mutated B cells were not selected based on the affinity of their BCR, but rather in an unguided manner.

## Results

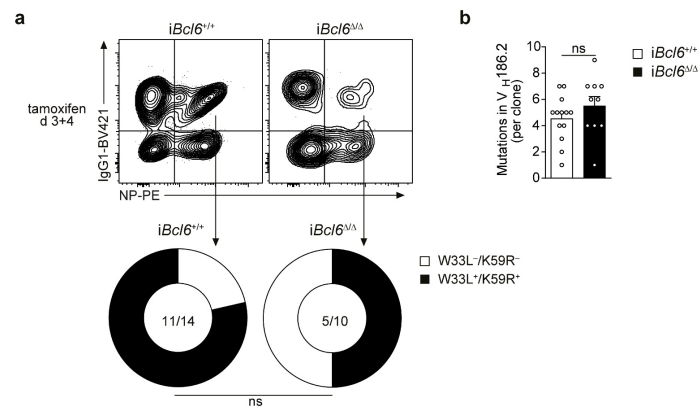


**Figure 18: Apparent defect in the selection of high-affinity GC B cells clones upon induced T cell-specific *Bcl6*-ablation.** Mice were immunized with NP-KLH/alum (s.c.), treated with tamoxifen on day 3+4 and analyzed on day 14. **a** Sorting strategy of IgG1<sup>+</sup>NP<sup>+</sup> GC B cell single clones from LNs of *iBcl6<sup>+/+</sup>* and *iBcl6<sup>Δ/Δ</sup>* mice. Cells were pre-gated as live CD19<sup>+</sup>CD4<sup>-</sup>IgD<sup>lo</sup>Fas<sup>hi</sup> lymphocytes. Below, proportion of V<sub>H</sub>186.2 sequences from single GC B cell clones from *iBcl6<sup>+/+</sup>* and *iBcl6<sup>Δ/Δ</sup>* mice bearing the high-affinity W33L or K59R mutation (n = 5). **b** Total number of mutations in V<sub>H</sub>186.2 sequences of GC B cell clones from (a). Two-tailed Fisher's exact test (a), nonparametric Mann-Whitney test (b); mean + s.e.m. in b.

### 7.2.3. Altered Th1/Tfh cell ratios upon induced loss of Bcl6 during acute viral infection

The findings from the previous experiments (**Fig. 13, 15, 16**) indicated that Bcl6 expression is particularly vital for the maintenance of GC Tfh cells. Unfortunately, in contrast to the induced *Cxcr5*-deletion in CD4<sup>+</sup> T cells, continued Tfh cell marker expression by *Bcl6*-ablated cells was not observed. This made it particularly difficult to track these polyclonal cells and investigate the cellular consequences of the loss of *Bcl6*.

To overcome this issue, we used CD4<sup>+</sup> T cells from SMARTA *iBcl6*<sup>Δ/Δ</sup> and *iBcl6*<sup>+/+</sup> mice (hereafter referred to as SM *iBcl6*<sup>Δ/Δ</sup> and SM *iBcl6*<sup>+/+</sup>), which express a TCR-transgene specific for the LCMV epitope GP<sub>61-80</sub> (Oxenius et al., 1998). Additionally, these mice expressed the congenic marker CD45.1/2 that can be used to differentiate between donor- and host-derived cells in adoptive transfer experiments and hence enabled us to track *Bcl6*-ablated cells (Baumjohann and Ansel, 2015). Naive CD4<sup>+</sup> T cells from SM *iBcl6*<sup>+/+</sup> or SM *iBcl6*<sup>Δ/Δ</sup> mice were transferred into CD45.2 WT recipients, followed by LCMV infection and tamoxifen application on day 3+4 to induce *Bcl6*-deficiency (**Fig. 19a**). Flow cytometric analysis on day 10 after infection showed that SM cells from control mice had differentiated into CXCR5<sup>+</sup>PSGL-1<sup>hi</sup> Th1 and CXCR5<sup>+</sup>PSGL-1<sup>lo</sup> Tfh cells at similar frequencies (**Fig. 19b**). Induced deletion of *Bcl6* in SM cells led to a near complete loss of CXCR5<sup>+</sup> Tfh cells that was paralleled by elevated Th1 cell frequencies and numbers (**Fig. 19b**). *Bcl6*-ablated cells appeared to have undergone

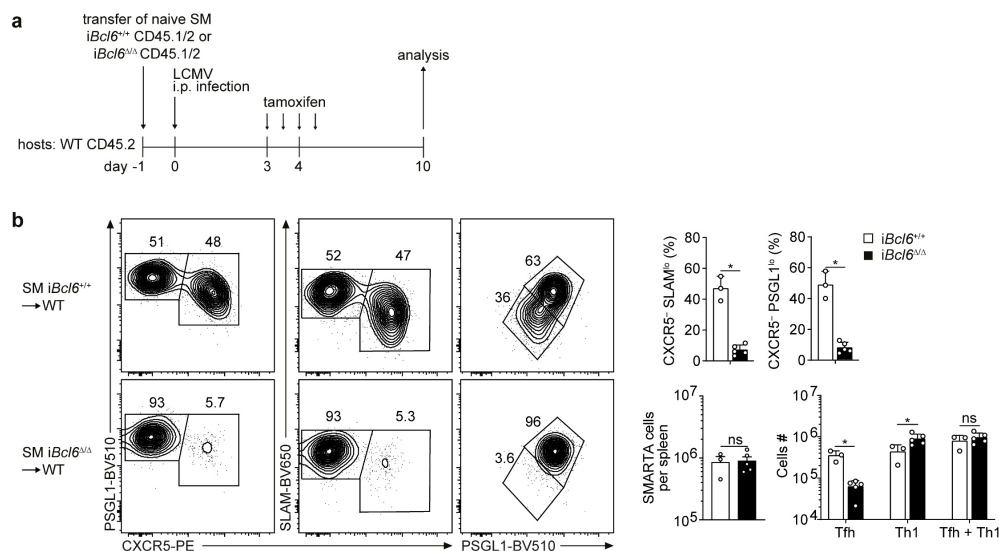


**Figure 19: Increased Th1 to Tfh cell ratio upon *Bcl6*-ablation during acute viral infection. a** Experimental scheme for the analysis of the impact of tamoxifen-induced and T-cell specific deletion of *Bcl6* in SM cells after infection with LCMV Armstrong (i.p.) **b** Flow cytometry of CD4<sup>+</sup> T cells from the spleens of tamoxifen-treated WT recipient that had been given adoptive transfers of SM *iBcl6*<sup>+/+</sup> and SM *iBcl6*<sup>Δ/Δ</sup> cells, followed by LCMV infection of recipients and analysis 10 days later. Pre-gated as live CD4<sup>+</sup>CD45.1/2CD19<sup>-</sup> lymphocytes. Gate frequencies indicate percent of CXCR5<sup>+</sup>PSGL-1<sup>hi</sup>, CXCR5<sup>-</sup>SLAMF6<sup>hi</sup> or PSGL-1<sup>hi</sup>SLAMF6<sup>hi</sup> Th1 cells and CXCR5<sup>+</sup> or PSGL-1<sup>lo</sup>SLAMF6<sup>lo</sup> Tfh cells. Quantification of the results (right panel); each symbol represents an individual mouse (n = 3-5). ns=not significant, \*P < 0.05 two-tailed nonparametric Mann-Whitney test (b); mean + s.e.m. in b.

normal expansion, as the total number of SM cells per spleen was unchanged (**Fig. 19b**). Low expression of the Th1 cell-associated markers PSGL-1 and SLAM, which are characteristic for Tfh cells (Choi et al., 2013b; Yusuf et al., 2010), were not maintained in the absence of *Bcl6* (**Fig. 19b**). It appeared that *Bcl6*-ablated cells upregulated the expression of these markers akin to Th1 cells. Indeed, we observed an increase in Th1 cell numbers concomitant with the decline in Tfh cells (**Fig 19b; bottom right**). The cell numbers added up to equal those of SM *iBcl6<sup>+/+</sup>* cells. On the one hand, this could potentially be explained through increased induction of cell death in Tfh cells caused by the loss of *Bcl6* and a simultaneous, compensatory Th1 cell expansion. On the other hand, it was also possible that Tfh cells transdifferentiated into Th1 or Th1-like cells. To address if former Tfh SM cells in this context adapted a Th1 cell transcriptional program or maintained the Tfh cell expression profile, RNA-seq was conducted.

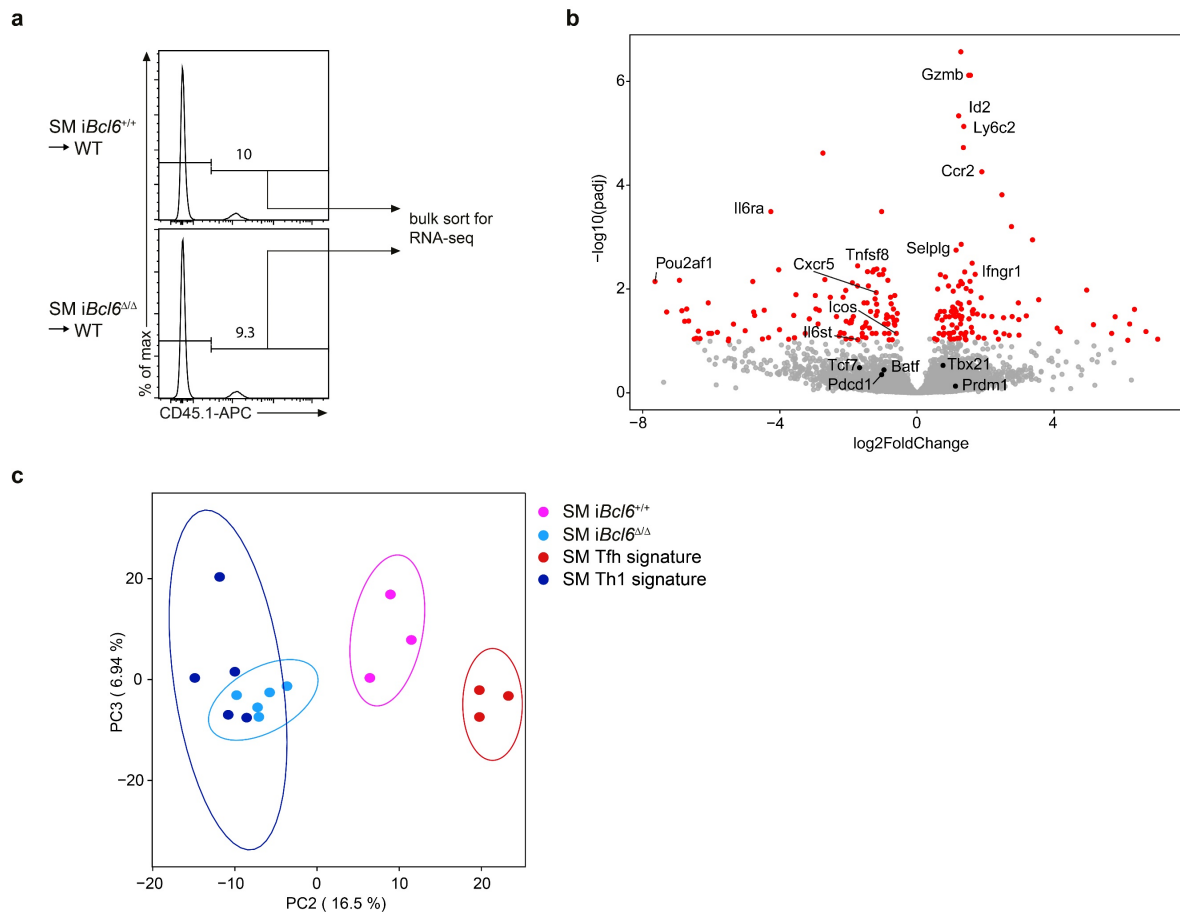


**Figure 20: *Bcl6*-deletion in CD4<sup>+</sup> T cells results in the adoption of a Th1-like transcription program.** WT recipient mice were given adoptive transfers of SM *iBcl6<sup>+/+</sup>* and SM *iBcl6<sup>Δ/Δ</sup>* cells, followed by infection with LCMV Armstrong (i.p.) and tamoxifen gavage on day 3+4 **a** Sorting strategy of donor-derived CD45.1 *iBcl6<sup>+/+</sup>* and *iBcl6<sup>Δ/Δ</sup>* SM cells from the spleens of host mice on day 10. Cells were pre-gated as live CD4<sup>+</sup>CD45.1CD19<sup>-</sup> lymphocytes. Gate frequencies indicate percent of CD45.1 cells. **b** Visualization of differentially expressed genes in *iBcl6<sup>+/+</sup>* and *iBcl6<sup>Δ/Δ</sup>* SM cells in a volcano plot. Relevant genes are labeled. Red dots depict significant genes (*P*<sub>adj</sub> < 0.1, fold change ≥ 0.5). **c** PCA of transcriptomes from *iBcl6<sup>+/+</sup>* and *iBcl6<sup>Δ/Δ</sup>* SM cells and additional signatures of *iCxcr5<sup>+/+</sup>* Th1 and Tfh SM cells from an analog experiment. Ellipses surrounding the data points delineate computed confidence ellipses with a 95% confidence level.

To this end, *iBcl6*<sup>ΔΔ</sup> or *iBcl6*<sup>+/+</sup> SM cells were sorted from the spleens of infected recipient mice on day 10 (**Fig. 20a**). The transcriptomic analysis revealed differential expression of >250 genes between *iBcl6*<sup>ΔΔ</sup> and *iBcl6*<sup>+/+</sup> SM cells that were visualized in a volcano plot (**Fig. 20b**). Many prominent Tfh cell genes were found among the downregulated transcripts, including *Cxcr5*, *Pou2af1*, *Il6ra* and *Il6st*. Th1 cell signature genes, in contrast, were generally upregulated, e.g. *Gzmb*, *Ifngr1*, *Id2* and *Ly6c2*. The similarity of Th1 cells and *Bcl6*-ablated SM cells was additionally assessed by a PCA using the 500 most variable genes. For this purpose, Th1 and Tfh cell signatures of SM cells obtained from control mice in an analog experimental setting were included in the analyses. When comparing independently generated RNA-seq data, batch effects occur naturally. Here, PC1 separated the datasets according to the different experiments. This is why PC2 and PC3 were used instead, which separated Th1 and Tfh cells adequately (**Fig. 20c; blue and red dots**). The transcriptomes of the *Bcl6*-sufficient SM cells were in between those of Tfh and Th1 cells (**Fig. 20c; magenta dots**). This appeared feasible as the cells contained a mixture of Tfh and Th1 cells (**Fig. 19b**). Moreover, the replicates of SM *iBcl6*<sup>ΔΔ</sup> cells were in close proximity to the Th1 cell samples (**Fig. 20c; light and dark blue dots**). This revealed that SM cells that lost *Bcl6* expression, were not able to maintain the Tfh cell transcriptional pattern, but rather switched to a Th1-like program. This supported the hypothesis that Tfh cells transdifferentiated into Th1-like cells upon *Bcl6* deletion.

#### 7.2.4. Transdifferentiation of *Bcl6*-deleted Tfh cells into Th1 cells during acute viral infection

To substantiate and extend these findings, the cell fate of *Bcl6*-ablated Tfh cells was examined in a re-transfer experiment. SM cells from *iBcl6*<sup>ΔΔ</sup> and *iBcl6*<sup>+/+</sup> mice were first co-transferred into primary hosts, where they differentiated into Th1 and Tfh cells after infection with LCMV (**Fig. 21a**). Four days after the infection, SM Th1 (CXCR<sup>-</sup>PSGL-1<sup>hi</sup>) and SM Tfh (CXCR5<sup>+</sup>PSGL-1<sup>lo</sup>) cells from both genotypes were sorted and each co-transferred into infection-matched secondary recipients (**Fig. 21b; left and middle panel**). On day 5+6, mice were treated with tamoxifen to induce the ablation of *Bcl6*. The co-transferred Th1 and Tfh cells were examined for the continued expression of Th1 and Tfh markers, respectively, on day 12 post infection. Regardless of *Bcl6* expression, more than 90% of the transferred Th1 cells maintained their expression patterns and were still CXCR5<sup>-</sup>PSGL-1<sup>hi</sup> (**Fig. 21b; right panel, upper row**). In contrast, phenotypic stability of the transferred SM Tfh cells was generally lower, as approximately 30% of the cells had gained Th1 cell marker expression (**Fig. 21b; right panel, lower row**). This effect was strongly amplified in *Bcl6*-ablated SM Tfh cells, which predominantly exhibited a Th1 cell phenotype. Importantly, these cells had a higher expression of the Th1 master regulator Tbet (Szabo et al., 2000) (**Fig. 21c**).

## Results

In summary, this data confirmed that the loss of *Bcl6* in pre-formed Tfh cells resulted in the transdifferentiation into *bona fide* Th1 cells.

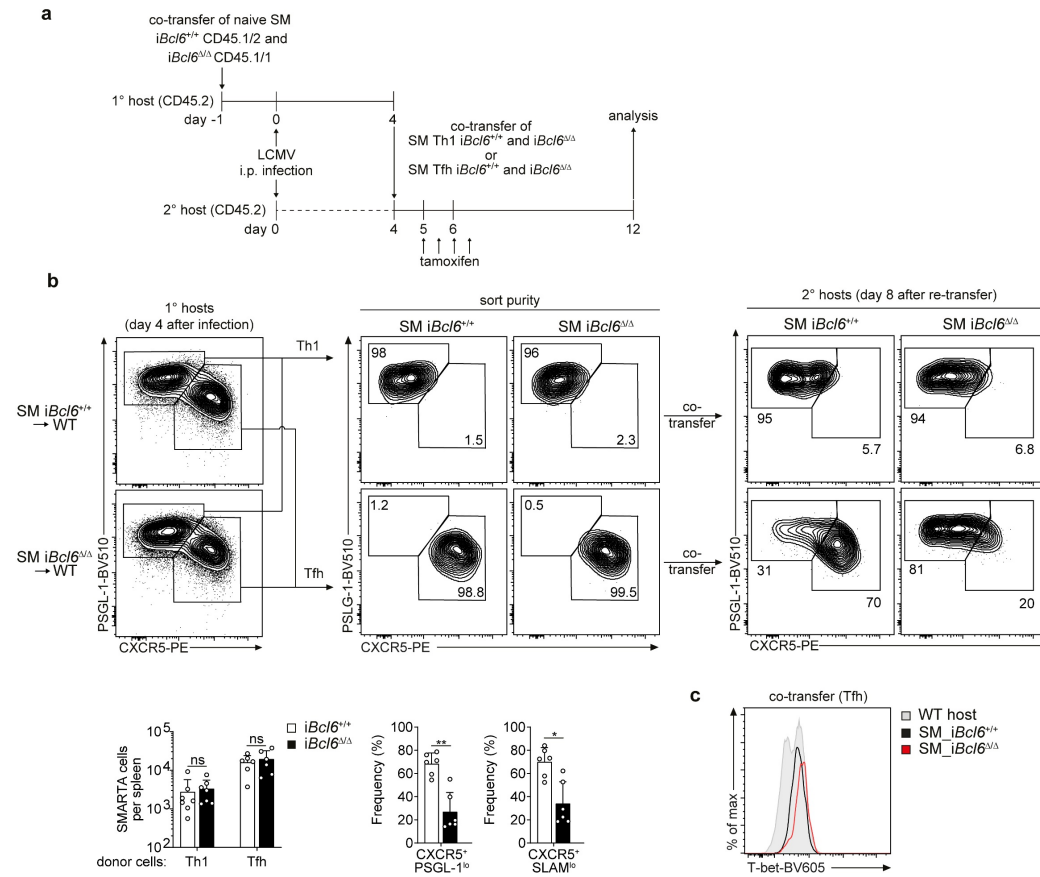


**Figure 21: *Bcl6* limits Tfh to Th1 cell transdifferentiation during acute viral infection.**  
**a** Experimental scheme for the analysis of the impact of tamoxifen-induced and T-cell specific deletion of *Bcl6* when Tfh and Th1 cells were first generated through LCMV infection and then separately co-transferred into secondary hosts followed by *Bcl6*-ablation through tamoxifen. **b** Flow cytometry of SM cells from the spleens of recipient mice on day 4 and day 12. SM Th1 (CXCR5<sup>+</sup>PSGL-1<sup>hi</sup>) and SM Tfh (CXCR5<sup>+</sup>PSGL-1<sup>lo</sup>) cells were sorted (middle panel) from the spleens of primary recipients on day 4 post infection, followed by a co-transfer of SM *iBcl6*<sup>+/+</sup> and *iBcl6*<sup>ΔΔ</sup> Th1 cells or SM *iBcl6*<sup>+/+</sup> and *iBcl6*<sup>ΔΔ</sup> Tfh cells into infection-matched secondary hosts (left panel). Co-transferred Th1 (right panel, upper row) and Tfh cells (right panel, lower row) were analyzed and quantified on day 12. Pre-gated as live CD4<sup>+</sup>CD19<sup>-</sup>CD45.1/2 (*iBcl6*<sup>+/+</sup>) or CD45.1 (*iBcl6*<sup>ΔΔ</sup>) lymphocytes. Gate frequencies indicate percent of CXCR5<sup>+</sup>PSGL-1<sup>hi</sup> Th1 and CXCR5<sup>+</sup>PSGL-1<sup>lo</sup> Tfh cells. Quantification of the results (lower panel); each symbol represents an individual mouse (n = 6). **c** Flow cytometry of co-transferred SM Tfh cells from mice as in (b). Overlay of Tbet expression in SM Tfh *iBcl6*<sup>+/+</sup> (black), SM Tfh *iBcl6*<sup>ΔΔ</sup> (red) donor and WT host cells (grey). ns = not significant, \*P < 0.05, \*\*P < 0.01 two-tailed nonparametric Mann-Whitney test (b); mean + s.e.m. in b.

### 7.2.5. *Bcl6*-ablation in the context of a type-II immune response yields enhanced Th2/memory T cell marker expression

Tfh cells in LCMV infection exhibit co-expression (Yusuf et al., 2010) of the otherwise mutually antagonistic TFs Tbet and *Bcl6* (Hatzi et al., 2015; Sheikh et al., 2019). It appeared feasible, that upon *Bcl6* loss, Tbet might be able to take over and convert the former Tfh cells into Th1 cells. Therefore, we set out to analyze the cell fate of *Bcl6*-ablated SMARTA cells in a model that does not involve substantial co-expression of TFs associated with other Th subsets in Tfh cells. This situation is generally found in the context of classical alum-based protein immunizations. To obtain results that are comparable with the findings during acute viral infections, we chose to use the SMARTA instead of the OT-II TCR-transgene (Barnden et al., 1998), which is more commonly used for studying Tfh cell responses during protein immunizations. The immunization was conducted with NP and SMARTA peptide GP<sub>61–80</sub> covalently linked to mouse serum albumin (NP-SM-MSA) as non-immunogenic carrier (Lahmann et al., 2019; Vu Van et al., 2016). Here, NP can be recognized by antigen-specific B cells that take up and process the complex and present the peptide on MHC-II molecules to SMARTA cells.

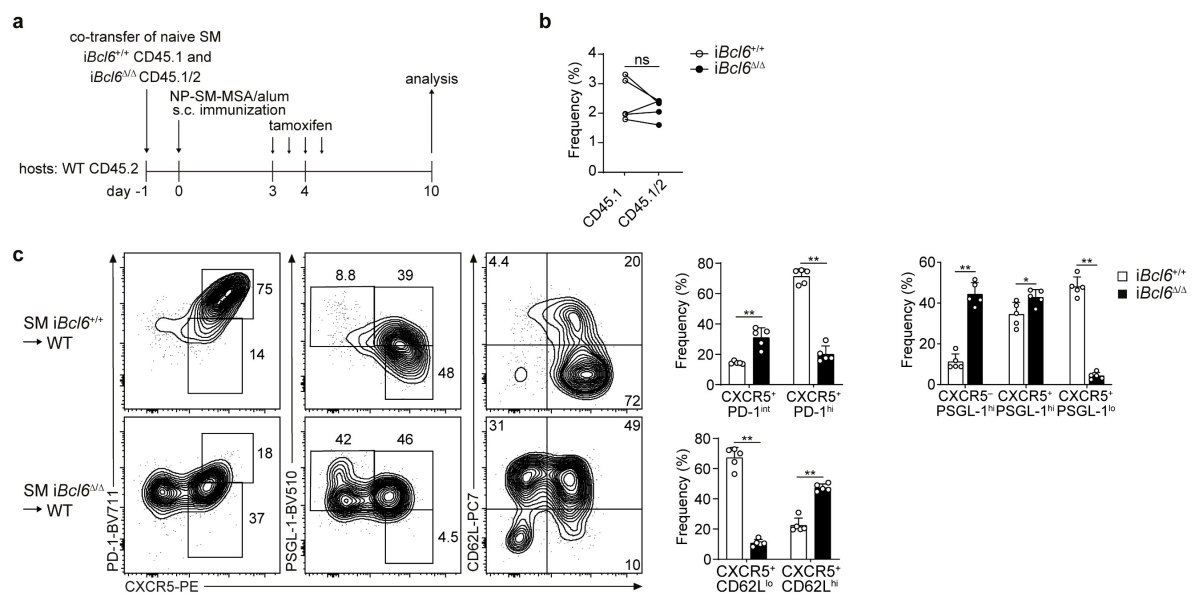


**Figure 22: Upregulation of the memory cell marker CD62L upon induced *Bcl6*-ablation.** **a** Experimental scheme for the analysis of the impact of tamoxifen-induced and T-cell specific deletion of *Bcl6* in SM cells after protein immunization. **b** Flow cytometric quantification of the frequencies of CD45.1 and CD45.1/2 CD4<sup>+</sup> T cells from the spleens of tamoxifen-treated WT recipients that had been given adoptive transfers of SM *iBcl6*<sup>+/+</sup> and SM *iBcl6*<sup>Δ/Δ</sup> cells, followed by immunization with NP-SM-MSA (s.c.) and analysis 10 days later. Pre-gated as live CD4<sup>+</sup>CD19<sup>-</sup>CD45.1 (*iBcl6*<sup>+/+</sup>) or CD45.1/2 (*iBcl6*<sup>Δ/Δ</sup>) lymphocytes. Each symbol represents an individual mouse (n = 5). **c** Flow cytometry of CD4<sup>+</sup> T cells from the spleens as in (b). Gate frequencies indicate percent of CXCR5<sup>+</sup>PD-1<sup>hi</sup> or CXCR5<sup>+</sup>PSGL-1<sup>lo</sup> GC Tfh cells and CXCR5<sup>+</sup>PD-1<sup>int</sup> or CXCR5<sup>+</sup>PSGL-1<sup>hi</sup> Tfh cells and CXCR5<sup>+</sup>CD62L<sup>hi</sup>, CXCR5<sup>+</sup>CD62L<sup>hi</sup> and CXCR5<sup>+</sup>CD62L<sup>lo</sup> cells. Quantification of the results (right panel). ns = not significant, \*\*P < 0.01 Wilcoxon matched-pairs signed rank test (b), two-tailed nonparametric Mann-Whitney test (c); mean + s.e.m. in c.

## Results

Analog to the previous experiments (**Fig 19, 21**), naive *iBcl6 $\Delta\Delta$*  or *iBcl6 $^{+/+}$*  SM cells were transferred into WT recipients, followed by subcutaneous immunization with NP-SM-MSA in alum and tamoxifen administration on day 3+4 (**Fig. 22a**). The total numbers of SMARTA cells on day 10 were unaffected by the induced KO (**Fig. 22b**). Flow cytometric assessment of Tfh cell markers revealed similarities to the observations made in the polyclonal Tfh cell response towards NP-KLH immunization (**Fig. 18**). The frequencies of CXCR5<sup>+</sup>PD-1<sup>hi</sup> GC Tfh cells were massively reduced from approximately 70% down to around 20% (**Fig. 22c**). As the fraction of CXCR5<sup>+</sup>PD-1<sup>int</sup> cells increased, it is feasible that the deletion of *Bcl6* caused a strong reduction of PD-1 and concomitantly also a rise of PSGL-1 levels in GC Tfh cells (**Fig. 22c**). Interestingly, CD62L, which is associated with memory Tfh cell formation (Kaji et al., 2016; Weber et al., 2012), was upregulated in both CXCR5<sup>-</sup> and CXCR5<sup>+</sup> CD4<sup>+</sup> T cells (**Fig. 22c**). However, although CCR7 levels were slightly increased (**Fig. 23**), the cells did not gain a CD62L<sup>hi</sup>CCR7<sup>hi</sup> memory phenotype (Hale et al., 2013; Kaji et al., 2016; Weber et al., 2012). In addition, the master regulator of the Th2 subset, GATA3, was significantly upregulated (**Fig. 23**), suggesting that the loss of *Bcl6* imposed a hybrid Th2/memory-like phenotype on the cells.

In summary, our data has demonstrated that continued *Bcl6* expression in CD4<sup>+</sup> T cells is required for the maintenance of Tfh and GC B cells. Particularly in GC Tfh cells, *Bcl6* was needed to obtain the highest levels of PD-1 and CXCR5 expression, while efficiently repressing PSGL-1 and CCR7. Concomitant with the loss of *Bcl6* in T cells, B cell response were only improperly sustained, with a pronounced defect in supporting class-switched GC B cells. Moreover, during an acute viral infection and protein immunization, *Bcl6* limited the phenotypic conversion into Th1 or Th2/memory T cell-like cells.

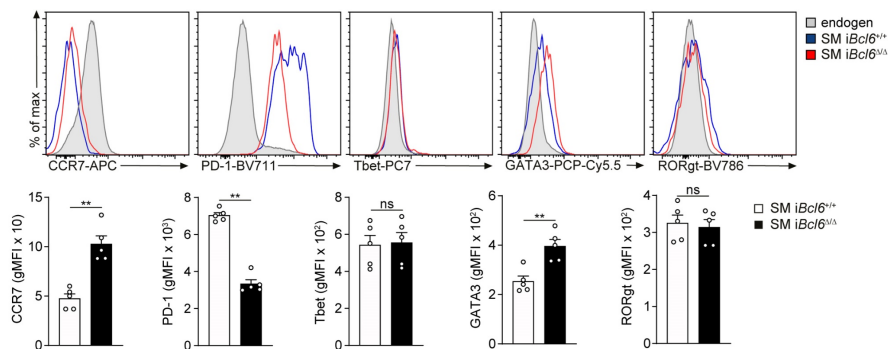


**Figure 23: GATA3 and CCR7 levels increase upon the loss of *Bcl6*.** WT recipient mice were given adoptive co-transfers of SM *iBcl6 $^{+/+}$*  and SM *iBcl6 $\Delta\Delta$*  cells, followed by immunization with NP-SM-MSA (s.c.) and tamoxifen gavage on day 3+4. Flow cytometric analyses of marker expression in SM cells on day 10. Pre-gated as live CD4<sup>+</sup>CD19<sup>-</sup>CD45.1<sup>+</sup> (*iBcl6 $^{+/+}$* ) or CD45.1<sup>+</sup>CD45.1<sup>-</sup> (*iBcl6 $\Delta\Delta$* ) lymphocytes. Quantification of the results as geometric mean (gMFI, lower panel), each symbol represents an individual mouse (n = 5). ns = not significant, \*\*P < 0.01 Student's t-test; mean + s.e.m.

## 8. Discussion

### 8.1. Tamoxifen-inducible KO mouse strains as tools to investigate the requirements of Tfh cell maintenance

Tfh cells are important regulators of humoral immune responses in health and disease. While the generation of these cells has been extensively studied (Crotty, 2011, 2019; Vinuesa et al., 2016), relatively little is known about the factors that regulate their cellular plasticity and maintenance (Baumjohann et al., 2013b; Meli et al., 2016; Weber et al., 2015). Investigating the molecular requirements of these processes is beneficial to obtain a better understanding of Tfh cell stability but also to explore the potential of targeting already formed Tfh cells in autoimmune diseases and cancer (Asai et al., 2019; Blanco et al., 2016; Ochando and Braza, 2017; Yan et al., 2017).

To assess the impact of an acute loss of Tfh cell hallmark molecules in pre-existing Tfh cells, a Tg (Aghajani et al., 2012) and a KI CD4-CreERT2 strain (Sledzinska et al., 2013) were compared to identify a suitable model allowing the temporally-guided deletion of genes specifically in CD4<sup>+</sup> T cells. This is particularly important as inducible Cre recombinases can vary greatly in terms of gene excision efficiency, specificity and toxicity (Becher et al., 2018; Kurachi et al., 2019; Reizis, 2019; Zeitrag et al., 2020). Although in our comparison experiments similar frequencies of recombination events were reported by the *Rosa26-eYFP* Cre reporter allele (Srinivas et al., 2001), as assessed by the fraction of eYFP<sup>+</sup>CD4<sup>+</sup> cells, profound differences between the two *Cd4-CreERT2* strains were observed.

First, deletion of a conditional *Cxcr5* allele in the Tg strain occurred almost exclusively within the eYFP<sup>+</sup>CD4<sup>+</sup> population, indicative of a lower Cre activity in the eYFP<sup>-</sup> cells. In contrast, efficient deletion of *Cxcr5* was evident in all CD4<sup>+</sup> T cells from KI mice regardless of eYFP expression, showing that the *Rosa26-eYFP* Cre reporter underestimates recombination at the *Cxcr5* locus in this system. Second, a striking difference was observed in the activation status of Cre reporter positive cells. While the frequencies of activated CD44<sup>hi</sup> cells in the KI strain were comparable between the eYFP<sup>-</sup> and eYFP<sup>+</sup> populations, a severe decrease in CD44<sup>hi</sup> cells was observed in the eYFP<sup>+</sup> fraction of the Tg strain. Cre toxicity was reported to primarily affect proliferating cells (Higashi et al., 2009; Kurachi et al., 2019), which are highly activated. This could explain why eYFP<sup>+</sup> cells with high Cre recombinase activity were mainly affected by this. Nevertheless, by this logic, eYFP<sup>-</sup>CD4<sup>+</sup> T cells should not be affected and have normal frequencies of CD44<sup>hi</sup> cells. Activated cells in this fraction were, however, significantly expanded, while the total frequencies of CD4<sup>+</sup> T cells with a CD44<sup>hi</sup> phenotype were comparable to WT mice. Therefore, it might be that the lower frequencies of activated cells were not a result of increased loss of proliferating cells, but rather a consequence of preferential Cre recombination in naive cells, resulting in an enrichment of naive cells within

the eYFP<sup>+</sup> population. Besides their construction strategies as Tg and KI mouse (Doyle et al., 2012), respectively, the observed deviations might also be due to differences in the CreERT2 fusion construct.

In summary, the two inducible-Cre strains are both suitable for certain applications. The broadly and commercially available Tg strain showed lower recombination efficiency for the conditional *Cxcr5* allele compared to the KI strain. Further, recombination appeared to occur preferentially in naive rather than in activated cells. Nevertheless, the *Rosa26-eYFP* allele reported faithfully on the recombination of *Cxcr5* in this system. This is advantageous, as eYFP<sup>-</sup> cells can be used as an intrinsic control here. The KI strain, in contrast, exhibited a higher efficiency of the recombination at the *Cxcr5* locus. Owing to the low number of cells that escaped the KO, it was possible to assess the impact on other cell types, similar to complete KO mice. These features rendered the strain suitable to study the effects of temporally-guided, CD4<sup>+</sup> T cell-specific gene ablation not only on Tfh cells, but also on the GC response. Consequently, the conditional *Cxcr5* and *Bcl6* alleles were crossed to the KI strain and used for all experiments thereafter. Finally, it has to be emphasized that it is crucial to use Cre positive animals without floxed alleles as controls to account for the adverse effects of inducible Cre recombinase expression described here and elsewhere (Becher et al., 2018; Kurachi et al., 2019; Zeitrag et al., 2020).

## 8.2. Induced *Cxcr5*-deficiency in CD4<sup>+</sup> T cells does not impair Tfh cell maintenance

After establishing a suitable and CD4-specific inducible-KO system, it was applied to address the T-cell intrinsic and extrinsic impact of an acute loss of CXCR5. The deletion of the hallmark chemokine receptor was induced at timepoints before and after the induction of a GC response. Upon early (day 3+4) or late (day 6+7) ablation in the context of a protein immunization, CXCR5<sup>+</sup> CD4<sup>+</sup> cells were nearly absent. The GC B cell response was generally intact and only mildly affected. Solely total GC B cell frequencies were about 2-fold decreased, while the fraction of antigen-specific and class-switched B cells were normal. Comparable results were obtained in studies with constitutively *Cxcr5*-deficient CD4<sup>+</sup> T cells (Arnold et al., 2007; Haynes et al., 2007). Either by transferring CXCR5<sup>-/-</sup> CD4<sup>+</sup> OTII T cells into WT hosts or by applying mixed-bone-marrow chimaeras, the authors showed that a lack of CXCR5 on T cells resulted in a diminished GC size and a 2-fold reduction in the frequencies of GC B and class-switched cells (Arnold et al., 2007; Haynes et al., 2007).

These findings were recently challenged by a publication showing that the GC B cell response was not affected in *Cd4-Cre<sup>+</sup>Cxcr5<sup>fl/fl</sup>* mice (Vanderleyden et al., 2020). On the one hand, this contradiction might be due to the different CXCR5 KO strategies: conditional allele versus straight KO in TCR-Tg cells. On the other hand, Vanderleyden et al. used an influenza infection model, in which antigen is highly abundant and CD4<sup>+</sup> T cells are strongly activated, while the

other studies applied conventional protein immunization (Arnold et al., 2007; Haynes et al., 2007). In fact, in the context of an acute LCMV infection, we did not observe an impaired GC B cell response upon induced *Cxcr5*-ablation. Furthermore, when *Cxcr5* was deleted prior to immunization, we were also able to confirm the findings from the aforementioned studies that reported decreased but not absent frequencies of GC B cells and class-switching (Arnold et al., 2007; Haynes et al., 2007). In contrast, *Cxcr5*-deletion after immunization did not result in an impairment of class-switching in this thesis. Recently, induction of CSR was shown to be an early event that precedes GC formation and depends on T-B cell interactions at the T-B cell border (Roco et al., 2019). This might explain why the loss of CXCR5 on day3 post immunization did not have an impact on CSR, while early *Cxcr5*-deficiency could have impeded the migration of early Tfh cells towards the B cell follicle.

In line with the generally intact B cell helper abilities, we found that *Cxcr5*-ablated CD4<sup>+</sup> T cells were able to maintain the localization within GCs. Similar findings were made using a priori CXCR5-lacking CD4<sup>+</sup> T cells (Arnold et al., 2007; Greczmiel et al., 2017; Haynes et al., 2007). This was surprising, as CXCR5 overexpression was shown to promote GC localization (Haynes et al., 2007; Shi et al., 2018). Potentially, CD4<sup>+</sup> T cells possess alternative modes of migration independent of CXCR5. A study by Okada et al. pointed out that CD4<sup>+</sup> T cells can also be passively dragged into the follicle by B cells (Okada et al., 2005). In addition, S1pr2 seems to be able to functionally compensate for the loss of CXCR5 to some extent, as only combined deletion of both factors yielded a complete abrogation of T cell recruitment into GCs (Moriyama et al., 2014). Furthermore, we observed in our experiments that induced *Cxcr5*-deficiency resulted in a loss of the Tfh cell-characteristic LZ polarization. This phenomenon was also observed with the constitutive *Cxcr5* KO system (Greczmiel et al., 2017; Haynes et al., 2007). The decrease in LZ T cells was associated with impaired affinity maturation in response to chronic LCMV infection (Greczmiel et al., 2017). Defective GC orientation of T cells that lack CXCR5 was intuitive, since the LZ is highly enriched for the CXCR5 ligand CXCL13 (Allen et al., 2004; Cyster et al., 2000). Furthermore, DZ/LZ cycling of B cells is mediated by alternating surface levels of CXCR4 and CXCR5, respectively (Allen et al., 2004). Hence, CXCR5-deficient B cells accumulate in the DZ and vice versa. Efficient T cell follicular entry could be important to ensure a diverse TCR repertoire in the GC reaction, which might not be crucial for model antigens, but for complex or mutating epitopes (Nikolich-Zugich et al., 2004). However, CCR7 downregulation seems to be the primary determinant to allow T cells to exit the T cell zone (Haynes et al., 2007). Taken together, this suggests that T cells do not only require CXCR5 for initial LZ positioning, but also to maintain this localization.

Notably, the phenotype of the CD4<sup>+</sup> T cells that were able to support GC responses independently of CXCR5 was not examined in these previous studies (Arnold et al., 2007;

Greczmiel et al., 2017; Haynes et al., 2007). In the model established in this work, a CXCR5<sup>-</sup> population co-expressing high levels of PD-1 and Bcl6 was observed when the KO was induced on day3 or day day6 following immunization. These cells appeared to be former Tfh cells that continued to express Tfh-associated molecules upon the loss of CXCR5. The maintenance of a Tfh-like expression pattern was also confirmed in antigen-specific CD4<sup>+</sup> T cells by analyzing LCMV tetramer-positive CD4<sup>+</sup> T cells in mice acutely infected with LCMV Armstrong. Even the global expression program was unaffected by *Cxcr5*-deletion as assessed by RNA-seq analysis of Tfh cells sufficient or deficient for *Cxcr5*. Furthermore, we did not observe a compensatory upregulation of chemokine receptors or other molecules associated with migration.

A possible disentanglement of CXCR5 and Tfh cell marker expression was reported in two studies in 2017. CD4<sup>+</sup> T cells with a CXCR5<sup>-</sup>PD-1<sup>hi</sup> phenotype, Tfh cell marker expression and B cell helper capacities are present in cancer tissues and in the joints of patients suffering from rheumatoid arthritis (Gu-Trantien et al., 2017; Rao et al., 2017). This is remarkable, as mice with a *Cxcr5*-deficient CD4<sup>+</sup> T cell compartment are resistant to collagen induced arthritis (Moschovakis et al., 2017). This might be due to species-specific differences in CXCR5 function or owing to the artificial nature of the collagen-induced mouse model. However, it is also conceivable that the entry into ectopic lymphoid-like structures, such as those found in patients with RA (Takemura et al., 2001; Timmer et al., 2007), does require CXCR5 expression, while the entry into GCs in lymphoid organs seems not to depend on CXCR5 (Arnold et al., 2007; Greczmiel et al., 2017; Haynes et al., 2007). Additionally, CXCR5-

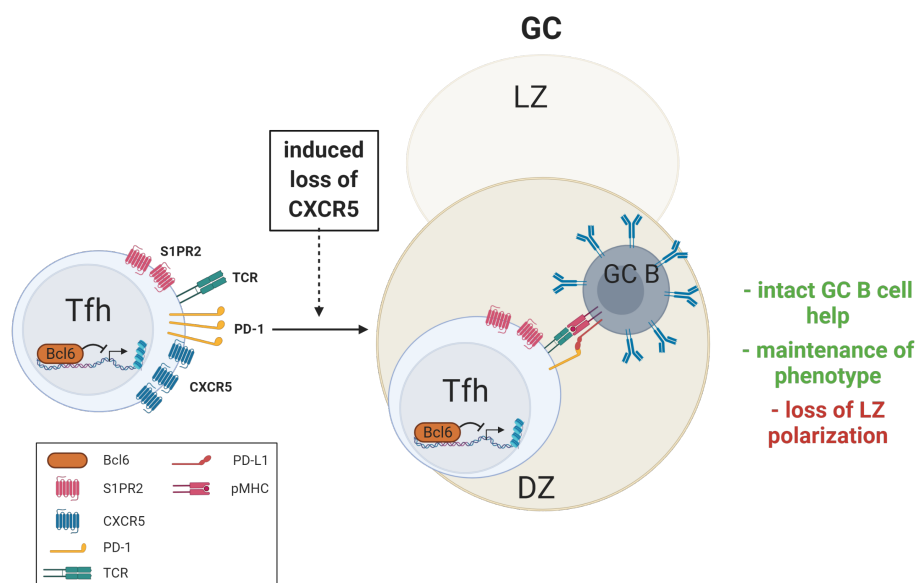


**Figure 24: The induced loss of *Cxcr5* in Tfh cells does not alter their phenotype, but abrogates the LZ polarization.** In the absence of CXCR5, Tfh cells continued to provide helper signals to GC B cells and maintained Tfh cell marker expression, while the characteristic LZ polarization in the GC was lost.

mediated LZ localization does not appear to play a role in the less organized ectopic GCs (Denton et al., 2019; Moyron-Quiroz et al., 2004). In summary, ablation of CXCR5 in pre-formed Tfh cells resulted in a moderate decrease of their GC B cell helper functions and a loss of the preferential LZ localization, while the overall Tfh cell phenotype was largely unaffected (**Fig. 24**).

It appears that CD4<sup>+</sup> T cells can not only bypass the need for surface CXCR5 expression to migrate into GCs (Moriyama et al., 2014), but even the maintenance of the Tfh cell phenotype was unaltered upon an acute loss of CXCR5, as suggested by the results in this work. In summary, this supports a model in which CXCR5 expression on CD4<sup>+</sup> T cells might serve different purposes during the distinct phases of the GC response. Initially, CXCR5 might enhance the efficiency of the migration of CD4<sup>+</sup> T towards and into the follicle, resulting in an increased size of the TCR repertoire within GCs. In established GCs, CXCR5 could function to restrain T cell help exclusively to the LZ, where GC B cells are selected based on BCR affinity.

### 8.3. Potential roles of *Bcl6* in established Tfh cells

*Bcl6* was shown to be necessary and sufficient to induce Tfh cell differentiation (Johnston et al., 2009; Nurieva et al., 2009; Yu et al., 2009), primarily by antagonizing the counterregulatory transcriptional repressor Blimp-1 (Johnston et al., 2009). T cell-specific *Bcl6*-deficiency abrogates Tfh cell differentiation and results in the absence of GC B cells (Hollister et al., 2013; Johnston et al., 2009; Nurieva et al., 2009; Yu et al., 2009). Studies applying ChIP-seq revealed that *Bcl6* regulates several important modules, comprising genes associated with migration, metabolism and differentiation into T effector cells (Hatzi et al., 2015; Liu et al., 2016b). Despite of its central role in promoting Tfh cell differentiation, it is not known if continued *Bcl6*-mediated repression of target genes is essential to maintain the Tfh cell phenotype.

In the experiments shown in this work, ablation of *Bcl6* in established Tfh cells through tamoxifen-induced Cre recombination resulted in a comprehensive loss of GC-Tfh cells in the context of protein immunization. This was observed for early ablation when tamoxifen was given on day 3+4 as well as for late ablation on day 6+7. The effect on non-GC Tfh cells, which reside in the follicle outside the GC or at the T-B cell border, was less critical. Seemingly, Tfh cells were more strongly affected when *Bcl6*-ablation was induced early. This could be due to a lower stability of Tfh cells at this timepoint of the immune response, although Tfh cells were reported to be fate committed early (Choi et al., 2013b). Alternatively, it could also be a result of the prolonged time period between KO induction and analysis, which allowed the effects to become more apparent. Regardless of the induction time point, the Tfh cell characteristic high levels of PD-1 were immediately lost upon *Bcl6*-deletion, while CXCR5 expression, which is strongly associated with *Bcl6* (Baumjohann et al., 2011; Choi et al., 2011; Johnston et al., 2009), persisted at reduced levels. Potentially, CXCR5 expression is maintained through other factors such as *Ascl-2* (Liu et al., 2014). As *Bcl6* was reported to positively regulate PD-1 expression, the observed downregulation might be a direct effect of the induced KO (Kroenke et al., 2012). Further, decreasing *Bcl6* levels were reported to result in a higher expression of Blimp-1 (Johnston et al., 2009), which restrains the expression of PD-1 in CD8<sup>+</sup> T cells (Lu et al., 2014). However, we did not look at Blimp-1 expression, as this is only weakly induced upon protein immunization and its flow cytometric detection is challenging (Kallies et al., 2004). Besides aberrant PD-1 expression, residual CXCR5<sup>+</sup> CD4<sup>+</sup> T cells also had increased PSGL-1 expression upon *Bcl6*-ablation. *Bcl6* was shown to directly bind and repress *Selplg*, which encodes PSGL-1, in human GC Tfh cells (Hatzi et al., 2015). Akin to the high levels of PD-1, low staining for PSGL-1 is characteristic for GC Tfh cells and separates them from Tfh cells (Crotty, 2014). The data presented in this thesis showed that GC Tfh cells were more strongly affected by the loss of *Bcl6* compared to Tfh cells.

GCs depict specified environments in which Tfh cells need to adapt to hypoxia (Zhu et al., 2019), run a chemotactic program to maintain LZ localization (Fuller et al., 1993; Haynes et al., 2007), and withstand an abundance of the counterregulatory cytokine IL-2 (Papillion et al., 2019). On the one hand, Bcl6 might serve here to repress migratory molecules that guide the migration towards the T cell zone, such as PSGL-1 and CCR7 or chemokine receptors that sense attractants outside the GC, e.g. EBI2 and S1PR1 (Hatzi et al., 2015; He et al., 2016; Vinuesa and Cyster, 2011). On the other hand, Bcl6 might protect GC Tfh from non-Tfh cell cues, e.g. IL-2 and IFN $\gamma$ , by inhibiting transcriptional programs of other Th cell subsets (Hatzi et al., 2015; Liu et al., 2016b). In contrast, Tfh cells outside the GC may not depend on Bcl6 in a similar manner. Generally, the observed loss of the Tfh cell phenotype upon *Bcl6*-ablation is comparable to studies in which T-B cell contacts were disrupted by blocking ICOSL:ICOS or other co-stimulatory pathways during the peak of the GC response (Akiba et al., 2005; Baumjohann et al., 2013b). Since co-stimulatory signaling through ICOS is able to stabilize Bcl6 levels by enhancing protein synthesis (Yi et al., 2017) and mRNA transcription (Stone et al., 2015; Xiao et al., 2014), it is conceivable that the effect of ICOS blocking antibodies is partly a result of diminished Bcl6 levels.

Interestingly, the frequencies of Tfr cells were hardly affected by the loss of Bcl6, and PD-1 expression by these cells was comparable to control mice. This is surprising, as Tfr cells are unable to form in mice with *Bcl6*-deficient Treg cells (Botta et al., 2017; Fu et al., 2018; Wu et al., 2016). However, Bcl6 expression levels in Tfr cells are lower compared to Tfh cells (Chung et al., 2011), and might potentially be dispensable after Tfr cell generation. Currently, the role of Bcl6 in Tfr cells is not well understood. It appears that Treg cells exploit the ability of Bcl6 to install a migratory program (Hatzi et al., 2015; Liu et al., 2016b), enabling the cells to localize to and enter follicles. Although our data showed that Tfr cells were phenotypically normal, it remains a possibility that their functionality is impaired when *Bcl6* is ablated. This was not addressed here, as the role of Tfr cells during protein immunization is still a matter of debate (Clement et al., 2019; Fu et al., 2018; Linterman et al., 2011; Wu et al., 2016) and suitable assays to assess Tfr cell functionality are still missing.

#### 8.4. Bcl6 as a gatekeeper of Tfh cell plasticity

GC Tfh cells are potent B cell helpers within the GC (Crotty, 2014) and their numbers correlate with those of GC B cells (Baumjohann et al., 2013b). Although a collapse of the GC Tfh cell population was observed upon *Bcl6*-ablation, GC B cells were not equally affected. Therefore, it is possible that residual CXCR5<sup>+</sup>PD-1<sup>lo</sup> CD4<sup>+</sup> T cells can functionally compensate for GC Tfh cells on certain aspects of GC biology, such as maintaining antigen-specific NP<sup>+</sup> GC B cells. In turn, normal frequencies of class-switched GC B cells were not sustained. The specific loss of IgG1<sup>+</sup> GC B cells might be a result of enhanced apoptosis, impaired proliferation (Gitlin et

al., 2015; Gitlin et al., 2014) or a premature exit from the GC of these cells (Li et al., 2018). Conceivably, CXCR5<sup>+</sup>PD-1<sup>lo</sup> cells fail to deliver suitable helper signals that are vital for class-switched GC B cells due to ineffective BCR signaling within GCs (Gitlin et al., 2016).

As opposed to *Cxcr5*, *Bcl6*-deletion resulted in a loss of Tfh-associated molecules that hampered the tracking and cell fate analyses of *Bcl6*-ablated cells. As congenically marked TCR-Tg cells can be easily followed *in vivo*, our data was complemented by observations from experiments with SM cells. During an acute viral infection, the total number of CD4<sup>+</sup> SM cells was not affected by the induced KO, indicating that *Bcl6*-deficiency did not result in diminished proliferation or enhanced apoptosis. Akin to the immunization experiments, GC Tfh cell frequencies were severely attenuated when *Bcl6* was ablated after GC induction. Moreover, Tfh cells were more strongly affected in the viral infection model, potentially because during a systemic viral infection non-Tfh cell cues, e.g. IL-2 and IFN $\gamma$ , are not only present in the GC, but throughout the secondary lymphoid organs. Therefore, Tfh cells in this context might also highly rely on the repression of Tfh-inappropriate genes by Bcl6. The decrease in Tfh cell numbers was paralleled by an increase in Th1 cells caused by a phenotypic conversion of ex-Tfh cells into Th1 cells when *Bcl6* was ablated. The bulk transcriptomes of *Bcl6*-deficient SM cells revealed that these cells were enriched for Th1 cell molecules while Tfh cell transcripts were diminished. This proved that *Bcl6*-ablation did not only result in a loss of certain Tfh cell-associated molecules, but indeed affected the global transcriptome. Hence, the cells underwent a profound transdifferentiation as opposed to mere local changes in the expression of hallmark molecules. It is important to mention that during acute LCMV infection, Tfh cells co-express Tbet and Bcl6 and possess certain traits of Th1 cells, such as IFN $\gamma$  production (Yusuf et al., 2010). Nevertheless, Th1 and Tfh cells still differ substantially during LCMV infection and Tfh cells express various other Tfh cell-defining TFs, e.g. TCF-1, LEF-1, *Ascl2* and *Thpok* (Choi et al., 2015; Liu et al., 2014; Vacchio et al., 2019; Xu et al., 2015), emphasizing the profound reprogramming the cells have to undergo to fully transdifferentiate into Th1 cells. Molecularly, the pronounced bias of Tfh cells to transdifferentiate towards Th1 cells when Bcl6 is not present, might be explained by an IL-6 dependent mechanism that was recently discovered (Papillion et al., 2019). Signaling via the IL-6-STAT3 axis during a viral infection mitigated strong IL-2 signals, which otherwise destabilized the Tfh cell phenotype. Upon *Bcl6*-ablation, we observed that *Il6st* and *Il6ra* transcripts were strongly reduced, which is very likely to result in impaired IL-6 signaling and thus enhanced susceptibility towards Th1 transdifferentiation.

Interestingly, *Bcl6*-deletion in the context of protein immunization with the SM-reactive LCMV epitope GP<sub>61-80</sub> resulted in upregulation of CD62L and the Th2 cell master regulator GATA3 in the transferred SM cells. Increased CD62L expression indicated memory Tfh cell formation

(Kaji et al., 2016; Weber et al., 2012), which also encompasses Bcl6 downregulation (Hale et al., 2013; Ise et al., 2014). However, upregulation of CCR7, another important characteristic of Tfh memory cells (Hale et al., 2013; Kaji et al., 2016; Weber et al., 2012), was not pronounced, arguing against the adoption of the memory cell fate. Instead, the increase in GATA3 expression suggested traits of a Th2 cell phenotype. Despite substantial IL-4 secretion, Tfh cells normally only express negligible amounts of GATA3 (Liang et al., 2011). Nevertheless, the *Gata3* locus in Tfh cells exhibits positive histone marks and is generally accessible (Lu et al., 2011). Furthermore, Tfh cells were reported to convert into pathogenic Th2 cells in the context of an *in vivo* allergy model (Ballesteros-Tato et al., 2016). It appeared that the loss of Bcl6 after protein immunization imposed a mixed Th2/memory-like phenotype on Tfh cells. In contrast, markers associated with memory or Th2 cells, were not seen to be upregulated in our transcriptomic analyses of *Bcl6*-deficient SMARTA cells during acute LCMV infection. The findings that *Bcl6*-ablated Tfh cells adopted a Th1 or a Th2 phenotype in an acute viral infection or during alum-based protein immunization, respectively, suggested that the direction of transdifferentiation is context-dependent. In conclusion, depending on the immune response type, *Bcl6*-ablation in Tfh cells resulted in a conversion into Th1 cells (LCMV) or Th2/memory-like T cells (LCMV peptide/alum) (Fig. 25).

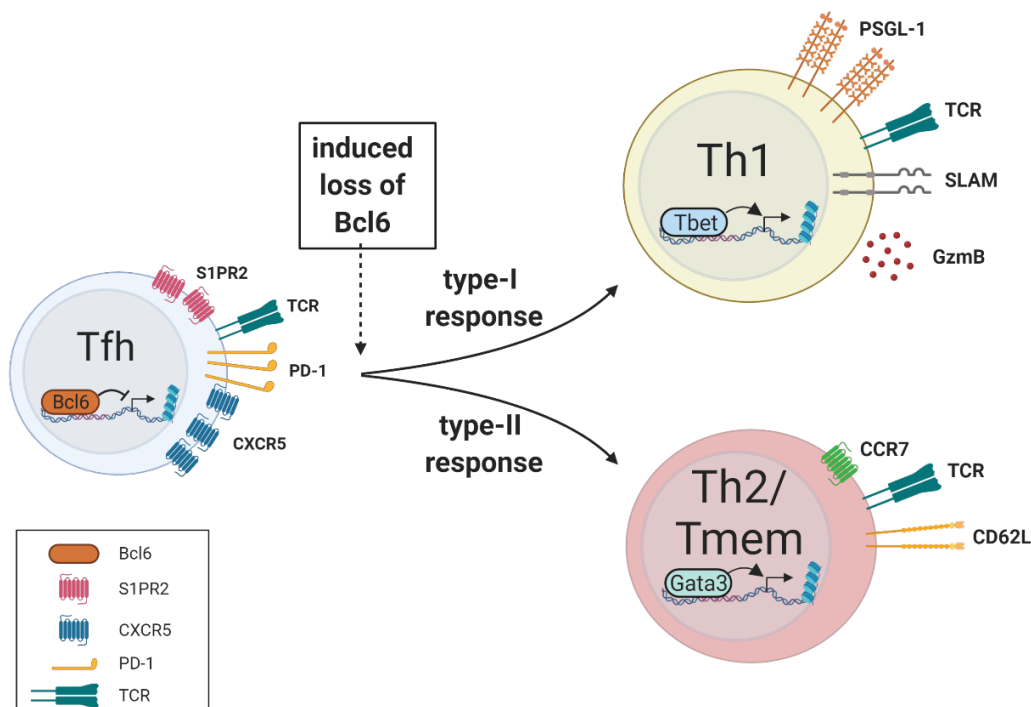


**Figure 25: Bcl6 as a gatekeeper of Tfh cell plasticity.** Depending on the context of an immune response, Bcl6 restricted the plasticity of Tfh cells towards Th1 cells (type I response) or Th2/memory-like T cells.

Taken together, our findings show that continued Bcl6 expression is required to preserve the identity and functionality of pre-formed Tfh cells. Particularly in GC Tfh cells, Bcl6 seems to be required to maintain the high expression levels of PD-1 and CXCR5, while efficiently repressing non-Tfh cell factors, e.g. PSGL-1 and SLAM. Additionally, Bcl6 appears to protect GC Tfh cells from non-Tfh cell cues abundantly present in GCs, where GC Tfh cells exert potent B cell helper functions to control affinity maturation and PC differentiation (Ersching et al., 2017; Gitlin et al., 2015; Krautler et al., 2017; Zhang et al., 2018). Here, Bcl6 also acts to restrain the transdifferentiation into the Th1 or Th2 cell subset to limit Tfh cell plasticity. As Tfh cells play detrimental roles in certain pathological situations such as follicular lymphoma and lupus (Ame-Thomas et al., 2012; Blanco et al., 2016; He et al., 2013), they have evolved as interesting therapeutic targets (Ochando and Braza, 2017; Yan et al., 2017). Instead of depletion, it might be beneficial to shift the phenotype of the harmful Tfh cells towards less pathogenic Th cells in lymphomas. This could be achieved by Bcl6 inhibition or degradation (Dupont et al., 2016; Kerres et al., 2017) in combination with Th1 cell cues, such as IL-2 (Ballesteros-Tato et al., 2012; He et al., 2016). As it was shown that Tfr cells can also develop from Foxp3<sup>-</sup> precursors (Aloulou et al., 2016), it might also be a promising approach to treat autoimmune diseases by converting Tfh into Tfr cells.

## 9. References

- Aghajani, K., Keerthivasan, S., Yu, Y., and Gounari, F. (2012). Generation of CD4CreER(T2) transgenic mice to study development of peripheral CD4-T-cells. *Genesis* *50*, 908-913.
- Ahmad, K.F., Melnick, A., Lax, S., Bouchard, D., Liu, J., Kiang, C.L., Mayer, S., Takahashi, S., Licht, J.D., and Prive, G.G. (2003). Mechanism of SMRT corepressor recruitment by the BCL6 BTB domain. *Mol Cell* *12*, 1551-1564.
- Akiba, H., Takeda, K., Kojima, Y., Usui, Y., Harada, N., Yamazaki, T., Ma, J., Tezuka, K., Yagita, H., and Okumura, K. (2005). The role of ICOS in the CXCR5+ follicular B helper T cell maintenance in vivo. *J Immunol* *175*, 2340-2348.
- Allen, C.D., Ansel, K.M., Low, C., Lesley, R., Tamamura, H., Fujii, N., and Cyster, J.G. (2004). Germinal center dark and light zone organization is mediated by CXCR4 and CXCR5. *Nat Immunol* *5*, 943-952.
- Allen, D., Simon, T., Sablitzky, F., Rajewsky, K., and Cumano, A. (1988). Antibody engineering for the analysis of affinity maturation of an anti-hapten response. *EMBO J* *7*, 1995-2001.
- Almishri, W., Santodomingo-Garzon, T., Le, T., Stack, D., Mody, C.H., and Swain, M.G. (2016). TNFalpha Augments Cytokine-Induced NK Cell IFNgamma Production through TNFR2. *J Innate Immun* *8*, 617-629.
- Alonso, M.N., Wong, M.T., Zhang, A.L., Winer, D., Suhoski, M.M., Tolentino, L.L., Gaitan, J., Davidson, M.G., Kung, T.H., Galel, D.M., *et al.* (2011). T(H)1, T(H)2, and T(H)17 cells instruct monocytes to differentiate into specialized dendritic cell subsets. *Blood* *118*, 3311-3320.
- Aloulou, M., Carr, E.J., Gador, M., Bignon, A., Liblau, R.S., Fazilleau, N., and Linterman, M.A. (2016). Follicular regulatory T cells can be specific for the immunizing antigen and derive from naive T cells. *Nat Commun* *7*, 10579.
- Ame-Thomas, P., Le Priol, J., Yssel, H., Caron, G., Pangault, C., Jean, R., Martin, N., Marafioti, T., Gaulard, P., Lamy, T., *et al.* (2012). Characterization of intratumoral follicular helper T cells in follicular lymphoma: role in the survival of malignant B cells. *Leukemia* *26*, 1053-1063.
- Amir, J., Scott, M.G., Nahm, M.H., and Granoff, D.M. (1990). Bactericidal and opsonic activity of IgG1 and IgG2 anticapsular antibodies to Haemophilus influenzae type b. *J Infect Dis* *162*, 163-171.
- Ansel, K.M., McHeyzer-Williams, L.J., Ngo, V.N., McHeyzer-Williams, M.G., and Cyster, J.G. (1999). In vivo-activated CD4 T cells upregulate CXC chemokine receptor 5 and reprogram their response to lymphoid chemokines. *J Exp Med* *190*, 1123-1134.
- Arnold, C.N., Campbell, D.J., Lipp, M., and Butcher, E.C. (2007). The germinal center response is impaired in the absence of T cell-expressed CXCR5. *European journal of immunology* *37*, 100-109.
- Asai, Y., Chiba, H., Nishikiori, H., Kamekura, R., Yabe, H., Kondo, S., Miyajima, S., Shigehara, K., Ichimiya, S., and Takahashi, H. (2019). Aberrant populations of circulating T follicular helper cells and regulatory B cells underlying idiopathic pulmonary fibrosis. *Respir Res* *20*, 244.
- Bagnoli, J.W., Ziegenhain, C., Janjic, A., Wange, L.E., Vieth, B., Parekh, S., Geuder, J., Hellmann, I., and Enard, W. (2018). Sensitive and powerful single-cell RNA sequencing using mcSCR-seq. *Nat Commun* *9*, 2937.
- Ballesteros-Tato, A., Leon, B., Graf, B.A., Moquin, A., Adams, P.S., Lund, F.E., and Randall, T.D. (2012). Interleukin-2 inhibits germinal center formation by limiting T follicular helper cell differentiation. *Immunity* *36*, 847-856.
- Ballesteros-Tato, A., Randall, T.D., Lund, F.E., Spolski, R., Leonard, W.J., and Leon, B. (2016). T Follicular Helper Cell Plasticity Shapes Pathogenic T Helper 2 Cell-Mediated Immunity to Inhaled House Dust Mite. *Immunity* *44*, 259-273.

## References

- Barnden, M.J., Allison, J., Heath, W.R., and Carbone, F.R. (1998). Defective TCR expression in transgenic mice constructed using cDNA-based alpha- and beta-chain genes under the control of heterologous regulatory elements. *Immunol Cell Biol* 76, 34-40.
- Basso, K., and Dalla-Favera, R. (2012). Roles of BCL6 in normal and transformed germinal center B cells. *Immunol Rev* 247, 172-183.
- Baumjohann, D., and Ansel, K.M. (2015). Tracking early T follicular helper cell differentiation in vivo. *Methods Mol Biol* 1291, 27-38.
- Baumjohann, D., Kageyama, R., Clingan, J.M., Morar, M.M., Patel, S., de Kouchkovsky, D., Bannard, O., Bluestone, J.A., Matloubian, M., Ansel, K.M., and Jeker, L.T. (2013a). The microRNA cluster miR-17 approximately 92 promotes TFH cell differentiation and represses subset-inappropriate gene expression. *Nat Immunol* 14, 840-848.
- Baumjohann, D., Okada, T., and Ansel, K.M. (2011). Cutting Edge: Distinct waves of BCL6 expression during T follicular helper cell development. *J Immunol* 187, 2089-2092.
- Baumjohann, D., Preite, S., Reboldi, A., Ronchi, F., Ansel, K.M., Lanzavecchia, A., and Sallusto, F. (2013b). Persistent antigen and germinal center B cells sustain T follicular helper cell responses and phenotype. *Immunity* 38, 596-605.
- Becher, B., Waisman, A., and Lu, L.F. (2018). Conditional Gene-Targeting in Mice: Problems and Solutions. *Immunity* 48, 835-836.
- Blanco, P., Ueno, H., and Schmitt, N. (2016). T follicular helper (Tfh) cells in lupus: Activation and involvement in SLE pathogenesis. *European journal of immunology* 46, 281-290.
- Boehm, T., Hirano, M., Holland, S.J., Das, S., Schorpp, M., and Cooper, M.D. (2018). Evolution of Alternative Adaptive Immune Systems in Vertebrates. *Annu Rev Immunol* 36, 19-42.
- Botta, D., Fuller, M.J., Marquez-Lago, T.T., Bachus, H., Bradley, J.E., Weinmann, A.S., Zajac, A.J., Randall, T.D., Lund, F.E., Leon, B., and Ballesteros-Tato, A. (2017). Dynamic regulation of T follicular regulatory cell responses by interleukin 2 during influenza infection. *Nat Immunol* 18, 1249-1260.
- Bradford, B.M., Reizis, B., and Mabbott, N.A. (2017). Oral Prion Disease Pathogenesis Is Impeded in the Specific Absence of CXCR5-Expressing Dendritic Cells. *J Virol* 91.
- Breitfeld, D., Ohl, L., Kremmer, E., Ellwart, J., Sallusto, F., Lipp, M., and Forster, R. (2000). Follicular B helper T cells express CXC chemokine receptor 5, localize to B cell follicles, and support immunoglobulin production. *J Exp Med* 192, 1545-1552.
- Cannons, J.L., Lu, K.T., and Schwartzberg, P.L. (2013). T follicular helper cell diversity and plasticity. *Trends Immunol* 34, 200-207.
- Cannons, J.L., Qi, H., Lu, K.T., Dutta, M., Gomez-Rodriguez, J., Cheng, J., Wakeland, E.K., Germain, R.N., and Schwartzberg, P.L. (2010). Optimal germinal center responses require a multistage T cell:B cell adhesion process involving integrins, SLAM-associated protein, and CD84. *Immunity* 32, 253-265.
- Cattoretti, G., Chang, C.C., Cechova, K., Zhang, J., Ye, B.H., Falini, B., Louie, D.C., Offit, K., Chaganti, R.S., and Dalla-Favera, R. (1995). BCL-6 protein is expressed in germinal-center B cells. *Blood* 86, 45-53.
- Chen, G., Shaw, M.H., Kim, Y.G., and Nunez, G. (2009). NOD-like receptors: role in innate immunity and inflammatory disease. *Annu Rev Pathol* 4, 365-398.
- Chi, H. (2012). Regulation and function of mTOR signalling in T cell fate decisions. *Nat Rev Immunol* 12, 325-338.
- Choi, Y.S., Eto, D., Yang, J.A., Lao, C., and Crotty, S. (2013a). Cutting edge: STAT1 is required for IL-6-mediated Bcl6 induction for early follicular helper cell differentiation. *J Immunol* 190, 3049-3053.

## References

- Choi, Y.S., Gullicksrud, J.A., Xing, S., Zeng, Z., Shan, Q., Li, F., Love, P.E., Peng, W., Xue, H.H., and Crotty, S. (2015). LEF-1 and TCF-1 orchestrate T(FH) differentiation by regulating differentiation circuits upstream of the transcriptional repressor Bcl6. *Nat Immunol* *16*, 980-990.
- Choi, Y.S., Kageyama, R., Eto, D., Escobar, T.C., Johnston, R.J., Monticelli, L., Lao, C., and Crotty, S. (2011). ICOS receptor instructs T follicular helper cell versus effector cell differentiation via induction of the transcriptional repressor Bcl6. *Immunity* *34*, 932-946.
- Choi, Y.S., Yang, J.A., Yusuf, I., Johnston, R.J., Greenbaum, J., Peters, B., and Crotty, S. (2013b). Bcl6 expressing follicular helper CD4 T cells are fate committed early and have the capacity to form memory. *J Immunol* *190*, 4014-4026.
- Chung, Y., Tanaka, S., Chu, F., Nurieva, R.I., Martinez, G.J., Rawal, S., Wang, Y.H., Lim, H., Reynolds, J.M., Zhou, X.H., *et al.* (2011). Follicular regulatory T cells expressing Foxp3 and Bcl-6 suppress germinal center reactions. *Nat Med* *17*, 983-988.
- Ci, W., Polo, J.M., Cerchiatti, L., Shaknovich, R., Wang, L., Yang, S.N., Ye, K., Farinha, P., Horsman, D.E., Gascoyne, R.D., *et al.* (2009). The BCL6 transcriptional program features repression of multiple oncogenes in primary B cells and is deregulated in DLBCL. *Blood* *113*, 5536-5548.
- Clement, R.L., Daccache, J., Mohammed, M.T., Diallo, A., Blazar, B.R., Kuchroo, V.K., Lovitch, S.B., Sharpe, A.H., and Sage, P.T. (2019). Follicular regulatory T cells control humoral and allergic immunity by restraining early B cell responses. *Nat Immunol* *20*, 1360-1371.
- Coffey, A.J., Brooksbank, R.A., Brandau, O., Oohashi, T., Howell, G.R., Bye, J.M., Cahn, A.P., Durham, J., Heath, P., Wray, P., *et al.* (1998). Host response to EBV infection in X-linked lymphoproliferative disease results from mutations in an SH2-domain encoding gene. *Nat Genet* *20*, 129-135.
- Coffman, R.L., Seymour, B.W., Hudak, S., Jackson, J., and Rennick, D. (1989). Antibody to interleukin-5 inhibits helminth-induced eosinophilia in mice. *Science* *245*, 308-310.
- Cooper, M.D., and Alder, M.N. (2006). The evolution of adaptive immune systems. *Cell* *124*, 815-822.
- Crotty, S. (2011). Follicular helper CD4 T cells (TFH). *Annu Rev Immunol* *29*, 621-663.
- Crotty, S. (2014). T follicular helper cell differentiation, function, and roles in disease. *Immunity* *41*, 529-542.
- Crotty, S. (2015). A brief history of T cell help to B cells. *Nat Rev Immunol* *15*, 185-189.
- Crotty, S. (2019). T Follicular Helper Cell Biology: A Decade of Discovery and Diseases. *Immunity* *50*, 1132-1148.
- Crotty, S., Johnston, R.J., and Schoenberger, S.P. (2010). Effectors and memories: Bcl-6 and Blimp-1 in T and B lymphocyte differentiation. *Nat Immunol* *11*, 114-120.
- Cumano, A., and Rajewsky, K. (1986). Clonal recruitment and somatic mutation in the generation of immunological memory to the hapten NP. *EMBO J* *5*, 2459-2468.
- Cyster, J.G., Ansel, K.M., Reif, K., Ekland, E.H., Hyman, P.L., Tang, H.L., Luther, S.A., and Ngo, V.N. (2000). Follicular stromal cells and lymphocyte homing to follicles. *Immunol Rev* *176*, 181-193.
- Davis, M.M., and Bjorkman, P.J. (1988). T-cell antigen receptor genes and T-cell recognition. *Nature* *334*, 395-402.
- De Silva, N.S., and Klein, U. (2015). Dynamics of B cells in germinal centres. *Nat Rev Immunol* *15*, 137-148.
- Deenick, E.K., Chan, A., Ma, C.S., Gatto, D., Schwartzberg, P.L., Brink, R., and Tangye, S.G. (2010). Follicular helper T cell differentiation requires continuous antigen presentation that is independent of unique B cell signaling. *Immunity* *33*, 241-253.

## References

- Denton, A.E., Innocentin, S., Carr, E.J., Bradford, B.M., Lafouresse, F., Mabbott, N.A., Morbe, U., Ludewig, B., Groom, J.R., Good-Jacobson, K.L., and Linterman, M.A. (2019). Type I interferon induces CXCL13 to support ectopic germinal center formation. *J Exp Med* 216, 621-637.
- Dobin, A., Davis, C.A., Schlesinger, F., Drenkow, J., Zaleski, C., Jha, S., Batut, P., Chaisson, M., and Gingeras, T.R. (2013). STAR: ultrafast universal RNA-seq aligner. *Bioinformatics* 29, 15-21.
- Dong, C., and Flavell, R.A. (2000). Control of T helper cell differentiation--in search of master genes. *Sci STKE* 2000, pe1.
- Dong, C., Juedes, A.E., Temann, U.A., Shresta, S., Allison, J.P., Ruddle, N.H., and Flavell, R.A. (2001). ICOS co-stimulatory receptor is essential for T-cell activation and function. *Nature* 409, 97-101.
- Doyle, A., McGarry, M.P., Lee, N.A., and Lee, J.J. (2012). The construction of transgenic and gene knockout/knockin mouse models of human disease. *Transgenic Res* 21, 327-349.
- Dupont, T., Yang, S.N., Patel, J., Hatzi, K., Malik, A., Tam, W., Martin, P., Leonard, J., Melnick, A., and Cerchietti, L. (2016). Selective targeting of BCL6 induces oncogene addiction switching to BCL2 in B-cell lymphoma. *Oncotarget* 7, 3520-3532.
- Dutko, F.J., and Oldstone, M.B. (1983). Genomic and biological variation among commonly used lymphocytic choriomeningitis virus strains. *J Gen Virol* 64 (Pt 8), 1689-1698.
- Elsner, R.A., Ernst, D.N., and Baumgarth, N. (2012). Single and coexpression of CXCR4 and CXCR5 identifies CD4 T helper cells in distinct lymph node niches during influenza virus infection. *J Virol* 86, 7146-7157.
- Ersching, J., Efeyan, A., Mesin, L., Jacobsen, J.T., Pasqual, G., Grabiner, B.C., Dominguez-Sola, D., Sabatini, D.M., and Vitorica, G.D. (2017). Germinal Center Selection and Affinity Maturation Require Dynamic Regulation of mTORC1 Kinase. *Immunity* 46, 1045-1058 e1046.
- Eto, D., Lao, C., DiToro, D., Barnett, B., Escobar, T.C., Kageyama, R., Yusuf, I., and Crotty, S. (2011). IL-21 and IL-6 are critical for different aspects of B cell immunity and redundantly induce optimal follicular helper CD4 T cell (Tfh) differentiation. *PLoS One* 6, e17739.
- Farrell, H.E., and Shellam, G.R. (1991). Protection against murine cytomegalovirus infection by passive transfer of neutralizing and non-neutralizing monoclonal antibodies. *J Gen Virol* 72 (Pt 1), 149-156.
- Fazilleau, N., McHeyzer-Williams, L.J., Rosen, H., and McHeyzer-Williams, M.G. (2009). The function of follicular helper T cells is regulated by the strength of T cell antigen receptor binding. *Nat Immunol* 10, 375-384.
- Ferguson, S.E., Han, S., Kelsoe, G., and Thompson, C.B. (1996). CD28 is required for germinal center formation. *J Immunol* 156, 4576-4581.
- Fu, W., Liu, X., Lin, X., Feng, H., Sun, L., Li, S., Chen, H., Tang, H., Lu, L., Jin, W., and Dong, C. (2018). Deficiency in T follicular regulatory cells promotes autoimmunity. *J Exp Med* 215, 815-825.
- Fujita, N., Jaye, D.L., Geigerman, C., Akyildiz, A., Mooney, M.R., Boss, J.M., and Wade, P.A. (2004). MTA3 and the Mi-2/NuRD complex regulate cell fate during B lymphocyte differentiation. *Cell* 119, 75-86.
- Fuller, K.A., Kanagawa, O., and Nahm, M.H. (1993). T cells within germinal centers are specific for the immunizing antigen. *J Immunol* 151, 4505-4512.
- Geng, H., Hurtz, C., Lenz, K.B., Chen, Z., Baumjohann, D., Thompson, S., Goloviznina, N.A., Chen, W.Y., Huan, J., LaTocha, D., et al. (2015). Self-enforcing feedback activation between BCL6 and pre-B cell receptor signaling defines a distinct subtype of acute lymphoblastic leukemia. *Cancer Cell* 27, 409-425.
- Gigoux, M., Shang, J., Pak, Y., Xu, M., Choe, J., Mak, T.W., and Suh, W.K. (2009). Inducible costimulator promotes helper T-cell differentiation through phosphoinositide 3-kinase. *Proceedings of the National Academy of Sciences of the United States of America* 106, 20371-20376.

## References

- Gitlin, A.D., Mayer, C.T., Oliveira, T.Y., Shulman, Z., Jones, M.J., Koren, A., and Nussenzweig, M.C. (2015). T cell help controls the speed of the cell cycle in germinal center B cells. *Science* **349**, 643-646.
- Gitlin, A.D., Shulman, Z., and Nussenzweig, M.C. (2014). Clonal selection in the germinal centre by regulated proliferation and hypermutation. *Nature* **509**, 637-640.
- Gitlin, A.D., von Boehmer, L., Gazumyan, A., Shulman, Z., Oliveira, T.Y., and Nussenzweig, M.C. (2016). Independent Roles of Switching and Hypermutation in the Development and Persistence of B Lymphocyte Memory. *Immunity* **44**, 769-781.
- Glasmacher, E., Hoefig, K.P., Vogel, K.U., Rath, N., Du, L., Wolf, C., Kremmer, E., Wang, X., and Heissmeyer, V. (2010). Roquin binds inducible costimulator mRNA and effectors of mRNA decay to induce microRNA-independent post-transcriptional repression. *Nat Immunol* **11**, 725-733.
- Goenka, R., Barnett, L.G., Silver, J.S., O'Neill, P.J., Hunter, C.A., Cancro, M.P., and Laufer, T.M. (2011). Cutting edge: dendritic cell-restricted antigen presentation initiates the follicular helper T cell program but cannot complete ultimate effector differentiation. *J Immunol* **187**, 1091-1095.
- Greczmiel, U., Krautler, N.J., Pedrioli, A., Bartsch, I., Agnellini, P., Bedenikovic, G., Harker, J., Richter, K., and Oxenius, A. (2017). Sustained T follicular helper cell response is essential for control of chronic viral infection. *Sci Immunol* **2**.
- Grimbacher, B., Hutloff, A., Schlesier, M., Glocker, E., Warnatz, K., Drager, R., Eibel, H., Fischer, B., Schaffer, A.A., Mages, H.W., *et al.* (2003). Homozygous loss of ICOS is associated with adult-onset common variable immunodeficiency. *Nat Immunol* **4**, 261-268.
- Gu-Trantien, C., Migliori, E., Buisseret, L., de Wind, A., Brohee, S., Garaud, S., Noel, G., Dang Chi, V.L., Lodewyckx, J.N., Naveaux, C., *et al.* (2017). CXCL13-producing TFH cells link immune suppression and adaptive memory in human breast cancer. *JCI insight* **2**.
- Gu, Z., Eils, R., and Schlesner, M. (2016). Complex heatmaps reveal patterns and correlations in multidimensional genomic data. *Bioinformatics* **32**, 2847-2849.
- Hale, J.S., Youngblood, B., Latner, D.R., Mohammed, A.U., Ye, L., Akondy, R.S., Wu, T., Iyer, S.S., and Ahmed, R. (2013). Distinct memory CD4<sup>+</sup> T cells with commitment to T follicular helper- and T helper 1-cell lineages are generated after acute viral infection. *Immunity* **38**, 805-817.
- Hatzi, K., Jiang, Y., Huang, C., Garrett-Bakelman, F., Gearhart, M.D., Giannopoulou, E.G., Zumbo, P., Kirouac, K., Bhaskara, S., Polo, J.M., *et al.* (2013). A hybrid mechanism of action for BCL6 in B cells defined by formation of functionally distinct complexes at enhancers and promoters. *Cell Rep* **4**, 578-588.
- Hatzi, K., Nance, J.P., Kroenke, M.A., Bothwell, M., Haddad, E.K., Melnick, A., and Crotty, S. (2015). BCL6 orchestrates Tfh cell differentiation via multiple distinct mechanisms. *J Exp Med* **212**, 539-553.
- Haynes, N.M., Allen, C.D., Lesley, R., Ansel, K.M., Killeen, N., and Cyster, J.G. (2007). Role of CXCR5 and CCR7 in follicular Th cell positioning and appearance of a programmed cell death gene-1high germinal center-associated subpopulation. *J Immunol* **179**, 5099-5108.
- Hazenbos, W.L., Heijnen, I.A., Meyer, D., Hofhuis, F.M., Renardel de Lavalette, C.R., Schmidt, R.E., Capel, P.J., van de Winkel, J.G., Gessner, J.E., van den Berg, T.K., and Verbeek, J.S. (1998). Murine IgG1 complexes trigger immune effector functions predominantly via Fc gamma RIII (CD16). *J Immunol* **161**, 3026-3032.
- He, J., Tsai, L.M., Leong, Y.A., Hu, X., Ma, C.S., Chevalier, N., Sun, X., Vandenberg, K., Rockman, S., Ding, Y., *et al.* (2013). Circulating precursor CCR7(lo)PD-1(hi) CXCR5(+) CD4(+) T cells indicate Tfh cell activity and promote antibody responses upon antigen reexposure. *Immunity* **39**, 770-781.
- He, J., Zhang, X., Wei, Y., Sun, X., Chen, Y., Deng, J., Jin, Y., Gan, Y., Hu, X., Jia, R., *et al.* (2016). Low-dose interleukin-2 treatment selectively modulates CD4(+) T cell subsets in patients with systemic lupus erythematosus. *Nat Med* **22**, 991-993.

## References

- Hemmi, H., Takeuchi, O., Kawai, T., Kaisho, T., Sato, S., Sanjo, H., Matsumoto, M., Hoshino, K., Wagner, H., Takeda, K., and Akira, S. (2000). A Toll-like receptor recognizes bacterial DNA. *Nature* *408*, 740-745.
- Higashi, A.Y., Ikawa, T., Muramatsu, M., Economides, A.N., Niwa, A., Okuda, T., Murphy, A.J., Rojas, J., Heike, T., Nakahata, T., *et al.* (2009). Direct hematological toxicity and illegitimate chromosomal recombination caused by the systemic activation of CreERT2. *J Immunol* *182*, 5633-5640.
- Hollister, K., Kusam, S., Wu, H., Clegg, N., Mondal, A., Sawant, D.V., and Dent, A.L. (2013). Insights into the role of Bcl6 in follicular Th cells using a new conditional mutant mouse model. *J Immunol* *191*, 3705-3711.
- Hutloff, A., Dittrich, A.M., Beier, K.C., Eljaschewitsch, B., Kraft, R., Anagnostopoulos, I., and Kroccek, R.A. (1999). ICOS is an inducible T-cell co-stimulator structurally and functionally related to CD28. *Nature* *397*, 263-266.
- Ichii, H., Sakamoto, A., Arima, M., Hatano, M., Kuroda, Y., and Tokuhisa, T. (2007). Bcl6 is essential for the generation of long-term memory CD4+ T cells. *Int Immunol* *19*, 427-433.
- Ichiyama, K., Gonzalez-Martin, A., Kim, B.S., Jin, H.Y., Jin, W., Xu, W., Sabouri-Ghomi, M., Xu, S., Zheng, P., Xiao, C., and Dong, C. (2016). The MicroRNA-183-96-182 Cluster Promotes T Helper 17 Cell Pathogenicity by Negatively Regulating Transcription Factor Foxo1 Expression. *Immunity* *44*, 1284-1298.
- Ise, W., Fujii, K., Shiroguchi, K., Ito, A., Kometani, K., Takeda, K., Kawakami, E., Yamashita, K., Suzuki, K., Okada, T., and Kurosaki, T. (2018). T Follicular Helper Cell-Germinal Center B Cell Interaction Strength Regulates Entry into Plasma Cell or Recycling Germinal Center Cell Fate. *Immunity* *48*, 702-715 e704.
- Ise, W., Inoue, T., McLachlan, J.B., Kometani, K., Kubo, M., Okada, T., and Kurosaki, T. (2014). Memory B cells contribute to rapid Bcl6 expression by memory follicular helper T cells. *Proceedings of the National Academy of Sciences of the United States of America* *111*, 11792-11797.
- Ise, W., Kohyama, M., Schraml, B.U., Zhang, T., Schwer, B., Basu, U., Alt, F.W., Tang, J., Oltz, E.M., Murphy, T.L., and Murphy, K.M. (2011). The transcription factor BATF controls the global regulators of class-switch recombination in both B cells and T cells. *Nat Immunol* *12*, 536-543.
- Jain, A., and Pasare, C. (2017). Innate Control of Adaptive Immunity: Beyond the Three-Signal Paradigm. *J Immunol* *198*, 3791-3800.
- Jeltsch, K.M., Hu, D., Brenner, S., Zoller, J., Heinz, G.A., Nagel, D., Vogel, K.U., Rehage, N., Warth, S.C., Edlmann, S.L., *et al.* (2014). Cleavage of roquin and regnase-1 by the paracaspase MALT1 releases their cooperatively repressed targets to promote T(H)17 differentiation. *Nat Immunol* *15*, 1079-1089.
- Johnson, J.L., Georgakilas, G., Petrovic, J., Kurachi, M., Cai, S., Harly, C., Pear, W.S., Bhandoola, A., Wherry, E.J., and Vahedi, G. (2018). Lineage-Determining Transcription Factor TCF-1 Initiates the Epigenetic Identity of T Cells. *Immunity* *48*, 243-257 e210.
- Johnston, R.J., Choi, Y.S., Diamond, J.A., Yang, J.A., and Crotty, S. (2012). STAT5 is a potent negative regulator of TFH cell differentiation. *J Exp Med* *209*, 243-250.
- Johnston, R.J., Poholek, A.C., DiToro, D., Yusuf, I., Eto, D., Barnett, B., Dent, A.L., Craft, J., and Crotty, S. (2009). Bcl6 and Blimp-1 are reciprocal and antagonistic regulators of T follicular helper cell differentiation. *Science* *325*, 1006-1010.
- Kageyama, R., Cannons, J.L., Zhao, F., Yusuf, I., Lao, C., Locci, M., Schwartzberg, P.L., and Crotty, S. (2012). The receptor Ly108 functions as a SAP adaptor-dependent on-off switch for T cell help to B cells and NKT cell development. *Immunity* *36*, 986-1002.
- Kaji, T., Hijikata, A., Ishige, A., Kitami, T., Watanabe, T., Ohara, O., Yanaka, N., Okada, M., Shimoda, M., Taniguchi, M., and Takemori, T. (2016). CD4 memory T cells develop and acquire functional competence by sequential cognate interactions and stepwise gene regulation. *Int Immunol* *28*, 267-282.

## References

- Kallies, A., Hasbold, J., Tarlinton, D.M., Dietrich, W., Corcoran, L.M., Hodgkin, P.D., and Nutt, S.L. (2004). Plasma cell ontogeny defined by quantitative changes in blimp-1 expression. *J Exp Med* *200*, 967-977.
- Kang, S.G., Liu, W.H., Lu, P., Jin, H.Y., Lim, H.W., Shepherd, J., Fremgen, D., Verdin, E., Oldstone, M.B., Qi, H., *et al.* (2013). MicroRNAs of the miR-17 approximately 92 family are critical regulators of T(FH) differentiation. *Nat Immunol* *14*, 849-857.
- Kelsoe, G. (1996). The germinal center: a crucible for lymphocyte selection. *Semin Immunol* *8*, 179-184.
- Kerres, N., Steurer, S., Schlager, S., Bader, G., Berger, H., Caligiuri, M., Dank, C., Engen, J.R., Ettmayer, P., Fischerauer, B., *et al.* (2017). Chemically Induced Degradation of the Oncogenic Transcription Factor BCL6. *Cell Rep* *20*, 2860-2875.
- Kipps, T.J., Parham, P., Punt, J., and Herzenberg, L.A. (1985). Importance of immunoglobulin isotype in human antibody-dependent, cell-mediated cytotoxicity directed by murine monoclonal antibodies. *J Exp Med* *161*, 1-17.
- Kitano, M., Moriyama, S., Ando, Y., Hikida, M., Mori, Y., Kurosaki, T., and Okada, T. (2011). Bcl6 protein expression shapes pre-germinal center B cell dynamics and follicular helper T cell heterogeneity. *Immunity* *34*, 961-972.
- Klaus, G.G., Pepys, M.B., Kitajima, K., and Askonas, B.A. (1979). Activation of mouse complement by different classes of mouse antibody. *Immunology* *38*, 687-695.
- Krautler, N.J., Suan, D., Butt, D., Bourne, K., Hermes, J.R., Chan, T.D., Sundling, C., Kaplan, W., Schofield, P., Jackson, J., *et al.* (2017). Differentiation of germinal center B cells into plasma cells is initiated by high-affinity antigen and completed by Tfh cells. *J Exp Med* *214*, 1259-1267.
- Krishnamoorthy, V., Kannanganat, S., Maienschein-Cline, M., Cook, S.L., Chen, J., Bahroos, N., Sievert, E., Corse, E., Chong, A., and Sciammas, R. (2017). The IRF4 Gene Regulatory Module Functions as a Read-Write Integrator to Dynamically Coordinate T Helper Cell Fate. *Immunity* *47*, 481-497 e487.
- Kroenke, M.A., Eto, D., Locci, M., Cho, M., Davidson, T., Haddad, E.K., and Crotty, S. (2012). Bcl6 and Maf cooperate to instruct human follicular helper CD4 T cell differentiation. *J Immunol* *188*, 3734-3744.
- Kurachi, M., Ngiow, S.F., Kurachi, J., Chen, Z., and Wherry, E.J. (2019). Hidden Caveat of Inducible Cre Recombinase. *Immunity* *51*, 591-592.
- Lahmann, A., Kuhrau, J., Fuhrmann, F., Heinrich, F., Bauer, L., Durek, P., Mashreghi, M.F., and Hutloff, A. (2019). Bach2 Controls T Follicular Helper Cells by Direct Repression of Bcl-6. *J Immunol* *202*, 2229-2239.
- Leavenworth, J.W., Verbinen, B., Yin, J., Huang, H., and Cantor, H. (2015). A p85alpha-osteopontin axis couples the receptor ICOS to sustained Bcl-6 expression by follicular helper and regulatory T cells. *Nat Immunol* *16*, 96-106.
- Lee, C.H., Melchers, M., Wang, H., Torrey, T.A., Slota, R., Qi, C.F., Kim, J.Y., Lugar, P., Kong, H.J., Farrington, L., *et al.* (2006). Regulation of the germinal center gene program by interferon (IFN) regulatory factor 8/IFN consensus sequence-binding protein. *J Exp Med* *203*, 63-72.
- Lee, J.Y., Skon, C.N., Lee, Y.J., Oh, S., Taylor, J.J., Malhotra, D., Jenkins, M.K., Rosenfeld, M.G., Hogquist, K.A., and Jameson, S.C. (2015). The transcription factor KLF2 restrains CD4(+) T follicular helper cell differentiation. *Immunity* *42*, 252-264.
- Lee, Y., Awasthi, A., Yosef, N., Quintana, F.J., Xiao, S., Peters, A., Wu, C., Kleinewietfeld, M., Kunder, S., Hafler, D.A., *et al.* (2012). Induction and molecular signature of pathogenic TH17 cells. *Nat Immunol* *13*, 991-999.

## References

- Lemercier, C., Brocard, M.P., Puvion-Dutilleul, F., Kao, H.Y., Albagli, O., and Khochbin, S. (2002). Class II histone deacetylases are directly recruited by BCL6 transcriptional repressor. *J Biol Chem* 277, 22045-22052.
- Lenschow, D.J., Su, G.H., Zuckerman, L.A., Nabavi, N., Jellis, C.L., Gray, G.S., Miller, J., and Bluestone, J.A. (1993). Expression and functional significance of an additional ligand for CTLA-4. *Proceedings of the National Academy of Sciences of the United States of America* 90, 11054-11058.
- Li, X., Gadzinsky, A., Gong, L., Tong, H., Calderon, V., Li, Y., Kitamura, D., Klein, U., Langdon, W.Y., Hou, F., *et al.* (2018). Cbl Ubiquitin Ligases Control B Cell Exit from the Germinal-Center Reaction. *Immunity* 48, 530-541 e536.
- Li, X.Y., Wu, Z.B., Ding, J., Zheng, Z.H., Li, X.Y., Chen, L.N., and Zhu, P. (2012). Role of the frequency of blood CD4(+) CXCR5(+) CCR6(+) T cells in autoimmunity in patients with Sjogren's syndrome. *Biochem Biophys Res Commun* 422, 238-244.
- Liang, H.E., Reinhardt, R.L., Bando, J.K., Sullivan, B.M., Ho, I.C., and Locksley, R.M. (2011). Divergent expression patterns of IL-4 and IL-13 define unique functions in allergic immunity. *Nat Immunol* 13, 58-66.
- Liang, L., Porter, E.M., and Sha, W.C. (2002). Constitutive expression of the B7h ligand for inducible costimulator on naive B cells is extinguished after activation by distinct B cell receptor and interleukin 4 receptor-mediated pathways and can be rescued by CD40 signaling. *J Exp Med* 196, 97-108.
- Lilienthal, G.M., Rahmoller, J., Petry, J., Bartsch, Y.C., Leliavski, A., and Ehlers, M. (2018). Potential of Murine IgG1 and Human IgG4 to Inhibit the Classical Complement and Fcgamma Receptor Activation Pathways. *Front Immunol* 9, 958.
- Linterman, M.A., Pierson, W., Lee, S.K., Kallies, A., Kawamoto, S., Rayner, T.F., Srivastava, M., Divekar, D.P., Beaton, L., Hogan, J.J., *et al.* (2011). Foxp3+ follicular regulatory T cells control the germinal center response. *Nat Med* 17, 975-982.
- Liu, D., Xu, H., Shih, C., Wan, Z., Ma, X., Ma, W., Luo, D., and Qi, H. (2015). T-B-cell entanglement and ICOSL-driven feed-forward regulation of germinal centre reaction. *Nature* 517, 214-218.
- Liu, S., Chan, H.L., Bai, F., Ma, J., Scott, A., Robbins, D.J., Capobianco, A.J., Zhu, P., and Pei, X.H. (2016a). Gata3 restrains B cell proliferation and cooperates with p18INK4c to repress B cell lymphomagenesis. *Oncotarget* 7, 64007-64020.
- Liu, X., Chen, X., Zhong, B., Wang, A., Wang, X., Chu, F., Nurieva, R.I., Yan, X., Chen, P., van der Flier, L.G., *et al.* (2014). Transcription factor achaete-scute homologue 2 initiates follicular T-helper-cell development. *Nature* 507, 513-518.
- Liu, X., Lu, H., Chen, T., Nallaparaju, K.C., Yan, X., Tanaka, S., Ichiyama, K., Zhang, X., Zhang, L., Wen, X., *et al.* (2016b). Genome-wide Analysis Identifies Bcl6-Controlled Regulatory Networks during T Follicular Helper Cell Differentiation. *Cell Rep* 14, 1735-1747.
- Liu, X., Nurieva, R.I., and Dong, C. (2013). Transcriptional regulation of follicular T-helper (Tfh) cells. *Immunol Rev* 252, 139-145.
- Livak, K.J., and Schmittgen, T.D. (2001). Analysis of relative gene expression data using real-time quantitative PCR and the 2<sup>-Delta Delta C(T)</sup> Method. *Methods* 25, 402-408.
- Love, M.I., Huber, W., and Anders, S. (2014). Moderated estimation of fold change and dispersion for RNA-seq data with DESeq2. *Genome Biol* 15, 550.
- Lu, K.T., Kanno, Y., Cannons, J.L., Handon, R., Bible, P., Elkahlon, A.G., Anderson, S.M., Wei, L., Sun, H., O'Shea, J.J., and Schwartzberg, P.L. (2011). Functional and epigenetic studies reveal multistep differentiation and plasticity of in vitro-generated and in vivo-derived follicular T helper cells. *Immunity* 35, 622-632.

## References

- Lu, P., Youngblood, B.A., Austin, J.W., Mohammed, A.U., Butler, R., Ahmed, R., and Boss, J.M. (2014). Blimp-1 represses CD8 T cell expression of PD-1 using a feed-forward transcriptional circuit during acute viral infection. *J Exp Med* 211, 515-527.
- Ma, J., Zhu, C., Ma, B., Tian, J., Baidoo, S.E., Mao, C., Wu, W., Chen, J., Tong, J., Yang, M., *et al.* (2012). Increased frequency of circulating follicular helper T cells in patients with rheumatoid arthritis. *Clin Dev Immunol* 2012, 827480.
- Maul, J., Alterauge, D., and Baumjohann, D. (2019). MicroRNA-mediated regulation of T follicular helper and T follicular regulatory cell identity. *Immunol Rev* 288, 97-111.
- McGeachy, M.J., Bak-Jensen, K.S., Chen, Y., Tato, C.M., Blumenschein, W., McClanahan, T., and Cua, D.J. (2007). TGF-beta and IL-6 drive the production of IL-17 and IL-10 by T cells and restrain T(H)-17 cell-mediated pathology. *Nat Immunol* 8, 1390-1397.
- McHeyzer-Williams, M.G., Nossal, G.J., and Lalor, P.A. (1991). Molecular characterization of single memory B cells. *Nature* 350, 502-505.
- Medzhitov, R., and Janeway, C.A., Jr. (1997). Innate immunity: the virtues of a nonclonal system of recognition. *Cell* 91, 295-298.
- Melamed, D., Benschop, R.J., Cambier, J.C., and Nemazee, D. (1998). Developmental regulation of B lymphocyte immune tolerance compartmentalizes clonal selection from receptor selection. *Cell* 92, 173-182.
- Meli, A.P., Fontes, G., Avery, D.T., Leddon, S.A., Tam, M., Elliot, M., Ballesteros-Tato, A., Miller, J., Stevenson, M.M., Fowell, D.J., *et al.* (2016). The Integrin LFA-1 Controls T Follicular Helper Cell Generation and Maintenance. *Immunity* 45, 831-846.
- Mendez, L.M., Polo, J.M., Yu, J.J., Krupski, M., Ding, B.B., Melnick, A., and Ye, B.H. (2008). CtBP is an essential corepressor for BCL6 autoregulation. *Mol Cell Biol* 28, 2175-2186.
- Mittrucker, H.W., Kohler, A., Mak, T.W., and Kaufmann, S.H. (1999). Critical role of CD28 in protective immunity against *Salmonella typhimurium*. *J Immunol* 163, 6769-6776.
- Miyauchi, K., Sugimoto-Ishige, A., Harada, Y., Adachi, Y., Usami, Y., Kaji, T., Inoue, K., Hasegawa, H., Watanabe, T., Hijikata, A., *et al.* (2016). Protective neutralizing influenza antibody response in the absence of T follicular helper cells. *Nat Immunol* 17, 1447-1458.
- Moriyama, S., Takahashi, N., Green, J.A., Hori, S., Kubo, M., Cyster, J.G., and Okada, T. (2014). Sphingosine-1-phosphate receptor 2 is critical for follicular helper T cell retention in germinal centers. *J Exp Med* 211, 1297-1305.
- Moschovakis, G.L., Bubke, A., Friedrichsen, M., Falk, C.S., Feederle, R., and Forster, R. (2017). T cell specific *Cxcr5* deficiency prevents rheumatoid arthritis. *Sci Rep* 7, 8933.
- Mosmann, T.R., Cherwinski, H., Bond, M.W., Giedlin, M.A., and Coffman, R.L. (1986). Two types of murine helper T cell clone. I. Definition according to profiles of lymphokine activities and secreted proteins. *J Immunol* 136, 2348-2357.
- Mosmann, T.R., and Coffman, R.L. (1989). TH1 and TH2 cells: different patterns of lymphokine secretion lead to different functional properties. *Annu Rev Immunol* 7, 145-173.
- Moyron-Quiroz, J.E., Rangel-Moreno, J., Kusser, K., Hartson, L., Sprague, F., Goodrich, S., Woodland, D.L., Lund, F.E., and Randall, T.D. (2004). Role of inducible bronchus associated lymphoid tissue (iBALT) in respiratory immunity. *Nat Med* 10, 927-934.
- Myles, A., Gearhart, P.J., and Cancro, M.P. (2017). Signals that drive T-bet expression in B cells. *Cell Immunol* 321, 3-7.
- Niessl, J., and Kaufmann, D.E. (2018). Harnessing T Follicular Helper Cell Responses for HIV Vaccine Development. *Viruses* 10.

## References

- Nikolich-Zugich, J., Slifka, M.K., and Messaoudi, I. (2004). The many important facets of T-cell repertoire diversity. *Nat Rev Immunol* 4, 123-132.
- Niu, H., Ye, B.H., and Dalla-Favera, R. (1998). Antigen receptor signaling induces MAP kinase-mediated phosphorylation and degradation of the BCL-6 transcription factor. *Genes Dev* 12, 1953-1961.
- Nurieva, R.I., Chung, Y., Hwang, D., Yang, X.O., Kang, H.S., Ma, L., Wang, Y.H., Watowich, S.S., Jetten, A.M., Tian, Q., and Dong, C. (2008). Generation of T follicular helper cells is mediated by interleukin-21 but independent of T helper 1, 2, or 17 cell lineages. *Immunity* 29, 138-149.
- Nurieva, R.I., Chung, Y., Martinez, G.J., Yang, X.O., Tanaka, S., Matskevitch, T.D., Wang, Y.H., and Dong, C. (2009). Bcl6 mediates the development of T follicular helper cells. *Science* 325, 1001-1005.
- Nurieva, R.I., Podd, A., Chen, Y., Alekseev, A.M., Yu, M., Qi, X., Huang, H., Wen, R., Wang, J., Li, H.S., *et al.* (2012). STAT5 protein negatively regulates T follicular helper (Tfh) cell generation and function. *J Biol Chem* 287, 11234-11239.
- O'Shea, J.J., Lahesmaa, R., Vahedi, G., Laurence, A., and Kanno, Y. (2011). Genomic views of STAT function in CD4+ T helper cell differentiation. *Nat Rev Immunol* 11, 239-250.
- Ochando, J., and Braza, M.S. (2017). T follicular helper cells: a potential therapeutic target in follicular lymphoma. *Oncotarget* 8, 112116-112131.
- Oestreich, K.J., Huang, A.C., and Weinmann, A.S. (2011). The lineage-defining factors T-bet and Bcl-6 collaborate to regulate Th1 gene expression patterns. *J Exp Med* 208, 1001-1013.
- Oestreich, K.J., Mohn, S.E., and Weinmann, A.S. (2012). Molecular mechanisms that control the expression and activity of Bcl-6 in TH1 cells to regulate flexibility with a TFH-like gene profile. *Nat Immunol* 13, 405-411.
- Oestreich, K.J., Read, K.A., Gilbertson, S.E., Hough, K.P., McDonald, P.W., Krishnamoorthy, V., and Weinmann, A.S. (2014). Bcl-6 directly represses the gene program of the glycolysis pathway. *Nat Immunol* 15, 957-964.
- Okada, T., Miller, M.J., Parker, I., Krummel, M.F., Neighbors, M., Hartley, S.B., O'Garra, A., Cahalan, M.D., and Cyster, J.G. (2005). Antigen-engaged B cells undergo chemotaxis toward the T zone and form motile conjugates with helper T cells. *PLoS Biol* 3, e150.
- Oxenius, A., Bachmann, M.F., Zinkernagel, R.M., and Hengartner, H. (1998). Virus-specific MHC-class II-restricted TCR-transgenic mice: effects on humoral and cellular immune responses after viral infection. *European journal of immunology* 28, 390-400.
- Ozaki, K., Spolski, R., Ettinger, R., Kim, H.P., Wang, G., Qi, C.F., Hwu, P., Shaffer, D.J., Akilesh, S., Roopenian, D.C., *et al.* (2004). Regulation of B cell differentiation and plasma cell generation by IL-21, a novel inducer of Blimp-1 and Bcl-6. *J Immunol* 173, 5361-5371.
- Papillion, A., Powell, M.D., Chisolm, D.A., Bachus, H., Fuller, M.J., Weinmann, A.S., Villarino, A., O'Shea, J.J., Leon, B., Oestreich, K.J., and Ballesteros-Tato, A. (2019). Inhibition of IL-2 responsiveness by IL-6 is required for the generation of GC-TFH cells. *Sci Immunol* 4.
- Parekh, S., Ziegenhain, C., Vieth, B., Enard, W., and Hellmann, I. (2018). zUMIs - A fast and flexible pipeline to process RNA sequencing data with UMIs. *Gigascience* 7.
- Pasqualucci, L., Migliazza, A., Basso, K., Houldsworth, J., Chaganti, R.S., and Dalla-Favera, R. (2003). Mutations of the BCL6 proto-oncogene disrupt its negative autoregulation in diffuse large B-cell lymphoma. *Blood* 101, 2914-2923.
- Pedros, C., Zhang, Y., Hu, J.K., Choi, Y.S., Canonigo-Balancio, A.J., Yates, J.R., 3rd, Altman, A., Crotty, S., and Kong, K.F. (2016). A TRAF-like motif of the inducible costimulator ICOS controls development of germinal center TFH cells via the kinase TBK1. *Nat Immunol* 17, 825-833.

## References

- Phan, R.T., Saito, M., Kitagawa, Y., Means, A.R., and Dalla-Favera, R. (2007). Genotoxic stress regulates expression of the proto-oncogene Bcl6 in germinal center B cells. *Nat Immunol* **8**, 1132-1139.
- Poholek, A.C., Hansen, K., Hernandez, S.G., Eto, D., Chandele, A., Weinstein, J.S., Dong, X., Odegard, J.M., Kaech, S.M., Dent, A.L., *et al.* (2010). In vivo regulation of Bcl6 and T follicular helper cell development. *J Immunol* **185**, 313-326.
- Pratama, A., Srivastava, M., Williams, N.J., Papa, I., Lee, S.K., Dinh, X.T., Hutloff, A., Jordan, M.A., Zhao, J.L., Casellas, R., *et al.* (2015). MicroRNA-146a regulates ICOS-ICOSL signalling to limit accumulation of T follicular helper cells and germinal centres. *Nat Commun* **6**, 6436.
- Qi, H. (2016). T follicular helper cells in space-time. *Nat Rev Immunol* **16**, 612-625.
- Qi, H., Cannons, J.L., Klauschen, F., Schwartzberg, P.L., and Germain, R.N. (2008). SAP-controlled T-B cell interactions underlie germinal centre formation. *Nature* **455**, 764-769.
- Ranuncolo, S.M., Polo, J.M., Dierov, J., Singer, M., Kuo, T., Greally, J., Green, R., Carroll, M., and Melnick, A. (2007). Bcl-6 mediates the germinal center B cell phenotype and lymphomagenesis through transcriptional repression of the DNA-damage sensor ATR. *Nat Immunol* **8**, 705-714.
- Ranuncolo, S.M., Polo, J.M., and Melnick, A. (2008). BCL6 represses CHEK1 and suppresses DNA damage pathways in normal and malignant B-cells. *Blood Cells Mol Dis* **41**, 95-99.
- Rao, D.A., Gurish, M.F., Marshall, J.L., Slowikowski, K., Fonseka, C.Y., Liu, Y., Donlin, L.T., Henderson, L.A., Wei, K., Mizoguchi, F., *et al.* (2017). Pathologically expanded peripheral T helper cell subset drives B cells in rheumatoid arthritis. *Nature* **542**, 110-114.
- Reinhardt, R.L., Liang, H.E., and Locksley, R.M. (2009). Cytokine-secreting follicular T cells shape the antibody repertoire. *Nat Immunol* **10**, 385-393.
- Reizis, B. (2019). The Specificity of Conditional Gene Targeting: A Case for Cre Reporters. *Immunity* **51**, 593-594.
- Roco, J.A., Mesin, L., Binder, S.C., Nefzger, C., Gonzalez-Figueroa, P., Canete, P.F., Ellyard, J., Shen, Q., Robert, P.A., Cappello, J., *et al.* (2019). Class-Switch Recombination Occurs Infrequently in Germinal Centers. *Immunity* **51**, 337-350 e337.
- Rogers, S., Wells, R., and Rechsteiner, M. (1986). Amino acid sequences common to rapidly degraded proteins: the PEST hypothesis. *Science* **234**, 364-368.
- Rolf, J., Bell, S.E., Kovcsdi, D., Janas, M.L., Soond, D.R., Webb, L.M., Santinelli, S., Saunders, T., Hebeis, B., Killeen, N., *et al.* (2010). Phosphoinositide 3-kinase activity in T cells regulates the magnitude of the germinal center reaction. *J Immunol* **185**, 4042-4052.
- Roufosse, F. (2018). Targeting the Interleukin-5 Pathway for Treatment of Eosinophilic Conditions Other than Asthma. *Front Med (Lausanne)* **5**, 49.
- Rudd, C.E., and Schneider, H. (2003). Unifying concepts in CD28, ICOS and CTLA4 co-receptor signalling. *Nat Rev Immunol* **3**, 544-556.
- Saito, M., Gao, J., Basso, K., Kitagawa, Y., Smith, P.M., Bhagat, G., Pernis, A., Pasqualucci, L., and Dalla-Favera, R. (2007). A signaling pathway mediating downregulation of BCL6 in germinal center B cells is blocked by BCL6 gene alterations in B cell lymphoma. *Cancer Cell* **12**, 280-292.
- Sebbag, M., Parry, S.L., Brennan, F.M., and Feldmann, M. (1997). Cytokine stimulation of T lymphocytes regulates their capacity to induce monocyte production of tumor necrosis factor-alpha, but not interleukin-10: possible relevance to pathophysiology of rheumatoid arthritis. *European journal of immunology* **27**, 624-632.
- Seder, R.A., Darrah, P.A., and Roederer, M. (2008). T-cell quality in memory and protection: implications for vaccine design. *Nat Rev Immunol* **8**, 247-258.

## References

- Sheikh, A.A., Cooper, L., Feng, M., Souza-Fonseca-Guimaraes, F., Lafouresse, F., Duckworth, B.C., Huntington, N.D., Moon, J.J., Pellegrini, M., Nutt, S.L., *et al.* (2019). Context-Dependent Role for T-bet in T Follicular Helper Differentiation and Germinal Center Function following Viral Infection. *Cell Rep* **28**, 1758-1772 e1754.
- Shi, J., Hou, S., Fang, Q., Liu, X., Liu, X., and Qi, H. (2018). PD-1 Controls Follicular T Helper Cell Positioning and Function. *Immunity* **49**, 264-274 e264.
- Shinnakasu, R., and Kurosaki, T. (2017). Regulation of memory B and plasma cell differentiation. *Curr Opin Immunol* **45**, 126-131.
- Shulman, Z., Gitlin, A.D., Weinstein, J.S., Lainez, B., Esplugues, E., Flavell, R.A., Craft, J.E., and Nussenzweig, M.C. (2014). Dynamic signaling by T follicular helper cells during germinal center B cell selection. *Science* **345**, 1058-1062.
- Simpson, N., Gatenby, P.A., Wilson, A., Malik, S., Fulcher, D.A., Tangye, S.G., Manku, H., Vyse, T.J., Roncador, G., Huttley, G.A., *et al.* (2010). Expansion of circulating T cells resembling follicular helper T cells is a fixed phenotype that identifies a subset of severe systemic lupus erythematosus. *Arthritis Rheum* **62**, 234-244.
- Sledzinska, A., Hemmers, S., Mair, F., Gorka, O., Ruland, J., Fairbairn, L., Nissler, A., Muller, W., Waisman, A., Becher, B., and Buch, T. (2013). TGF-beta signalling is required for CD4(+) T cell homeostasis but dispensable for regulatory T cell function. *PLoS Biol* **11**, e1001674.
- Snell, L.M., Osokine, I., Yamada, D.H., De la Fuente, J.R., Elsaesser, H.J., and Brooks, D.G. (2016). Overcoming CD4 Th1 Cell Fate Restrictions to Sustain Antiviral CD8 T Cells and Control Persistent Virus Infection. *Cell Rep* **16**, 3286-3296.
- Snook, J.P., Kim, C., and Williams, M.A. (2018). TCR signal strength controls the differentiation of CD4(+) effector and memory T cells. *Sci Immunol* **3**.
- Srinivas, S., Watanabe, T., Lin, C.S., William, C.M., Tanabe, Y., Jessell, T.M., and Costantini, F. (2001). Cre reporter strains produced by targeted insertion of EYFP and ECFP into the ROSA26 locus. *BMC Dev Biol* **1**, 4.
- Stathopoulou, C., Gangaplara, A., Mallett, G., Flomerfelt, F.A., Liniany, L.P., Knight, D., Samsel, L.A., Berlinguer-Palmini, R., Yim, J.J., Felizardo, T.C., *et al.* (2018). PD-1 Inhibitory Receptor Downregulates Asparaginyl Endopeptidase and Maintains Foxp3 Transcription Factor Stability in Induced Regulatory T Cells. *Immunity* **49**, 247-263 e247.
- Stockinger, B. (1992). Capacity of antigen uptake by B cells, fibroblasts or macrophages determines efficiency of presentation of a soluble self antigen (C5) to T lymphocytes. *European journal of immunology* **22**, 1271-1278.
- Stone, E.L., Pepper, M., Katayama, C.D., Kerdiles, Y.M., Lai, C.Y., Emslie, E., Lin, Y.C., Yang, E., Goldrath, A.W., Li, M.O., *et al.* (2015). ICOS coreceptor signaling inactivates the transcription factor FOXO1 to promote Tfh cell differentiation. *Immunity* **42**, 239-251.
- Streeck, H., D'Souza, M.P., Littman, D.R., and Crotty, S. (2013). Harnessing CD4(+) T cell responses in HIV vaccine development. *Nat Med* **19**, 143-149.
- Suan, D., Nguyen, A., Moran, I., Bourne, K., Hermes, J.R., Arshi, M., Hampton, H.R., Tomura, M., Miwa, Y., Kelleher, A.D., *et al.* (2015). T Follicular Helper Cells Have Distinct Modes of Migration and Molecular Signatures in Naive and Memory Immune Responses. *Immunity*.
- Suan, D., Sundling, C., and Brink, R. (2017). Plasma cell and memory B cell differentiation from the germinal center. *Curr Opin Immunol* **45**, 97-102.
- Suresh, M., Singh, A., and Fischer, C. (2005). Role of tumor necrosis factor receptors in regulating CD8 T-cell responses during acute lymphocytic choriomeningitis virus infection. *J Virol* **79**, 202-213.

## References

- Szabo, S.J., Kim, S.T., Costa, G.L., Zhang, X., Fathman, C.G., and Glimcher, L.H. (2000). A novel transcription factor, T-bet, directs Th1 lineage commitment. *Cell* *100*, 655-669.
- Tada, H., Aiba, S., Shibata, K., Ohteki, T., and Takada, H. (2005). Synergistic effect of Nod1 and Nod2 agonists with toll-like receptor agonists on human dendritic cells to generate interleukin-12 and T helper type 1 cells. *Infect Immun* *73*, 7967-7976.
- Tafuri, A., Shahinian, A., Blatt, F., Yoshinaga, S.K., Jordana, M., Wakeham, A., Boucher, L.M., Bouchard, D., Chan, V.S., Duncan, G., *et al.* (2001). ICOS is essential for effective T-helper-cell responses. *Nature* *409*, 105-109.
- Tahilian, V., Hutchinson, T.E., Abboud, G., Croft, M., and Salek-Ardakani, S. (2017). OX40 Cooperates with ICOS To Amplify Follicular Th Cell Development and Germinal Center Reactions during Infection. *J Immunol* *198*, 218-228.
- Takemura, S., Braun, A., Crowson, C., Kurtin, P.J., Cofield, R.H., O'Fallon, W.M., Goronzy, J.J., and Weyand, C.M. (2001). Lymphoid neogenesis in rheumatoid synovitis. *J Immunol* *167*, 1072-1080.
- Timmer, T.C., Baltus, B., Vondenhoff, M., Huizinga, T.W., Tak, P.P., Verweij, C.L., Mebius, R.E., and van der Pouw Kraan, T.C. (2007). Inflammation and ectopic lymphoid structures in rheumatoid arthritis synovial tissues dissected by genomics technology: identification of the interleukin-7 signaling pathway in tissues with lymphoid neogenesis. *Arthritis Rheum* *56*, 2492-2502.
- Tonegawa, S. (1983). Somatic generation of antibody diversity. *Nature* *302*, 575-581.
- Toney, L.M., Cattoretti, G., Graf, J.A., Merghoub, T., Pandolfi, P.P., Dalla-Favera, R., Ye, B.H., and Dent, A.L. (2000). BCL-6 regulates chemokine gene transcription in macrophages. *Nat Immunol* *1*, 214-220.
- Tschopp, J., Masson, D., and Stanley, K.K. (1986). Structural/functional similarity between proteins involved in complement- and cytotoxic T-lymphocyte-mediated cytolysis. *Nature* *322*, 831-834.
- Tunyaplin, C., Shaffer, A.L., Angelin-Duclos, C.D., Yu, X., Staudt, L.M., and Calame, K.L. (2004). Direct repression of *prdm1* by Bcl-6 inhibits plasmacytic differentiation. *J Immunol* *173*, 1158-1165.
- Ueno, H. (2019). Tfh cell response in influenza vaccines in humans: what is visible and what is invisible. *Curr Opin Immunol* *59*, 9-14.
- Vacchio, M.S., Ciucci, T., Gao, Y., Watanabe, M., Balmaceno-Criss, M., McGinty, M.T., Huang, A., Xiao, Q., McConkey, C., Zhao, Y., *et al.* (2019). A Thpok-Directed Transcriptional Circuitry Promotes Bcl6 and Maf Expression to Orchestrate T Follicular Helper Differentiation. *Immunity* *51*, 465-478 e466.
- Vanderleyden, I., Fra-Bido, S.C., Innocenti, S., Stebbeg, M., Okkenhaug, H., Evans-Bailey, N., Pierson, W., Denton, A.E., and Linterman, M.A. (2020). Follicular Regulatory T Cells Can Access the Germinal Center Independently of CXCR5. *Cell Rep* *30*, 611-619 e614.
- Victoria, G.D., Dominguez-Sola, D., Holmes, A.B., Deroubaix, S., Dalla-Favera, R., and Nussenzweig, M.C. (2012). Identification of human germinal center light and dark zone cells and their relationship to human B-cell lymphomas. *Blood* *120*, 2240-2248.
- Victoria, G.D., Schwickert, T.A., Fooksman, D.R., Kamphorst, A.O., Meyer-Hermann, M., Dustin, M.L., and Nussenzweig, M.C. (2010). Germinal center dynamics revealed by multiphoton microscopy with a photoactivatable fluorescent reporter. *Cell* *143*, 592-605.
- Vinuesa, C.G., and Cyster, J.G. (2011). How T cells earn the follicular rite of passage. *Immunity* *35*, 671-680.
- Vinuesa, C.G., Linterman, M.A., Yu, D., and MacLennan, I.C. (2016). Follicular Helper T Cells. *Annu Rev Immunol* *34*, 335-368.
- Vogel, K.U., Edelmann, S.L., Jeltsch, K.M., Bertossi, A., Heger, K., Heinz, G.A., Zoller, J., Warth, S.C., Hoefig, K.P., Lohs, C., *et al.* (2013). Roquin paralogs 1 and 2 redundantly repress the *Icos* and *Ox40* costimulator mRNAs and control follicular helper T cell differentiation. *Immunity* *38*, 655-668.

## References

- Vu Van, D., Beier, K.C., Pietzke, L.J., Al Baz, M.S., Feist, R.K., Gurka, S., Hamelmann, E., Kroczek, R.A., and Hutloff, A. (2016). Local T/B cooperation in inflamed tissues is supported by T follicular helper-like cells. *Nat Commun* 7, 10875.
- Walker, J.A., and McKenzie, A.N.J. (2018). TH2 cell development and function. *Nat Rev Immunol* 18, 121-133.
- Wang, C., Collins, M., and Kuchroo, V.K. (2015a). Effector T cell differentiation: are master regulators of effector T cells still the masters? *Curr Opin Immunol* 37, 6-10.
- Wang, C.J., Heuts, F., Ovcinnikovs, V., Wardzinski, L., Bowers, C., Schmidt, E.M., Kogimtzis, A., Kenefeck, R., Sansom, D.M., and Walker, L.S. (2015b). CTLA-4 controls follicular helper T-cell differentiation by regulating the strength of CD28 engagement. *Proceedings of the National Academy of Sciences of the United States of America* 112, 524-529.
- Wang, P., Wang, Y., Xie, L., Xiao, M., Wu, J., Xu, L., Bai, Q., Hao, Y., Huang, Q., Chen, X., *et al.* (2019). The Transcription Factor T-Bet Is Required for Optimal Type I Follicular Helper T Cell Maintenance During Acute Viral Infection. *Front Immunol* 10, 606.
- Wang, X., Li, Z., Naganuma, A., and Ye, B.H. (2002). Negative autoregulation of BCL-6 is bypassed by genetic alterations in diffuse large B cell lymphomas. *Proceedings of the National Academy of Sciences of the United States of America* 99, 15018-15023.
- Watanabe, M., Fujihara, C., Radtke, A.J., Chiang, Y.J., Bhatia, S., Germain, R.N., and Hodes, R.J. (2017). Co-stimulatory function in primary germinal center responses: CD40 and B7 are required on distinct antigen-presenting cells. *J Exp Med* 214, 2795-2810.
- Weber, J.P., Fuhrmann, F., Feist, R.K., Lahmann, A., Al Baz, M.S., Gentz, L.J., Vu Van, D., Mages, H.W., Haftmann, C., Riedel, R., *et al.* (2015). ICOS maintains the T follicular helper cell phenotype by down-regulating Kruppel-like factor 2. *J Exp Med* 212, 217-233.
- Weber, J.P., Fuhrmann, F., and Hutloff, A. (2012). T-follicular helper cells survive as long-term memory cells. *European journal of immunology* 42, 1981-1988.
- Weinstein, J.S., Herman, E.I., Lainez, B., Licona-Limon, P., Esplugues, E., Flavell, R., and Craft, J. (2016). TFH cells progressively differentiate to regulate the germinal center response. *Nat Immunol* 17, 1197-1205.
- Wickham, H. (2016). *ggplot2: Elegant Graphics for Data Analysis*. Springer-Verlag New York 978-3-319-24277-4.
- Wu, H., Chen, Y., Liu, H., Xu, L.L., Teuscher, P., Wang, S., Lu, S., and Dent, A.L. (2016). Follicular regulatory T cells repress cytokine production by follicular helper T cells and optimize IgG responses in mice. *European journal of immunology* 46, 1152-1161.
- Wynn, T.A. (2003). IL-13 effector functions. *Annu Rev Immunol* 21, 425-456.
- Xiao, N., Eto, D., Elly, C., Peng, G., Crotty, S., and Liu, Y.C. (2014). The E3 ubiquitin ligase Itch is required for the differentiation of follicular helper T cells. *Nat Immunol* 15, 657-666.
- Xiong, H., Dolpady, J., Wabl, M., Curotto de Lafaille, M.A., and Lafaille, J.J. (2012). Sequential class switching is required for the generation of high affinity IgE antibodies. *J Exp Med* 209, 353-364.
- Xu, H., Li, X., Liu, D., Li, J., Zhang, X., Chen, X., Hou, S., Peng, L., Xu, C., Liu, W., *et al.* (2013). Follicular T-helper cell recruitment governed by bystander B cells and ICOS-driven motility. *Nature* 496, 523-527.
- Xu, L., Cao, Y., Xie, Z., Huang, Q., Bai, Q., Yang, X., He, R., Hao, Y., Wang, H., Zhao, T., *et al.* (2015). The transcription factor TCF-1 initiates the differentiation of T(FH) cells during acute viral infection. *Nat Immunol* 16, 991-999.
- Yan, L., de Leur, K., Hendriks, R.W., van der Laan, L.J.W., Shi, Y., Wang, L., and Baan, C.C. (2017). T Follicular Helper Cells As a New Target for Immunosuppressive Therapies. *Front Immunol* 8, 1510.

## References

- Yang, J., Lin, X., Pan, Y., Wang, J., Chen, P., Huang, H., Xue, H.H., Gao, J., and Zhong, X.P. (2016). Critical roles of mTOR Complex 1 and 2 for T follicular helper cell differentiation and germinal center responses. *Elife* 5.
- Yi, W., Gupta, S., Ricker, E., Manni, M., Jessberger, R., Chinenov, Y., Molina, H., and Pernis, A.B. (2017). The mTORC1-4E-BP-eIF4E axis controls de novo Bcl6 protein synthesis in T cells and systemic autoimmunity. *Nat Commun* 8, 254.
- Yu, D., Rao, S., Tsai, L.M., Lee, S.K., He, Y., Sutcliffe, E.L., Srivastava, M., Linterman, M., Zheng, L., Simpson, N., *et al.* (2009). The transcriptional repressor Bcl-6 directs T follicular helper cell lineage commitment. *Immunity* 31, 457-468.
- Yusuf, I., Kageyama, R., Monticelli, L., Johnston, R.J., Ditoro, D., Hansen, K., Barnett, B., and Crotty, S. (2010). Germinal center T follicular helper cell IL-4 production is dependent on signaling lymphocytic activation molecule receptor (CD150). *J Immunol* 185, 190-202.
- Zakroff, S.G., Beck, L., Platzer, E.G., and Spiegelberg, H.L. (1989). The IgE and IgG subclass responses of mice to four helminth parasites. *Cell Immunol* 119, 193-201.
- Zeitrag, J., Alterauge, D., Dahlstrom, F., and Baumjohann, D. (2020). Gene dose matters: Considerations for the use of inducible CD4-CreER(T2) mouse lines. *European journal of immunology*.
- Zeng, H., Cohen, S., Guy, C., Shrestha, S., Neale, G., Brown, S.A., Cloer, C., Kishton, R.J., Gao, X., Youngblood, B., *et al.* (2016). mTORC1 and mTORC2 Kinase Signaling and Glucose Metabolism Drive Follicular Helper T Cell Differentiation. *Immunity* 45, 540-554.
- Zhang, S., Zhang, H., and Zhao, J. (2009). The role of CD4 T cell help for CD8 CTL activation. *Biochem Biophys Res Commun* 384, 405-408.
- Zhang, Y., Tech, L., George, L.A., Acs, A., Durrett, R.E., Hess, H., Walker, L.S.K., Tarlinton, D.M., Fletcher, A.L., Hauser, A.E., and Toellner, K.M. (2018). Plasma cell output from germinal centers is regulated by signals from Tfh and stromal cells. *J Exp Med* 215, 1227-1243.
- Zhu, J., Yamane, H., and Paul, W.E. (2010). Differentiation of effector CD4 T cell populations (\*). *Annu Rev Immunol* 28, 445-489.
- Zhu, Y., Zhao, Y., Zou, L., Zhang, D., Aki, D., and Liu, Y.C. (2019). The E3 ligase VHL promotes follicular helper T cell differentiation via glycolytic-epigenetic control. *J Exp Med* 216, 1664-1681.

## 10. Acknowledgement

First of all, I would like to thank Prof. Dr. Dirk Baumjohann for his continued support, his trust in my abilities and the comprehensive introduction into the methods of immunology. The entire Baumjohann lab being crowded around the BD Cantos in the Goethestraße, is still a famous anecdote among IFI alumni. This is where my passion for immunology started, thank you for introducing me to this great field. Best of luck for your future career in Bonn.

In addition, I would like to thank Markus Müschen, Neil Mabbott and Thorsten Buch for providing mouse strains that were critical for this work and also Andreas Hutloff who shared important reagents and protocols with us. Moreover, I would like to thank Stefan Krebs (LAFUGA Genomics) and LAFUGA Genomics for preparing and sequencing the samples.

As a 'junior' PhD student it was not always easy digging into new and fancy methods such as single cell RNA-seq. I was very lucky to be supported by Prof. Wolfgang Enards group. Setting up the Drop-seq device with Christoph Ziegenhain was a lab DIY dream come true for every amateur craftsman. A big thanks has to go to Chris not only for introducing me into the wet lab part of RNA-seq, but also for supporting me with the challenging dry lab part. This was greatly taken over by his successor, Johannes Bagnoli, who thoroughly analyzed my RNA-seq data, and thereby had an enormous part in shaping the experimental data into a story for a manuscript. Thank you for that Johannes and also for answering reviewer questions already before 7 am. All the best for your future in Lyon. Bonne chance! I would also like to thank Lucas Wange, Aleks Janjic, Johanna Geuder and Daniel Richter for helping out with consultation, reagents, etc. Finally, a big thank you to Wolfgang Enard, who supported me with such great manpower, and also through his elaborate input in meetings and in my TAC committee.

From the IFI, I would like to particularly thank Christine Ried and Jan for introducing me into the world of microscopy ("how do you turn this thing on?") and for always making the time for a nice chat. Thank you Christine for taking such good care of those many invisible things. We would have probably drowned in dirty dishes without you.

I am extremely happy to have had the opportunity to work together with such nice, funny and clever colleagues. I would like to thank all the members of the Baumjohann lab and especially the 'core crew': Frank, Julia and Johanna who really made the lab routine more than just joyful. Without Frank taking the exhausting genotyping work off our backs, we probably would not have gotten anything done at all. Thank you very much for that and for all the nice chats on our walks over to Chicco.

## Acknowledgement

Being able to choose a 'career' path that starts with an extended time of studying is nothing that I take for granted. My parents always supported me in my decisions and made it possible for me to take this journey. I am so happy to have you.

I was often told that people recognize that I am a younger brother and I am proud to admit it. My bigger sister has had such a great influence on me and how I see and do things. Without her, I would probably still not know how to ride a bike ;). Thank you Caro for always being there for me.

After five years of doing a PhD, the question arises at last, what can be taken from it. Important skills, valuable experiences and an entitling diploma are fantastic, but meeting the love of your life still outranks them all. Working together with you was funny, chaotic and somehow still productive. Getting to know you was exciting, thrilling and upsetting. There are no words to describe what it is like to be loved and supported by you. Thank you Katharina, I love you.